ABSTRACT

Title of Dissertation: REGULATION OF ENDOCYTOSIS AT MAMMALIAN CENTRAL SYNAPSES

Bo Shi
Doctor of Philosophy
2022

Dissertation directed by: Dr. Ling-Gang Wu
National Institute of Neurological Disorders and Stroke
National Institutes of Health

Dr. Leslie Pick
Department of Entomology
University of Maryland, College Park

Synaptic endocytosis retrieves exocytosed vesicles and maintains synaptic transmission which is essential to neural circuit functions. Accumulated studies suggest that calcium influx triggers synaptic vesicle endocytosis, which must undergo membrane pit formation and fission of the pit's neck to generate vesicles. However, the calcium sensor that links calcium to endocytic machinery remains not well understood; whether pit formation involves clathrin remains debated, what mechanism controls the endocytic vesicle size remains not well understood either; the mechanism that couples exo- to endocytosis remains not fully understood either. My thesis work aims at

improving our understanding of each of these questions. I studied endocytosis using a combination of techniques, including gene knockout, gene knockdown, fluorescence imaging, electron microscopy, and molecular biology techniques. I identified the calcium sensors that link calcium influx to endocytosis – the protein kinase C α and β isoforms and calmodulin. I found that clathrin is involved in mediating endocytosis at synapses, which may clarify the doubts on whether clathrin is indispensable for synaptic vesicle endocytosis. I found that dynamin is crucial not only for fission as generally thought, but also for controlling the vesicle size at hippocampal synapses, which enhances our understanding on how vesicle size is regulated at synapses. I found that NSF, which disassembles the SNARE complex, is crucial for mediating synaptic vesicle endocytosis, which enhance our understanding of the mechanisms that couple exo- to endocytosis. Consequently, In summary, I identified endocytosis calcium sensor as protein kinase C (α and β isoforms) and calmodulin; found clathrin in playing a role in pit formation, discovered a novel function of dynamin in controlling vesicle size, and reveal NSF in coupling exo- to endocytosis. These findings contribute to better understanding regulation of endocytosis at synapses.

REGULATION OF ENDOCYTOSIS AT MAMMALIAN CENTRAL SYNAPSES

by

Bo Shi

Dissertation submitted to the Faculty of the Graduate School of the
University of Maryland, College Park, in partial fulfillment
of the requirements for the degree of
Doctor of Philosophy
2022

Advisory Committee:
Professor Leslie Pick
Dr. Ling-Gang Wu
Professor Joshua Singer (Dean's Representative)
Professor Quentin Gaudry
Professor Lisa Taneyhill

Acknowledgements

I would like to first thank my advisors, Dr. Ling-Gang Wu and Dr. Leslie Pick, for their mentoring, teaching and guiding.

Besides my advisors, I would like to thank the rest of my committee members for raising questions, giving advice and comments.

Moreover, I would like to thank the lab members: Xinsheng Wu and Yinghui Jin taught me cell culture and pHluorin imaging; Wonchul Shin taught me using software for analyzing data; Seth Villarreal helped me in EM experiments; Xiaoli Guo, Lisi Wei, Keith Chan, Sue Han, Xin Wang, Min Sun, and Nico Cordero gave me advice in the lab meetings.

Last but of course not least, I would like to thank my family for their support and understanding.

Table of Contents

List of Figures

List of Abbreviations

ANTH	AP180 N-terminal homology
AP180	assembly protein 180
AP2	adaptor protein complex 2
AP-5	D,L-2-amino-5- phosphonovaleric acid
ARP2/3	actin related protein 2/3
BAR	bin/amphiphysin/rvs
CALM	clathrin assembly lymphoidmyeloid leukemia
CaM	calmodulin
CaN	calcineurin
CCP	clathrin-coated pit
CCV	clathrin coated vesicle
Cdk5	cyclin dependent kinase 5
CHC	clathrin heavy chain
CLC	clathrin light chain
CME	clathrin medicated endocytosis
CNQX	6-cyano-7- nitroquinoxaline-2, 3-dione
Dnm	dynamin
Doc2	double C2-like domain-containing protein
EM	electron microscopy
EPS15	epidermal growth factor receptor substrate 15
GSK3	glycogen synthase kinase 3
NIH	National Institutes of Health
Hip1R	huntingtin interacting protein 1 related
HRP	horseradish peroxidase
HSC70	heat shock protein 70
NA	numerical aperture
Norm N_{ves}	normalized number of vesicles
NPF	asparagine-proline-phenyalanine
NSF	N-ethylmaleimide sensitive factor
PH	pleckstrin homology
PI	phosphoinositide
PIP_2	phosphatidylinositol-2-bisphosphate
$PI(3,4,5)P_3$	phosphatidylinositol 3,4,5-trisphosphate
$PI(4,5)P_2$	phosphatidylinositol 4,5-bisphosphate
PIP5K	phosphatidylinositol-4-phosphate [PI(4)P]-5-Kinase
PKC	protein kinase C
RRP	readily releasable pool

SH3	src homology 3
SNAP25	synaptosome associated protein 25
STED	stimulated emission depletion
SypH	pH-sensitive pHluorin2X
v-Glut	vesicular glutamate transporter
VAMP4	vesicle associated membrane protein 4
WT	wild-type

Chapter 1: Introduction

1.1 Synaptic transmission and vesicle recycling

The nervous system processes environmental information to guide behaviors. Such processes are carried out by neural circuits, in which neurons interconnect with each other via a structure called a synapse. Signal transmission at synapses is mostly chemical, but can also be electrical. The present study focuses on chemical transmission at synapses, the release of neurotransmitters and their effects on postsynaptic neurons. A synapse is composed of a presynaptic axon terminal, a synaptic cleft, and a postsynaptic compartment usually located at the dendrite of the postsynaptic neuron. Neurotransmitters are produced, transported into vesicles, released from exocytotic vesicles into the synaptic cleft, and finally bind to receptors on postsynaptic dendrites or cell bodies to generate a postsynaptic potential.

To release transmitters from vesicles, vesicles fuse with the plasma membrane, a process called exocytosis. Vesicle fusion opens a pore to discharge vesicular contents, including neurotransmitters, to the synaptic cleft. There are three modes of fusion, full-collapse fusion, kiss-and-run, and compound fusion (Figure 1.1). Full-collapse fusion expands the fusion pore until the vesicle is flat, having fused with the plasma membrane (Figure 1.1), allowing for rapid and complete release of vesicular contents (Ceccarelli et al., 1973). Kiss-and-run involves only fusion pore opening and closure, without the vesicle flattening at the plasma membrane characteristic of full-collapse fusion (Ceccarelli et al., 1973) (Figure 1.1). The fusion pore during kiss-and-run fusion is thought to be narrow, which may slow down transmitter release and even cause

incomplete release if the pore closes quickly enough (Albillos et al., 1997; Ceccarelli et al., 1973; De Toledo et al., 1993; He et al., 2006; Klyachko & Jackson, 2002). Compound fusion involves vesicle-vesicle fusion before exocytosis (Figure 1.1). It may enhance synaptic strength and mediate a large portion of post-tetanic potentiation after repetitive stimulation (Fioravante et al., 2011; He et al., 2009; L.-G. Wu et al., 2014; Xue & Wu, 2010).

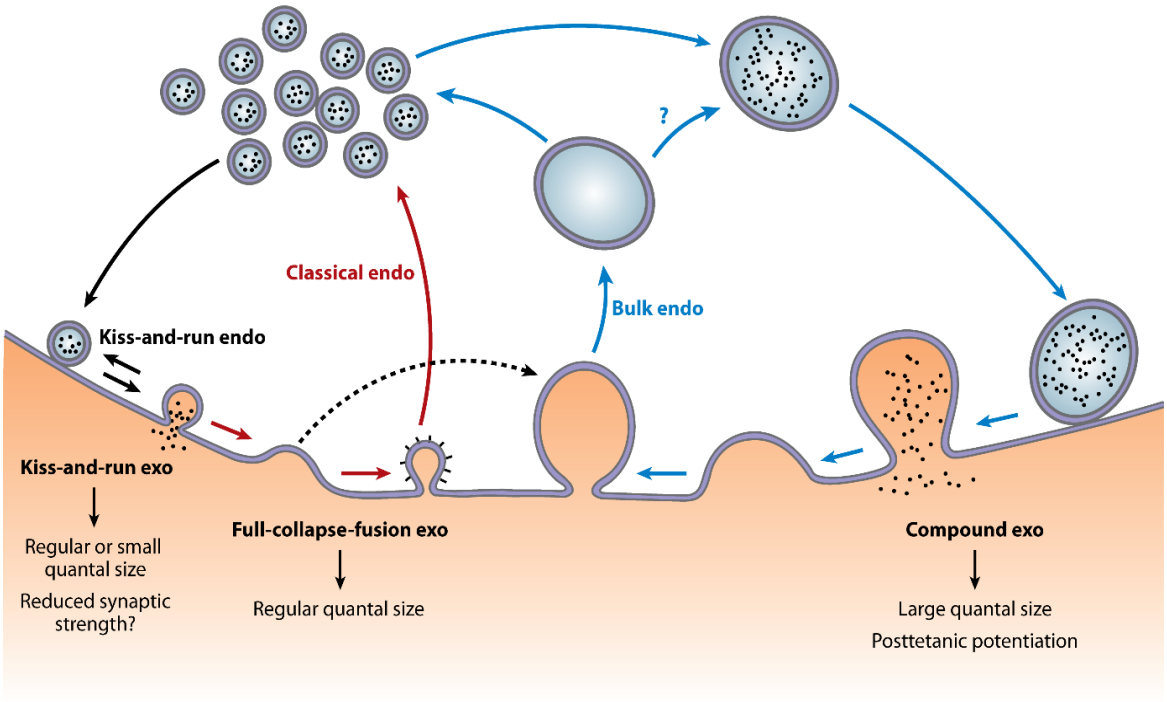

Wu L-G, et al. 2014.
Annu. Rev. Physiol. 76:301–31

Figure 1.1. Three modes of exocytosis, full-collapse fusion, kiss-and-run, and compound fusion, may be associated with clathrin-mediated endocytosis, kiss-and-run, and bulk endocytosis, respectively.

Exocytosed vesicles are recycled via a process called endocytosis, which prevents the vesicle pool from being exhausted by exocytosis. Endocytosis is thus crucial in maintaining vesicle pools, exocytosis, and synaptic transmission (Ceccarelli et al., 1973; Heuser & Reese, 1973; Kononenko & Haucke, 2015; Wu et al., 2014). In addition,

endocytosis preserves the morphological integrity of the cells (Alabi & Tsien, 2013; Bittner & Kennedy, 1970).

1.2 Modes of endocytosis

1.2.1 Modes of endocytosis differing in speed, vesicle size, or amount

The kinetics of endocytosis depend on the parameters of stimulation, as demonstrated at many synapses. For example, at calyx of held synapses, where endocytosis can be measured with capacitance measurements, rapid endocytosis (time constant: ~1-3 s) is observed after an action-potential-like stimulus, whereas slow endocytosis (time constant: ~10-30 s) is observed after a brief train of action-potential-like stimuli or a 20-ms depolarization (Renden & von Gersdorff, 2007; Sun & Wu, 2001; Sun et al., 2002; Wu et al., 2005; Wu et al., 2009). In addition to inducing rapid endocytosis, an increase in stimulation intensity also increases the frequency of bulk endocytosis, a mode of endocytosis that retrieves vesicles much larger than regular vesicles (Wu et al., 2005; Wu et al., 2009). Further increases in stimulation intensity induce endocytosis overshoot, a form of endocytosis that retrieves more vesicles than were exocytosed (Renden & von Gersdorff, 2007; Wu et al., 2009; Xue et al., 2012).

1.2.2 Four mechanistically different modes of endocytosis

1.2.2.1 Clathrin-mediated endocytosis

Clathrin-mediated endocytosis (CME), a classical form of endocytosis, involves the generation of clathrin-coated pits (CCPs) and membrane scission at the neck of pits that converts them into vesicles (Fig. 1.1). CCPs accumulate after exocytosis (Heuser,

1989; Heuser & Reese, 1973). Blockage of scission, the final step of endocytosis, leads to accumulation of CCPs and clathrin-coated vesicles (CCVs). Blockage of CME by perturbations leads to inhibition of vesicle recycling (Ferguson et al., 2007; Granseth et al., 2006; Hayashi et al., 2008; Heerssen et al., 2008; Kasprowicz et al., 2008; Milosevic et al., 2011; Raimondi et al., 2011; Shupliakov, 1997; von Kleist et al., 2011; Zhang et al., 1998). These results suggest that CME plays a role in synaptic vesicle endocytosis. However, recent studies suggest that clathrin is not necessary for synaptic transmission, indicating that clathrin-mediated endocytosis is not essential at synapses (Kim & Ryan, 2009; Kononenko, 2014). Thus, whether clathrin is indispensable for synapses remains debated. This point will be further discussed in a later chapter.

Three clathrin heavy chains (CHCs) and three clathrin light chains (CLCs) combine to form a clathrin triskelion. Clathrin triskelia combine to form pentagons and hexagons, assemble lattices, and coat plasma membrane in CME. The first step of CME is called nucleation, which is thought to start with interaction among clathrin triskelia, adaptor proteins and phosphatidylinositol-2-bisphosphate (PIP_2) (Cocucci et al., 2012; Heuser, 1980; Kelly et al., 2014; Lampe et al., 2016). After nucleation, clathrin, adaptor proteins, cargos, and accessory factors interact with each other while the "coat" grows, and subsequently forming an invaginated bud with a narrow neck. Then, fission takes place at the neck, mediated by a GTPase, dynamin. Fission results in the pinch off of a vesicle from plasma membrane, followed by uncoating of the clathrin-coat (Ferguson & De Camilli, 2012; Koenig & Ikeda, 1996; Saheki & De Camilli, 2012).

Currently, there are two hypotheses regarding how CCPs grow and form curvatures, the curvature constant model and the area constant model (Lampe et al., 2016;

Saffarian et al., 2009). In the curvature constant model, the CCP grows continuously as an invaginated bud as it sustains a constant curvature (Kirchhausen, 2009). In the area constant model, the clathrin triskelia polymerize and extend to a larger but less curved coat, called a coated plaque. The plaque moves inward from the plasma membrane shortly before vesicle fission (Avinoam et al., 2015; Heuser, 1980; Larkin et al., 1986). The second model is energetically unfavorable because of the conversion from hexagons to pentagons during curvature formation (Den Otter & Briels, 2011; Heuser, 1980; Kirchhausen, 2009; Saffarian et al., 2009).

The clathrin-coat consists of two layers, the interior layer formed by adaptors and the exterior layer formed by clathrin. The adaptor proteins bind to phosphoinositides (PIs), such as phosphatidylinositol 4,5-bisphosphate ($PI(4,5)P_2$) and phosphatidylinositol 3,4,5-trisphosphate ($PI(3,4,5)P_3$) (Beck & Keen, 1991; Edeling et al., 2006; Schmid & McMahon, 2007). These proteins also bind to the N-terminal, β-propeller domain of the clathrin heavy chain (Edeling et al., 2006; Schmid & McMahon, 2007) and some other cargos, adaptors, and endocytic proteins (Haucke, 1999; Saheki & De Camilli, 2012). Adaptor protein complex 2 (AP2) is abundant at the plasma membrane. This adaptor complex comprises four subunits, including two large subunits, α and β2 (~100 kDa), a medium subunit, μ2 (~50kDa), and a small one, δ2 (~20kDa) (Edeling et al., 2006). The complex interacts with transmembrane proteins carrying tyrosine-based motifs and dileucine-based motifs (Kononenko & Haucke, 2015). For instance, by interaction with tyrosine-based motifs, AP2 plays a role in internalization of synaptotagmin, a calcium sensor in exocytosis, by binding to its C2B domain (Haucke, 1999; Ullrich et al., 1994; Zhang et al., 1994).

Another adaptor protein, stonin 2 (*Drosophila* homolog stoned B or *C. elegans* homolog unc41) contains a C-terminal μ-homology domain with similarities in sequence to the sorting signal motif of the μ subunit of AP2. Thereby, stonin 2 also recognizes the C2 domains of synaptotagmin and plays an organizational role in endocytic internalization and synaptotagmin recycling (Diril et al., 2006; Fergestad & Broadie, 2001; Kononenko et al., 2013; Maritzen et al., 2010; Mullen et al., 2012). Moreover, stonin 2 regulates interactions between AP2 and synaptotagmin (Fergestad & Broadie, 2001) just as AP2 regulates the ability of stonin 2 to facilitate endocytic internalization and recycling of synaptagmin also depends on AP2 (Diril et al., 2006). In addition, stonin 2 contains two asparagine-proline-phenyalanine (NPF) motifs which bind to epidermal growth factor receptor substrate 15 (EPS15) and intersectin, two accessory proteins involved in scaffolding (Maritzen et al., 2010).

There are two AP180 N-terminal homology (ANTH) domain proteins as adaptors: clathrin coat assembly protein 180 (AP180), expressed in neurons, and its homolog, clathrin assembly lymphoidmyeloid leukemia (CALM), expressed ubiquitously (Morgan et al., 1999; Saheki & De Camilli, 2012; Yao et al., 2003). These two proteins regulate sorting of synaptobrevin, a key factor in exocytosis, via its direct association with their ANTH domain (Burston et al., 2009; Dittman & Kaplan, 2006; Koo et al., 2011; Nonet et al., 1999; Sharon et al., 2011).

As mentioned above, nucleation in CME requires clathrin triskelia, adaptor proteins, and PIP_2. PIP_2 is phosphorylated derivative of PIs, which are key elements of membrane identity. Different PIs associate with specific lipid binding motifs of proteins, so the distribution of PIs is critical for targeting these proteins to their correct subcellular

locations (Behnia & Munro, 2005; Lemmon, 2008; Matteis & Godi, 2004; Simonsen et al., 2001). $PI(4,5)P_2$, one PIP_2, plays a crucial role in endocytosis. It binds adaptor proteins, like AP2, AP180, CALM, and some accessory proteins, including members of the bin/amphiphysin/rvs (BAR) domain protein family (Posor et al., 2015; Simonsen et al., 2001). Furthermore, $PI(4,5)P_2$ activates AP2, changing it from its closed conformation to its open conformation (Jackson et al., 2010). In addition, it is required for vesicle fission mediated by dynamin (Lee et al., 1999; Vallis et al., 1999).

Beyond the core molecules that are required for and very involved in CME, there are accessory proteins that assist in or regulate CME. These accessory proteins provide protein or lipid interactions and contain typical domains for such a purpose, such as ANTH, BAR, pleckstrin homology (PH), and src homology 3 (SH3) domains; also commonly found are NPF motifs or other motifs for binding proteins (Dittman & Ryan, 2009; Slepnev & De Camilli, 2000). Besides protein binding, these proteins may play roles in phosphorylation, phosphoinositide metabolization, scaffold generation, curvature generation, or curvature sensing (Saheki & De Camilli, 2012). For instance, EPS15 and intersectin are accessory proteins provide scaffolding function (Kaksonen & Roux, 2018).

$PI(4,5)P_2$ metabolizing enzymes are involved in CME. $PI(4,5)P_2$ is synthesized by phosphatidylinositol-4-phosphate [PI(4)P]-5-Kinases (PIP5Ks) (Krauß & Haucke, 2007), and type I PIP5K interacts with the μ2 subunit of AP2, which is involved in nucleation (Krauss et al., 2006). On the other hand, before fission, synaptojanin 1, a $PI(4,5)P_2$ phosphatase, is recruited to the necks of CCVs (Saheki & De Camilli, 2012), and the dephosphorylation of $PI(4,5)P_2$ facilitates AP2 disassembly from the membrane (Edeling et al., 2006).

Formation of curvature buds follows nucleation. Membrane curving requires: 1) insertion of amphipathic helices of endocytic proteins into the cytosolic leaflet of the membrane to generate asymmetry of the lipid bilayer (Antonny, 2011; Farsad et al., 2001; Ford et al., 2002; Gallop et al., 2006; Masuda et al., 2006) and 2) formation of homodimers or heterodimers of proteins containing BAR domains. The dimers are crescent-shaped and positively charged on their surface, allowing them to bind optimally to the negatively charged lipid bilayer to induce and sense membrane curvature (Frost et al., 2008; Frost et al., 2009; Gallop et al., 2006; Masuda et al., 2006; Peter, 2004; Shimada et al., 2007; Weissenhorn, 2005). For example, endophilin contains N-terminal amphipathic helices and a BAR domain, and the two motifs work together as a functional module (called the N-BAR domain), to promote dimerization and membrane deformation. This protein also contains an SH3 domain and plays a role in fission and uncoating by interacting with the proline-rich domains of dynamin and synaptojanin (Dittman & Ryan, 2009; Farsad et al., 2001; Gallop et al., 2006; Ringstad et al., 2001).

In addition to curvature-generation proteins, actin cytoskeleton may be required to overcome resistance forces from the spontaneous tendency of the lipid bilayer to remain flat (Kessels & Qualmann, 2021). In addition, some actin regulatory factors also regulate endocytosis indirectly. For example, huntingtin interacting protein 1 related (Hip1R) blocks actin assembly associated with endocytosis by forming a complex with cortactin, a protein that binds to actin filament and actin related protein 2/3 (ARP2/3) complex (Le Clainche et al., 2007).

Dynamin mediates CCP fission, a process whose details will be illustrated in a later section. After CCVs are released from plasma membrane, two mechanisms are used

to uncoat them. First, because clathrin coat shedding is an ATP dependent process, heat shock protein 70 (HSC70), an ATPase, is involved. HSC70 and its cofactor auxilin regulate this uncoating process (Braell et al., 1984; Kaksonen & Roux, 2018; Schlossman et al., 1984; Ungewickell, 1985; Ungewickell et al., 1995; Xing et al., 2010). Second, synaptojanin catalyzes $PI(4,5)P_2$ hydrolysis, which is required for adaptor proteins to separate from the inner layer of CCVs (Edeling et al., 2006; Kaksonen & Roux, 2018; Saheki & De Camilli, 2012).

1.2.2.2 Kiss-and-run

Kiss-and-run is a combined process of exocytosis and endocytosis in which fusing vesicles do not collapse into cell membrane during or after neurotransmitter release (Fig. 1.1). Thereby, kiss-and-run keeps vesicular identity and bypasses the sorting mechanism. Kiss-and-run was originally proposed by Ceccarelli and his colleagues in 1973, based on the Ω-shaped pits visible in electron microscopy (EM) imaging at the frog neuromuscular junction (Ceccarelli et al., 1973). However, there was no convincing evidence to determine whether the Ω-shaped pits were an intermediate status of full collapse or pore closure until capacitance recordings shed light on the subject. Capacitance flickers were observed, and the pores were determined to be ~0.5-3 nm in diameter, as measured by pore conductance (Albillos et al., 1997; De Toledo et al., 1993; He et al., 2006; Klyachko & Jackson, 2002).

Recently, the process of kiss-and-run has been directly observed under the stimulated emission depletion (STED) microscope (Shin et al., 2018; Shin et al., 2021; Zhao et al., 2016). Hemi-fusion (one layer of the lipid bilayer of the exocytic vesicle

fuses with the plasma membrane) and hemi-fission (one layer of the lipid bilayer of the endocytic vesicle fissions from the plasma membrane) stages have also been observed in live imaging. Additionally, pore opening and closure are regulated by actin and dynamin (Shin et al., 2018; Shin et al., 2021; Zhao et al., 2016).

1.2.2.3 Bulk endocytosis

When synaptic vesicles fuse with the plasma membrane after a stimulus, sometimes extra membrane is retrieved through large infoldings at the distal area of the active zone. Then, the infoldings undergo fission to produce intracellular endosome-like structures or cisternae, which are much larger than regular vesicles. This retrieval process is called bulk endocytosis, a nonselective endocytosis for membrane uptake (Clayton et al., 2008; Hayashi et al., 2008; Heuser & Reese, 1973; Holt et al., 2003; Miller & Heuser, 1984; Paillart et al., 2003; Wu & Wu, 2007) (Fig. 1.1). The size of synaptic vesicles reformed from bulk endocytosis is less homogeneous compared to that at rest or under mild stimulation, and hence fidelity of vesicle size is partially lost (Saheki & De Camilli, 2012). Nonetheless, some endocytic cargoes, including synaptophysin, Synaptobrevin 2, and vesicular glutamate transporter (v-Glut) are recycled by bulk endocytosis, though the underlying mechanism of this recycling remains largely unknown (Chanaday et al., 2019). In addition, vesicle associated membrane protein 4 (VAMP4) is favorably accumulated by bulk endocytosis, suggesting VAMP4 involvement in bulk endocytosis (Nicholson-Fish et al., 2015).

Bulk endocytosis retrieves membrane in a time span from less than a second to a much longer time, resulting in endosome-like structures or cisternae with an average

diameter of 150 nm. This process is actin and formin dependent, but clathrin and AP2 independent (Clayton & Cousin, 2009; Soykan et al., 2017; Wu et al., 2016). Cyclin dependent kinase 5 (Cdk5) and glycogen synthase kinase 3 (GSK3) facilitate bulk endocytosis via several endocytic proteins, such as syndapin and dynamin (Evans & Cousin, 2007; Renard & Boucrot, 2021; Smillie et al., 2013). Flower is a synaptic-vesicle-associated calcium channel located near the active zone. This channel provides calcium influx to trigger bulk endocytosis during intense stimulations (Yao et al., 2017; Yao et al., 2009). Furthermore, calcium sensors are expected to play a key role, and calcineurin (CaN) could be involved in bulk endocytosis. CaN is a calcium-dependent phosphatase that dephosphorylates many endocytic proteins at synapses, including dynamin. Dephosphorylated dynamin associates with syndapin to activate bulk endocytosis (Clayton et al., 2009; Nguyen et al., 2014). CaN may be involved in bulk endocytosis, as supported by three pieces of evidence. First, this protein is located in the cytosol with a low affinity for calcium, and thus can only be activated during large calcium influxes caused by strong nerve activity (Nguyen et al., 2014). Second, dynamin 1 is dephosphorylated by CaN only when stimulation reaches the threshold to activate bulk endocytosis (Clayton & Cousin, 2009). Third, bulk endocytosis is inhibited by CaN chemical blockers in neuron cultures (Evans & Cousin, 2007).

The role of dynamin in bulk endocytosis is somewhat debated. On the one hand, mutation of phosphorylation sites of dynamin 1 inhibits bulk endocytosis (Clayton & Cousin, 2009). On the other hand, bulk endocytosis still proceeds in mouse neurons with double knockouts of dynamin 1 and dynamin 3, although dynamin 2 involvement cannot be ruled out (Y. Wu et al., 2014). Nevertheless, shibire (dynamin homolog in *Drosophila*)

inactivation does not cause large pit accumulation, but rather causes bulk membrane invagination at the plasma membrane, suggesting that dynamin is involved in fission during bulk endocytosis (Kasprowicz et al., 2014).

1.2.2.4 Ultrafast endocytosis

Another category of vesicle recycling is called “ultrafast endocytosis” (add jorgenson paper citation here). Ultrafast endocytosis is clathrin-independent endocytosis, and it is triggered within 30 ms to 1 s after a single optical stimulation through channelrhodopsin at physiological temperature. This form of endocytosis is found at the lateral edges of active zones. It generates relatively homogenously sized vesicles with a diameter ~60-80 nm (Delvendahl et al., 2016; Soykan et al., 2017; Watanabe, Liu, et al., 2013; Watanabe, Rost, et al., 2013). Single vesicle pHluorin experiments from another publication demonstrate that ultrafast endocytosis (with mean duration of 200-300 ms) also can be triggered at 24 ℃, even though it is not dominant (Chanaday & Kavalali, 2018). After ultrafast endocytosis, the large vesicles are converted to small vesicles via clathrin-coated vesicle formation from these large endosome-like structures in ~10-20 s (Watanabe et al., 2014).

Ultrafast endocytosis is inhibited by latrunculin-A, which blocks actin polymerization, and dynasore, which blocks dynamin (Watanabe, Rost, et al., 2013). However, dynasore blocks actin, cholesterol, and lipid rafts as well, so further evidence is required to prove whether dynamin mediates ultrafast endocytosis (Preta et al., 2015). Moreover, ultrafast endocytosis shares other components of CME, such as synaptojanin

and endophilin. These two proteins enhance ultrafast endocytosis during vesicle neck formation and clathrin uncoating (Watanabe et al., 2018).

1.2.2.5 Comparison of the mechanisms of endocytosis

Ultrafast endocytosis is less understood for two reasons. First, common imaging systems have difficulty capturing ultrafast dynamics. Second, live assays typically make indirect measurements. For example, pHluorin experiments measure pH changes instead of endocytosis.

Both ultrafast endocytosis and kiss-and-run recycle vesicles quickly, but they differ in location and vesicle size. Ultrafast endocytosis is triggered at lateral edges of the active zone, while kiss-and-run occurs within the active zone. Furthermore, the synaptic vesicles do not collapse during kiss-and-run, and thus the vesicle size does not change. The vesicle size of ultrafast endocytosis is larger than that of synaptic vesicles.

Both ultrafast endocytosis and bulk endocytosis form endosomes, but the former process is much faster. Moreover, ultrafast endocytosis forms uniform vesicles with a diameter of ~60-80 nm, whereas vesicles formed during bulk endocytosis are larger and more heterogeneous in size.

1.2.3 Correlation between endocytosis dyanmics and mechanisms

CME may contribute to slow endocytosis since slow endocytosis is blocked when CME-related proteins are perturbed (Artalejo et al., 1995; Granseth et al., 2006; Jockusch et al., 2005; Kim & Ryan, 2009; Milosevic et al., 2011; Schuske et al., 2003; von Kleist et al., 2011; Willox & Royle, 2012; Wu et al., 2009; Yim et al., 2010). Mostly, kiss-and-

run is fast, which contributes to rapid endocytosis, but a small portion of kiss-and-run, called cavicapture, is slow in chromaffin cells, and probably mediates slow endocytosis (Elhamdani, 2006; Perrais et al., 2004). Bulk endocytosis takes a few seconds or more, and hence it could mediate slow and fast endocytosis (Wu & Wu, 2007; Wu et al., 2009). Last, ultrafast endocytosis is the fastest mode of endocytosis (Watanabe, Liu, et al., 2013; Watanabe, Rost, et al., 2013).

As mentioned before, rapid endocytosis (time constant: ~1-3 s) is observed after an action-potential-like stimulus at calyx of held synapses, and both rapid and slow endocytosis are evoked by more intense stimulation. Rapid endocytosis is inhibited by loss of actin, suggesting actin involvement in rapid endocytosis (Wu et al., 2016). Furthermore, dynamin is likely involved in rapid endocytosis because it is blocked by dynamin inhibitors (Wu et al., 2009; Yamashita et al., 2005).

1.3 Coupling between exocytosis and endocytosis

1.3.1 Endocytosis maintains exocytosis

First, endocytosis prevents the vesicle exhaustion that is an inevitable consequence of unopposed exocytosis, evident from experiments on the *shibire* *Drosophila* mutant (whose homolog is *dynamin* in mammals). This mutant is temperature sensitive, and its function is deactivated over 29 °C. Its deactivation blocks endocytosis and eventually paralyzes the animal (Delgado et al., 2000; Koenig & Ikeda, 1989; Koenig & Ikeda, 1996). Furthermore, endocytosis may maintain the size of synaptic vesicles and thereby sustain neural transmission at boutons (Wu & Wu, 2009).

Moreover, endocytosis retrieves comparable membrane area to that fused during exocytosis over a time course from tens of milliseconds to a few minutes. This compensatory endocytosis tightly couples with exocytosis, which prevents cells from swelling or shrinking (Haucke et al., 2011; Smith & Neher, 1997; Watanabe, Rost, et al., 2013; Wu et al., 2007).

1.3.2 Mode coupling for exo-endocytosis

Furthermore, not only amount and timing are coupled, but also certain types of exocytosis may couple with specific types of endocytosis. For instance, full-collapse fusion is proposed to associate with CME given that CCVs are similar to synaptic vesicles in size (Heuser & Reese, 1973, 1981; Miller & Heuser, 1984). As mentioned, kiss-and-run retrieves the same vesicle as a combination of exocytosis and endocytosis. Compound fusion is thought to be coupled with bulk endocytosis (Fig. 1.1).

1.3.3 Endocytosis clear the active zone to facilitate endocytosis

Endocytosis may be critical in clearing exocytic proteins from the active zone, and thus may enhance replenishment of the readily releasable pool (RRP). There are two pieces of evidence for this claim. First, short-term depression is enhanced within 20-40 ms at 50 Hz stimulation in neuromuscular junctions of fruitflies by clathrin knockdown or shibire mutation (Kawasaki et al., 2000; Wu & Borst, 1999). This response is so rapid that it could not result from vesicular recycling. It has been proposed that endocytosis promotes RRP refilling by clearing exocytotic proteins and membrane to facilitate vesicle docking at the active zone (Hosoi et al., 2009; Kawasaki et al., 2000; Wu et al., 2009).

Second, the calyx of held is a high-frequency firing synapse, and this high frequency firing is maintained by clearance of the active zone (Haucke et al., 2011; Neher, 2010). Some endocytic proteins, like intersectin 1 (aforementioned), are critical for this clearance (Hosoi et al., 2009; Sakaba et al., 2013). In sum, endocytosis removes fused membrane and proteins to facilitate subsequent docking of synaptic vesicles (Hosoi et al., 2009).

1.3.4 Exocytosis plays roles in initiation of endocytosis

SNARE proteins (synaptobrevin, syntaxin and synaptosome associated protein 25 [SNAP25]) mediate exocytosis. Studies suggest that these three proteins also play roles in endocytosis at calyx and hippocampal synapses. For example, both rapid and slow endocytosis are blocked by tetanus toxin and botulinum neurotoxins that cleave these SNARE proteins at the calyx (Xu et al., 2013). Synaptobrevin or SNAP25 knockdown also blocks endocytosis at hippocampal synapses (Zhang et al., 2013).

Moreover, synaptotagmin is the calcium sensor for exocytosis and critical for initiation of endocytosis. Its loss causes inhibition of endocytosis in mouse hippocampal synapses, the calyx of Held, and neuromuscular junctions (Hosoi et al., 2009; Jorgensen et al., 1995; Littleton et al., 2001; Nicholson-Tomishima & Ryan, 2004; Poskanzer et al., 2003; J. Yao et al., 2012).

1.3.5 Lipid involvement in exo-endocytosis coupling

Beyond the role of PIP_2 in endocytosis described in Section 1.2.2.1, $PI(4,5)P_2$ also promotes exocytosis by increasing the probability of vesicle release. The mechanism of

this promotion is still not fully understood. It has been suggested that $PI(4,5)P_2$ may facilitate recruitment of several $PI(4,5)P_2$ binding proteins, such as Munc13 and synaptotagmin (Lauwers et al., 2016; Martin, 2015; Walter et al., 2017). In addition, $PI(4,5)P_2$ interacts with some other exocytic proteins, including Double C2-Like Domain-Containing Protein (Doc2) and syntaxin (Koch & Holt, 2012). Consequently, PIP_2 play key roles in both exo- and endocytosis. It may play a role in exo-endocytosis coupling.

1.4 Medical significance

Understanding endocytosis may help medically because some endocytic proteins are associated with neurodegenerative diseases. For examples, mutation of α-synuclein, which causes dementia and Parkinson's disease, blocks rapid endocytosis, slow endocytosis, and replenishment of the RRP at calyces (Xu et al., 2016). AP2 and AP180 are linked to Alzheimer's disease. Auxilin and synaptojanin are associated with Parkinsonism (Edvardson et al., 2012; Krebs et al., 2013; Yao & Coleman, 1998). Endophilin, a curvature sensing protein in CME, is linked to ataxia (John et al., 2016).

1.5 Background and Significance of thesis projects

1.5.1 Calcium Sensors in endocytosis

Two pieces of evidence demonstrate that calcium triggers endocytosis (Hosoi et al., 2009; L.-G. Wu et al., 2014; Wu et al., 2009). First, at the calyx of Held, decreasing the extracellular calcium concentration or adding a calcium chelator, BAPTA, decreases the rate of slow and rapid endocytosis up to 1500 fold and blocks endocytic overshoot. Accordingly, increasing the calcium current charge enhances the rate and overshoot of

endocytosis significantly. Second, the calcium chelator EGTA inhibits bulk endocytosis. Moreover, calcium influx enhances rapid and slow endocytosis at chromaffin cells and hippocampal cells (Artalejo et al., 1995; Chiang et al., 2014; Sun et al., 2010).

How does calcium triggers endocytosis? To address this question, the first task is to identify the calcium sensor(s). CaN is a candidate mentioned earlier. Calmodulin (CaM) is another candidate, because chemical blockers and knockdown of CaM inhibit endocytosis (Sun et al., 2010). However, we do not know whether CaM involvement in endocytosis depends on calcium binding to CaM. Thus, it remains unclear whether CaM is a calcium sensor for endocytosis.

Our lab studied these calcium sensors by knockout calcium-activated protein kinase C (PKC) α or β isoform (PKC_{α} or PKC_{β}) and CaM isoform 2 (CaM_2) in mice (Fig.1.2B). The hypothesis was that CaM and PKC are calcium sensors for calcium-triggered endocytosis. The lab found that PKC_{α}, PKC_{β} and CaM_2 serve as calcium sensors at conventional hippocampal synapses. This finding suggests that calcium triggers endocytosis via PKC-mediated phosphorylation and CaM-mediated dephosphorylation.

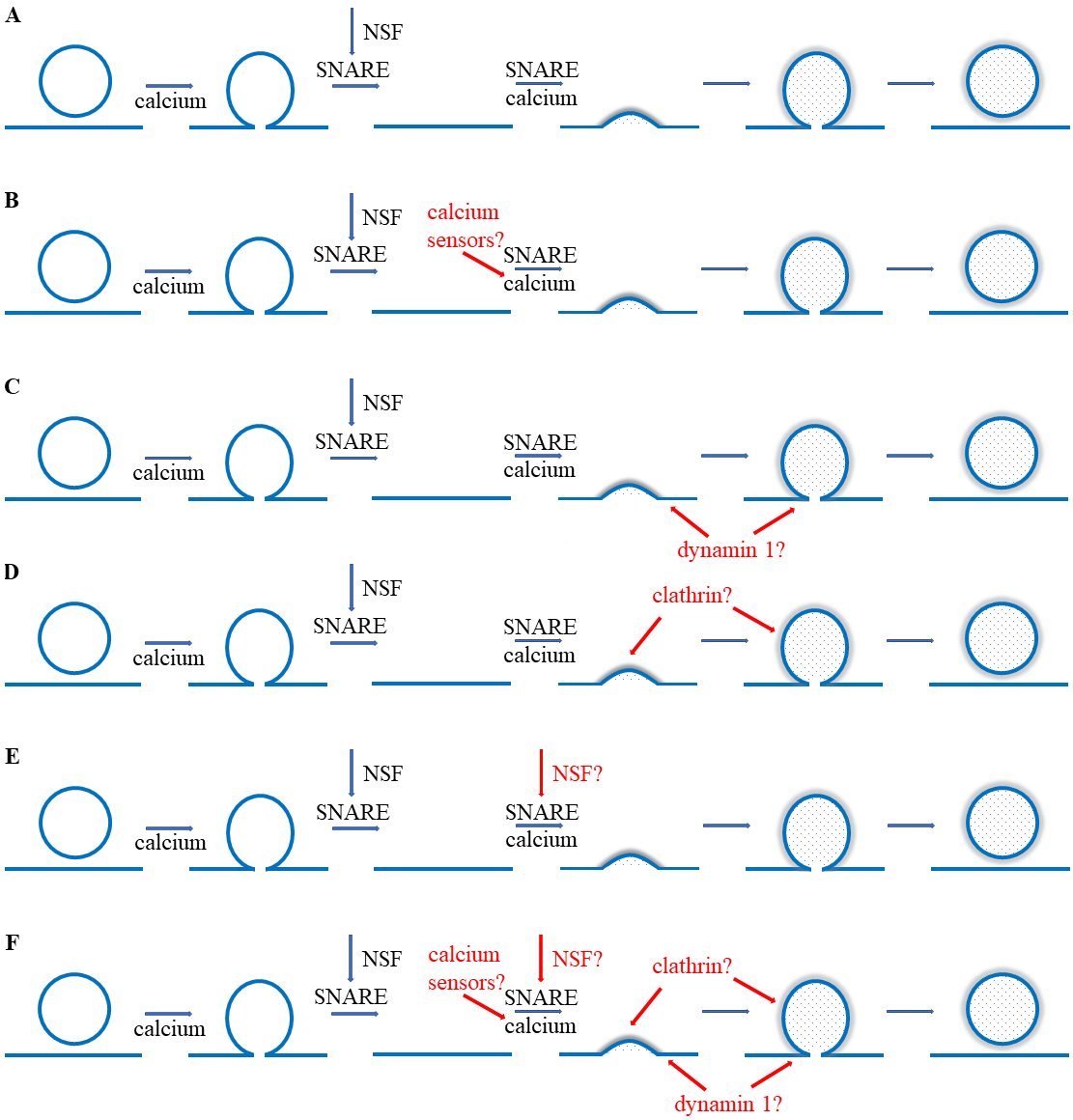

Figure 1.2. ***A***, Calcium triggers SNARE-dependent vesicle fusion, then triggers endocytosis, which is also SNARE-dependent. This panel shows the starting point of the present research. ***B-E***, Four research projects with question marks showing the questions being addressed in the present thesis: ***B***, What are the calcium sensors of endocytosis? ***C***, Does dynamin have an additional role before fission? ***D***, Is clathrin involved in synaptic vesicle endocytosis? ***E***, Is NSF (for disassembling SNARE proteins) involved in coupling exocytosis to endocytosis? ***F***, Summary of all four projects with four question marks.

1.5.2 Dynamin

Dynamin is a GTPase that mediates vesicle fission during endocytosis. There are three isoforms of dynamin in mammals, where dynamin 1 is expressed most abundantly and specifically in the nervous system (Saheki & De Camilli, 2012). Previous studies

show that knocking out dynamin 1 only significantly inhibits endocytosis in cortical neurons during, not after, stimulation (Ferguson et al., 2007; Raimondi et al., 2011). Consequently, the current view on dynamin 1 is that it increases endocytic capacity and velocity during stimulation in small, conventional, central synapses. Here, this issue is re-examined in hippocampal synapses containing conventional small boutons (Gan & Watanabe, 2018; Kavalali & Jorgensen, 2014; Kononenko & Haucke, 2015; L.-G. Wu et al., 2014).

In contrast to the results obtained at cortical synapses, the present research found that dynamin 1 plays a critical role in endocytosis after both low and high frequency action potential trains at hippocampal synapses (Fig.1.2C). Unexpectedly, it was also found that dynamin 1 is important in controlling vesicle size, a function that must occur at a step before fission, during formation of the endocytic vesicle. Thus, dynamin 1 is more important than previously recognized in mediating endocytosis and controlling vesicle size at conventional small-bouton hippocampal synapses.

1.5.3 Clathrin

Although traditionally CME is considered essential to synaptic transmission, recent studies at hippocampal synapses reported that clathrin knockdown, conditional knockout of AP2 (Kononenko, 2014), or ~96% knockdown of AP2 (Kim and Ryan, 2009) only inhibits vesicle protein endocytosis to a rather minor extent at room temperature, suggesting that clathrin is dispensable for vesicular protein endocytosis (Kononenko, 2014). However, ultrastructural examination suggests that clathrin is required for vesicle budding from endosomes (Kononenko, 2014). Using ‘flash-and-

freeze' electron microscopy (EM), where high-pressure freezing is timed after action potentials evoked by light-induced channelrhodopsin activation, recent studies suggest that an ultrafast (~50-100 ms) clathrin-independent mechanism, which forms large endosomes from the plasma membrane, mediates synaptic vesicle endocytosis at physiological temperature, whereas clathrin mediates vesicle budding from endosomes (Watanabe, Liu, et al., 2013; Watanabe, Rost, et al., 2013; Watanabe et al., 2014). Only at room temperature, clathrin mediates synaptic vesicle endocytosis (Watanabe et al., 2014). Consistent with these EM results, acute photo-inactivation of clathrin light chain or clathrin heavy chain does not inhibit membrane internalization, but rather blocks vesicle budding from endosomes in *Drosophila* neuromuscular junctions (Heerssen et al., 2008; Kasprowicz et al., 2008); reducing clathrin in *Caenorhabditis elegans* does not affect vesicle number in nerve terminals or spontaneous release (Sato et al., 2009). Taken together, except an early study (Granseth et al., 2006), most recent studies seem to agree that endocytosis is mediated by a clathrin-independent mechanism at synapses. However, although these studies agree that endocytosis is clathrin-independent at synapses, they disagree about the details, such as the temperatures at which this rule applies. For example, the flash-and-freeze EM suggests that synaptic vesicle endocytosis in hippocampal synapses is clathrin-independent only at physiological temperature and clathrin-dependent at room temperature (Watanabe et al., 2014), which is in conflict with a study suggesting that clathrin is not necessary at room temperature in hippocampal synapses (Kononenko, 2014).

Here we determined whether synaptic vesicle endocytosis depends on clathrin at hippocampal synapses by knocking out clathrin (Fig.1.2D). We found that endocytosis of

vesicular proteins at hippocampal synapses is clathrin-dependent, suggesting that clathrin is required for vesicular protein endocytosis at these synapses. We found that the clathrin dependency was not evident until clathrin was reduced by more than ~74%, which may help to reconcile the conflict of whether clathrin is essential for vesicular protein endocytosis at hippocampal synapses between previous and present studies (Granseth et al., 2006; Kononenko, 2014). It is concluded that clathrin is indispensable for synaptic vesicular protein endocytosis.

1.5.4 NSF

After a synaptic vesicle is released, the SNARE complex is dissociated by an ATPase N-Ethylmaleimide Sensitive Factor (NSF). Following exocytosis, disassembly of SNARE proteins by NSF is required (Jackson & Chapman, 2008; Südhof, 2004). Whether NSF plays a role in endocytosis and thus may contribute to exo-endocytosis coupling is not well understood. However, this possibility seems likely considering that SNARE proteins are involved in endocytosis. I hypothesized that NSF is involved in mediating endocytosis (Fig.1.2E). This hypothesis was tested, and the results indicate that NSF is involved in endocytosis at small conventional hippocampal synapses. This finding suggests a new endocytosis model in which newly disassembled SNARE proteins are involved in endocytosis by binding and recruiting endocytosis proteins to mediate endocytosis.

Chapter 2: Protein kinase C and calmodulin serve as calcium sensors for calcium-stimulated endocytosis at synapses

This chapter is derived from Jin, Y.H., Wu, X.S.*, Shi, B.*, Zhang, Z., Guo, X., Gan, L., Chen, Z., Wu, L.G. (2019) Protein Kinase C and Calmodulin Serve as Calcium Sensors for Calcium-Stimulated Endocytosis at Synapses. *J Neurosci.* 39(48):9478-9490. (*Jin, Y.H., Wu, XS and Shi, B. contributed equally to this work.)

*The transgenic mice were produced by Lin Gan. The pHluorin imaging data was produced by Yinghui Jin, Xinsheng Wu and me. I am responsible for EM data.

2.1 Introduction

Endocytosis mediates fundamental functions, such as vesicle re- cycling to sustain synaptic transmission, intracellular trafficking of proteins and lipids vital for every cell, and viral entry (Kononenko & Haucke, 2015; L.-G. Wu et al., 2014). Two sets of evidence at calyx of Held synapses suggest that calcium triggers slow endocytosis (10 s), rapid endocytosis (<~3 s), bulk endocytosis, and endocytosis overshoot (Hosoi et al., 2009; Wu et al., 2009; Yamashita et al., 2010) (for review, see L.G. Wu et al., 2014). First, lowering extracellular calcium or buffering calcium with BAPTA reduces the rate of rapid and slow endocytosis by ~50 to 1500 folds and abolishes endocytosis overshoot, whereas increasing calcium current charges increases endocytosis rate by hundreds of folds and promotes endocytosis overshoot. Second, calcium chelator EGTA inhibits bulk endocytosis and reduces the fission pore closure rate. Consistent with these results, calcium influx triggers rapid endocytosis at chromaffin cells (Artalejo et al., 1995; Chiang et al., 2014) and slow endocytosis at hippocampal synapses (Sun et al., 2010); calcium influx upregulates rapid, slow, bulk, and/or overshoot endocytosis at hippocampal synapses, retinal nerve terminals, hair cells, chromaffin cells and pituitary

neurons (Balaji et al., 2008; Clayton et al., 2009; Moser & Beutner, 2000; Neves et al., 2001; Sankaranarayanan & Ryan, 2001; Smith & Neher, 1997; Thomas et al., 1994).

Like calcium-induced exocytosis, the first step in the study of calcium-stimulated endocytosis is to identify calcium sensor. The candidate being considered for the last two decades is calcium/ calmodulin-activated CaN, which dephosphorylates endocytic proteins (Cousin & Robinson, 2001). Pharmacological block or knock-down of CaM and knockout of CaN led to slower endocytosis at synapses, raising the possibility that CaM and CaN serve as the calcium sensors for endocytosis (Cottrell et al., 2016; Sun et al., 2010; X.-S. Wu et al., 2014). However, whether CaM or CaN involvement in endocytosis depends on their calcium binding, the condition required for establishing CaM/CaN as the calcium sensor, has not been tested.

My lab researched on the calcium sensors by knockout calcium-activated protein kinase C (PKC) α or β isoform (PKC_{α} or PKC_{β}), and CaM isoform 2 (CaM_2) in mice. Our hypothesis was these knockouts inhibit endocytosis at mouse hippocampal boutons. We also tested whether the inhibition could be rescued by the wild-type (WT) or the calcium-binding-deficient proteins. I found out that PKC_{α}, PKC_{β} and CaM_2 serve as calcium at small conventional synapses. The results suggest that calcium triggers endocytosis via PKC-mediated phosphorylation and CaM-mediated dephosphorylation.

2.2 Materials and Methods

2.2.1 Animals.

Animal care and use were performed according to National Institutes of Health (NIH) guidelines and were approved by the NIH Animal Care and Use Committee.

$PKC\alpha^{+/-}$ mice were purchased from The Jackson Laboratory; $PKC\beta^{-/-}$ and $CaM_2^{-/-}$ mice were generated by us, as described in detail in the legends to Figures 2.1A and 2.3A. Knockout mice of either sex were obtained by heterozygous and homozygous breeding using standard mouse husbandry procedures. Mouse genotypes were determined by PCR. WT littermates and WT non-littermates of either sex were used as controls.

2.2.2 Hippocampal culture and imaging.

Mouse hippocampal culture was prepared as described previously (Sankaranarayanan & Ryan, 2000; Sun et al., 2010). Hippocampal CA1-CA3 regions from P0 mice were dissected, dissociated, and plated on Poly-D-lysine-treated coverslips. Cells were maintained at 37°C in a 5% CO_2 humidified incubator with a culture medium consisting of Neurobasal A (Invitrogen), 10% fetal bovine serum (Invitrogen), 2% B-27 (Invitrogen), 1% Glutamax-1 (Invitrogen). On 5–7 d after plating, neurons were transfected with plasmids using Lipofectamine LTX (Invitrogen).

Hippocampal cultures were transfected with a plasmid containing synaptophysin tagged with the pH-sensitive pHluorin2X (SypH, provided by Dr. Yong-Ling Zhu) (Zhu et al., 2009) for imaging of endocytosis. cDNA encoding human $PKC\alpha$ WT was amplified from pHACE-$PKC\alpha$ (Add- gene, 21232) and subcloned into PmCherry-N1 (Clontech) (mCherry used for recognition of transfection). Mutant $PKC\alpha^{D/A}$ was generated by replacing the five aspartates in the calcium binding C2 domain (Nalefski & Falke, 1996) with alanines through site-directed mutagenesis (QuikChange Lightning; Agilent Technologies). Similar to WT $PKC\alpha$, $PKC\beta^{D/A}$ was subcloned into PmCherry-N1.

The cDNA encoding CaM or CaM_{1234}, provided by the late Dr. David Yue, was subcloned into PmCherry-N1. For PKC or CaM rescue experiments (see Figs. 2.2, 2.4), we transfected PKC or CaM plasmid along with SypH. PKC or CaM plasmid contained mCherry, which was used for us to recognize transfected cells. After transfection, neurons were maintained at 37°C in a 5% CO_2-humidified incubator for another 8 –12 day before experiments.

Action potential was evoked by a 1 ms pulse (20 mA) through a platinum electrode. The bath solution contained the following (in mM): 119 NaCl, 2.5 KCl, 2 $CaCl_2$, 2 $MgCl_2$, 25 HEPES, 30 glucose, 0.01 6-cyano-7- nitroquinoxaline-2, 3-dione (CNQX), and 0.05 D,L-2-amino-5- phosphonovaleric acid (AP-5), pH 7.4 , adjusted with NaOH. In temperature experiments, we heated the culture chamber using a temperature controller (TC344B; Warner Instruments, Hamden, CT). Imaging was performed after the culture was at 34 –37°C for 15–30 min. The temperature was verified with another small thermometer (BAT-7001H; Physitemp Instruments) in the chamber. SypH images were acquired at 1 Hz using Nikon A1 confocal microscope (60X, 1.4 numerical aperture [NA]), and analyzed with Nikon software.

2.2.3 Western blot.

Neurons were washed three times with ice-cold PBS. Cell lysates were prepared in the modified RIPA buffer containing protease inhibitors (Thermo Scientific). Equal amounts of proteins, determined by BCA protein assay (Thermo Scientific), were loaded onto SDS-PAGE gel and immunoblotted using antibodies against PKC_{α} (1: 250; Sigma-Aldrich), PKC_{β} (1:250; u), CaM (1:200, Millinpore), clathrin heavy chain (1:1000; BD

Bioscience), dynamin (1:1000; BD Biosciences; recognizing all dynamin isoforms, including 1, 2, and 3) and β-actin (1:2000; Abcam).

2.2.4 Data collection and measurements of T and $Rate_{decay}$.

For SypH signal in hippocampal cultures, the $Rate_{decay}$ was measured from boutons' SypH fluorescence trace in the first 4 –10 s after stimulation.

2.2.5 Electron microscopy.

Hippocampal cultures were fixed with 4% glutaraldehyde (freshly prepared, Electron microscopy sciences, Hatfield, PA) in 0.1 M Na-cacodylate buffer solution containing for at least 1 h at 22–24°C and stored in 4°C refrigerator overnight. The next day, cultures were washed with 0.1 M cacodylate buffer, and treated with 1% OsO_4 in cacodylate buffer for1h on ice, and 0.25% uranyl acetate in acetate buffer at pH 5.0 overnight at 4°C, dehydrated with ethanol, and embedded in epoxy resin. Thin sections were counterstained with uranyl acetate and lead citrate then examined in a JEOL200CX TEM. Images were collected with a CCD digital camera system (XR-100; AMT) at a primary magnification of 10,000 –20,000X. Synapses were selected based on the structural specialization including synaptic vesicle clustering, synaptic cleft and the postsynaptic density.

2.2.6 Experimental design and statistical analyses.

Data are presented as means ± s.e.m. The statistical test used was t test with equal variance, although t test with unequal variance gave the same result.

For pHluorin imaging, each experiment included 20 –30 boutons showing fluorescence increase (region of interest: 2 µm X 2 µm). Approximately one to three experiments were taken from each culture. Each culture was from 3–5 mice. Each group of data was obtained from at least four batches of cultures (4–12 cultures).

For electron microscopy, synapses were selected based on the structural specialization, including synaptic vesicle clustering, synaptic cleft, and the postsynaptic density. Each group of data was taken from 100–132 synaptic profiles from 4–12 mice.

2.3 Results

2.3.1 PKC Knockout mouse generation.

We generated $PKC_{\alpha}^{-/-}$ mice by breeding $PKC_{\alpha}^{-/-}$ mice from The Jackson Laboratory and generated $PKC_{\beta}^{-/-}$ mice by ourselves (Fig. 1A). Targeted embryonic stem cells ($Prkcb^{tm1a(EUCOMM)Wtsi}$ line EPD0233_5_F09) obtained from The International Mouse Phenotyping Consortium were injected into C57BL/6J blastocysts to generate chimeras (Fig. 2.1A). Chimeric mice were then bred with C57BL/6J mice to generate PKC_{β} targeted germline mice ($PKC_{\beta}^{+/loxP}$). $PKC_{\beta}^{+/loxP}$ mice were bred with CMV-Cre mice (The Jackson Laboratory, 006054) to delete exon 4 of PKC_{β} 3 gene, which resulted in the generation of $PKC_{\beta}^{-/+}$ mice (Fig. 2.1A). $PKC_{\beta}^{-/+}$ mice were used to establish the $PKC_{\beta}^{-/-}$ mouse line (Fig. 2.1A). Western blot at $PKC_{\alpha}^{-/-}$ or $PKC_{\beta}^{-/-}$ hippocampal cultures showed that PKC_{α} or PKC_{β} were not expressed, whereas other endocytic proteins, including clathrin, dynamin and AP2 were not affected (Fig. 2.1B).

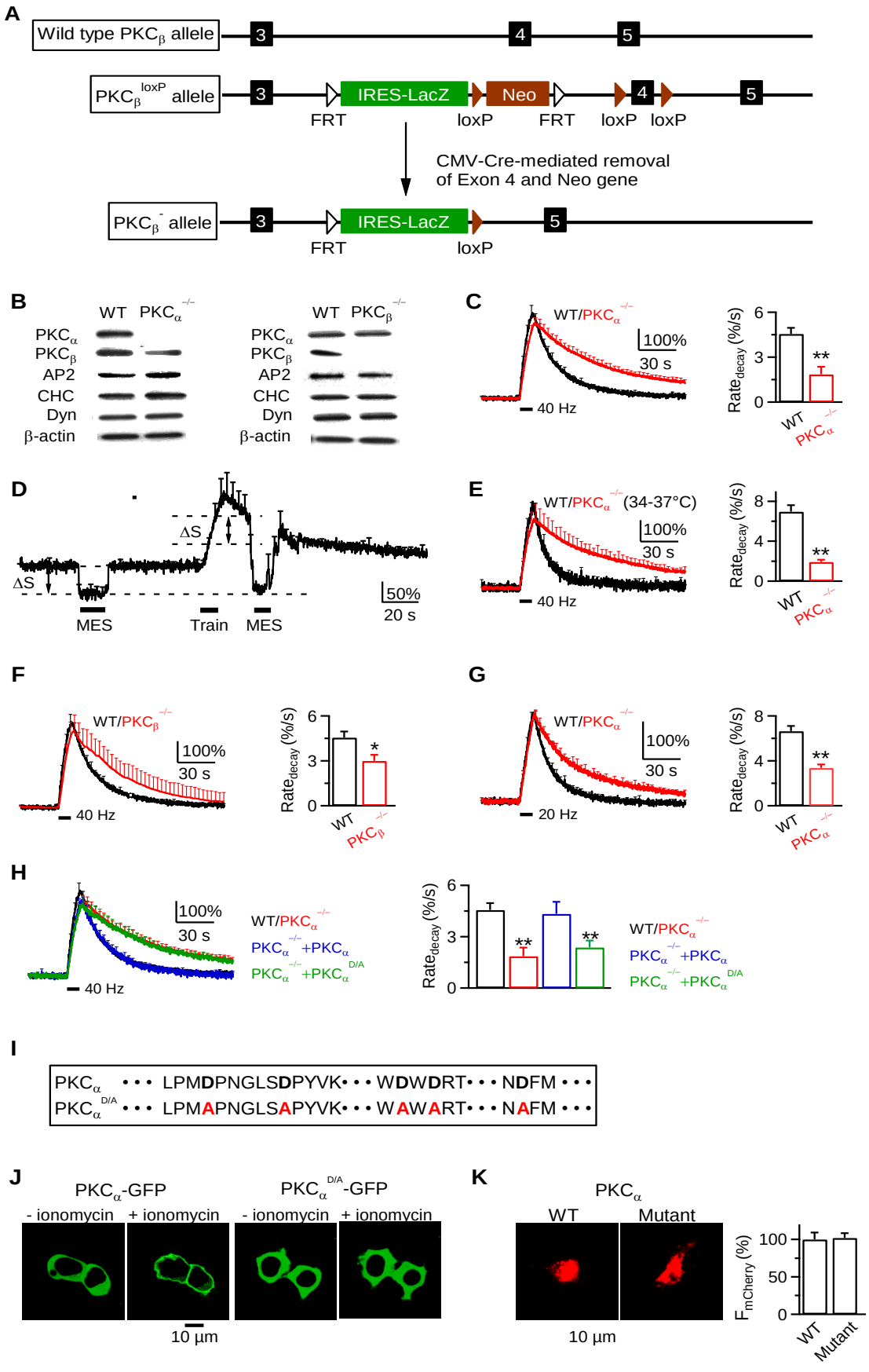
A
Wild type PKCβ allele
PKCβ loxP allele
PKCβ - allele
IRES-LacZ
Neo
FRT
loxP
CMV-Cre-mediated removal
of Exon 4 and Neo gene
B
WT
PKCα −/−
PKCβ −/−
PKCα
PKCβ
AP2
CHC
Dyn
β-actin
C
WT/PKCα −/−
100%
30 s
40 Hz
Rate decay (%/s)
D
ΔS
MES
Train
50%
20 s
E
WT/PKCα −/− (34-37°C)
F
WT/PKCβ −/−
G
20 Hz
H
WT/PKCα −/−
PKCα −/− +PKCα
PKCα −/− +PKCα D/A
I
PKCα • • • LPMDPNGLSDPYVK• • • WDWDRT• • • NDFM • • •
PKCα D/A • • • LPMAPNGLSAPYVK• • • WAWART• • • NAFM • • •
J
PKCα-GFP
PKCα D/A-GFP
- ionomycin
+ ionomycin
10 μm
K
PKCα
WT
Mutant
FmCherry (%)

Figure 2.1. PKC and its calcium-binding domain are required for endocytosis at hippocampal synapses. ***A***, Schematic illustration of the generation of $PKC_{\beta}^{-/-}$ mice. PKC_{β} gene has five exons, three of which (3, 4, and 5) are shown. Targeted embryonic stem (ES) cells ($Prkcb^{tm1a(EUCOMM)Wtsi}$ line EPD0233_5_F09) were obtained from The International Mouse Phenotyping Consortium and were injected into C57BL/6J blastocysts to generate chimeras. Chimeric mice were then bred with C57BL/6J to generate PKC_{β} targeted germline mice ($PKC_{\beta}^{+/loxP}$). $PKC_{\beta}^{+/loxP}$ mice were bred with CMV-Cre mice (The Jackson Laboratory, 006054) to delete exon 4, generating $PKC_{\beta}^{-/+}$ mice, which were used to establish the $PKC_{\beta}^{-/-}$ mouse line. Mouse genotypes were determined by PCR. ***B***, Western blot of PKC_{α}, PKC_{β}, adaptor protein 2 (AP2), clathrin heavy chain (CHC), dynamin, and β-actin in WT, $PKC_{\alpha}^{-/-}$ (***A***), and $PKC_{\beta}^{-/-}$- (B) hippocampal culture. Results in ***A*** and ***B*** were repeated by 2– 4 times. ***C***, F_{SypH} traces (normalized to baseline, left) and $Rate_{decay}$ (right) induced by Train40Hz (bar) in WT (n = 14 experiments) or $PKC_{\alpha}^{-/-}$ (n = 28 experiments) hippocampal culture at 22–24°C. Data plotted as mean + s.e.m.; *p < 0.05; **p < 0.01, t test (applies to all similar graphs). Throughout the study, each experiment contained 20 –30 boutons; 1–3 experiments were taken from 1 culture; each culture was from 3–5 mice; each group was from 4 –12 cultures. ***D***, Applying MES solution (pH:5.5, bars) quenched F_{SypH} (mean + s.e.m.) to a similar level (lowest dash line) before and after a 10 s train of stimuli in $PKC_{\alpha}^{-/-}$ boutons (n = 6 experiments, 22–24°C). ΔS, SypH at resting plasma membrane quenched by MES. E–G, Similar to C, but at 34 –37°C (***E***), in $PKC_{\beta}^{-/-}$ culture (***F***), or after a 10 s train at 20 Hz (***G***). ***E***, WT, n = 6 experiments; $PKC_{\alpha}^{-/-}$, n = 6. ***F***, WT, n = 14; $PKC_{\beta}^{-/-}$, n = 5. ***G***, WT, n = 16; $PKC_{\alpha}^{-/-}$, n = 22. ***H***, F_{SypH} traces and $Rate_{decay}$ induced by $Train_{40Hz}$ (bar) in WT boutons (n = 14), $PKC_{\alpha}^{-/-}$ boutons ($PKC_{\alpha}^{-/-}$-, n = 28), $PKC_{\alpha}^{-/-}$ boutons rescued with WT PKC_{α} (containing mCherry for recognition, $PKC_{\alpha}^{-/-}$+ PKC_{α}, n = 7), and in $PKC_{\alpha}^{-/-}$ boutons rescued with $PKC_{\alpha}^{D/A}$ and mCherry ($PKC_{\alpha}^{-/-}$+ $PKC_{\alpha}^{D/A}$, n = 8). ***I***, Protein sequence of PKC_{α} and $PKC_{\alpha}^{D/A}$ C2 domain. The Ca 2+-coordinating aspartates of PKC_{α} (bold) were mutated to alanines (red) in $PKC_{\alpha}^{D/A}$. ***J***, we expressed PKC_{α}-GFP (left two panels) or $PKC_{\alpha}^{D/A}$ -GFP (right two panels) in HEK293T cells and monitored the subcellular distribution of the kinase. The Ca^{2+} ionophore, ionomycin (10 μM, 15 min), induced translocation of PKC_{α}-GFP toward the plasma membrane, but did not alter the intracellular distribution of $PKC_{\alpha}^{D/A}$ -GFP. Such results were observed in 3 experiments (each experiment had 2–3 cells). ***K***, Left, $PKC_{\alpha}^{-/-}$ neurons rescued with WT PKC_{α} (containing mCherry for recognition, $PKC_{\alpha}^{-/-}$+ PKC_{α}), or with PKC_{α} D/A and mCherry ($PKC_{\alpha}^{-/-}$+ $PKC_{\alpha}^{D/A}$). Right, Fluorescence intensity of mCherry ($F_{mCherry}$) in $PKC_{\alpha}^{-/-}$+ PKC_{α} neurons (n = 10) and $PKC_{\alpha}^{-/-}$+ $PKC_{\alpha}^{D/A}$ neurons (n = 13). $F_{mCherry}$ was measured from both soma and branches. *, p < 0.05; **, p < 0.01 (t test). The transgenic mice were produced by Lin Gan. The data was produced by Yinghui Jin, Xinsheng Wu and me.

2.3.2 PKC calcium-binding domain is needed for endocytosis at hippocampal synapses.

In cultures transfected with pH- sensitive synaptophysin-pHluorin2X (SypH), a 10 s train of stimuli (1 ms/20 mA) at 40 Hz ($Train_{40Hz}$), which generated an action potential train, induced a SypH fluorescence (F_{SypH}) increase (ΔF) and then decrease (Fig. 1C), reflecting exocytosis and endocytosis, respectively. In WT at 22–24°C (applies if not mentioned otherwise), F_{SypH} decayed mono-exponentially with a τ of 20.0 ± 1.4 s, reflecting slow endocytosis; the initial decay rate ($Rate_{decay}$) was 4.6 ± 0.4%/s (n = 14

experiments, 7 cultures, each culture from 3–5 mice; Fig. 2.1C). In $PKC_{\alpha}^{-/-}$ cultures, F_{SypH} decay was slower with a $Rate_{decay}$ ~41% of WT (Fig. 2.1C).

Is the slower F_{SypH} decay due to slower reacidification or endocytosis? In $PKC_{\alpha}^{-/-}$ cultures, MES solution with a pH of 5.5 applied before Train10s quenched F_{SypH} to the background level and decreased F_{SypH} by ΔS (Fig. 2.1D), which reflected the preexisting SypH molecules at the plasma membrane. Washing out MES solution led to recovery of F_{SypH} to baseline (Fig. 2.1D). We then applied a 10 s train of stimuli and applied MES solution at 10 s after the stimulation train, at which F_{SypH} remained well above the baseline. F_{SypH} was quenched to a level similar to that in MES solution before the stimulation train (lower dotted line; Fig. 2.1D), but much lower than that predicted, if F_{SypH} decay is due to reacidification (upper dotted line; Fig. 2.1D, n = 6). Quenched F_{SypH} recovered above baseline after MES washout, confirming the prolonged presence of SypH at the plasma membrane (Fig. 2.1D). Thus, slower F_{SypH} decay in $PKC_{\alpha}^{-/-}$ cultures primarily reflected slower endocytosis.

Prolonged F_{SypH} decay and reduced $Rate_{decay}$ were also observed at 34 –37°C (Fig. 2.1E, $PKC_{\alpha}^{-/-}$ culture), at $PKC_{\beta}^{-/-}$ culture (Fig. 2.1F), and after a 10 s action potential train at 20 Hz (Fig. 2.1G, $PKC_{\alpha}^{-/-}$ culture). $Rate_{decay}$ in $PKC_{\alpha}^{-/-}$ culture was rescued to the WT level by transfection of WT PKC_{α}, but not a mutant PKC_{α} (Fig. 2.1H), in which 5 aspartates in its calcium binding C2 domain were mutated to alanines ($PKC_{\alpha}^{D/A}$; Fig. 2.1I) (Nalefski & Falke, 1996).

$PKC_{\alpha}^{D/A}$ neither binds calcium nor is translocated to the plasma membrane by calcium as WT PKC (Newton, 2010) (D. Fiorovante and W. Regehr, personal communication. see also Fig. 2.1J). The fluorescence of mCherry was similar in $PKC_{\alpha}^{-/-}$

neurons overexpressed with PKC_{α} and mCherry or with $PKC_{\alpha}^{D/A}$ and mCherry (Fig. 2.1K, t test, p = 0.84), consistent with similar expression level of PKCα and $PKC_{\alpha}^{D/A}$. Together, these results suggest that PKC calcium binding domain is needed for endocytosis. PKC may thus serve as an endocytosis calcium sensor.

2.3.3 EM suggests PKC involvement in endocytosis of regular vesicles and bulk endosomes.

We performed EM to examine ultrastructural changes in $PKC_{\alpha}^{-/-}$ hippocampal cultures. Horseradish peroxidase (HRP, 5 mg/ml, bath) was added for assay of vesicular uptake. At rest, HRP-positive [HRP(+)] vesicles were minimal; most vesicles were HRP-negative [HRP(-)] (Fig. 2.2A, B); the number of HRP(+) and HRP(-) vesicles and their sum in boutons were similar in WT and $PKC_{\alpha}^{-/-}$ cultures (data not shown). To ex- amine endocytosis, we applied 90 mM KCl with HRP for 1.5 min, and fixed samples at 0, 3 and 10 min after KCl/HRP application. In WT boutons, compared with the resting condition, HRP(+) vesicles increased from time 0 to 10 min after KCl, reflecting vesicle endocytosis (Fig. 2.2A, B) as previously shown (Wu et al., 2016; Y. Wu et al., 2014). Compared with WT boutons, HRP(+) vesicles were significantly reduced at each time point after KCl in $PKC_{\alpha}^{-/-}$ boutons (Fig. 2.2A, B), suggesting inhibition of endocytosis.

In WT boutons, we observed HRP(+) bulk endosomes (Fig. 2.2A), defined as vesicles with a diameter 80 nm or with a cross section area more than that of a 80 nm vesicle (~0.005 μm^2). Bulk endosome area increased at time 0, then decreased at 3 and 10 min (Fig. 2.2A, C), suggesting generation of bulk endosomes and subsequent conversion to vesicles as previously shown (Wu et al., 2016; Y. Wu et al., 2014). Similar trends were

observed in PKC$_\alpha^{-/-}$, but at a lower level, which was significant at 10 min time point (Fig. 2.2C), suggesting inhibition of bulk endocytosis. These EM data confirmed the involvement of PKC in endocytosis. Results shown in Figure 5, A–C, were obtained at room temperature (22–24°C). Results similar to Figure 2.2A–C, were also observed at physiological temperature (37°C; Fig. 2.2D, E), at which bulk endocytosis was more severely inhibited, suggesting more involvement of PKC in bulk endocytosis in physiological temperature.

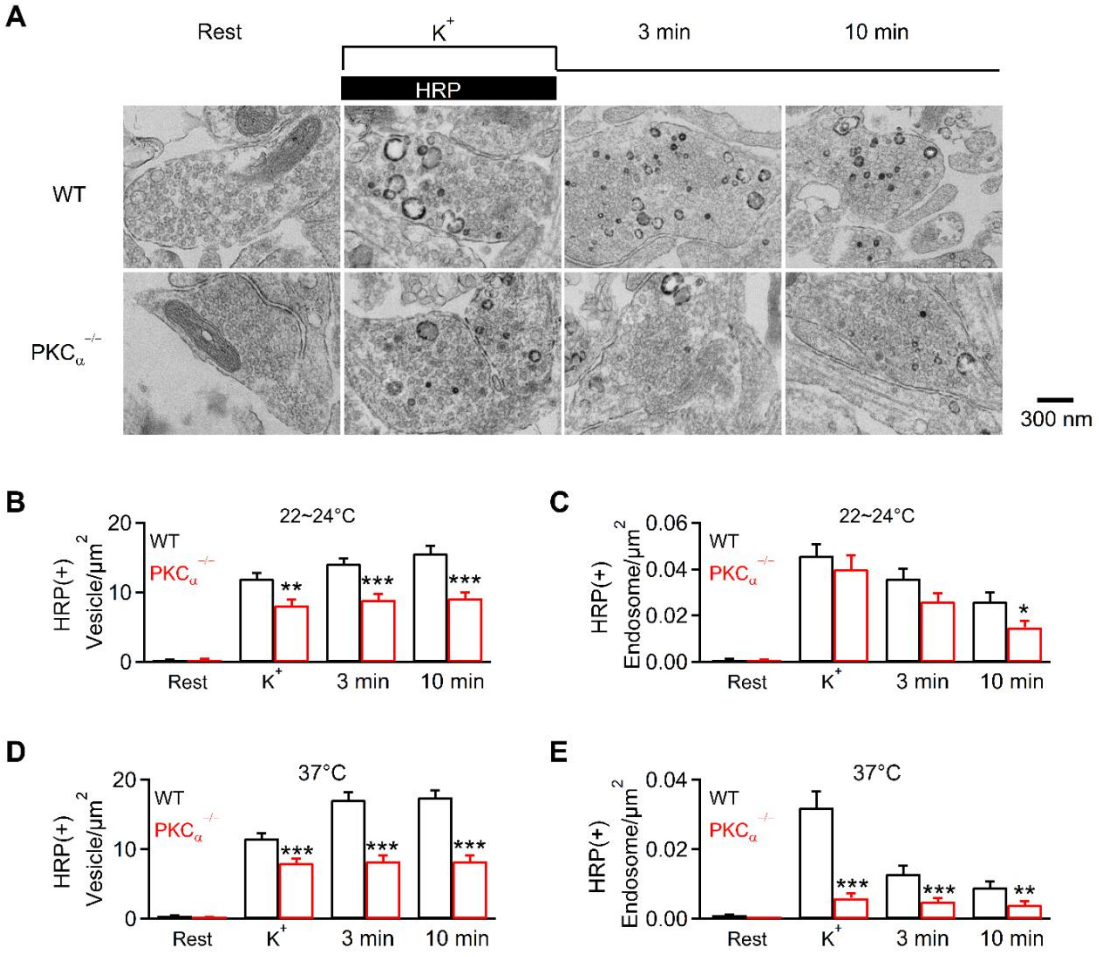

Figure 2.2. PKC$_\alpha$ knockout affects endocytosis examined with EM at hippocampal synapses. ***A***, EM images of WT and PKC$_\alpha^{-/-}$ hippocampal boutons at rest (Rest) and at 0 min (K+), 3 min and 10 min after

1.5 min 90 mM KCl application. For Rest, HRP was included for 1.5 min; for KCl application, HRP was included only during KCl application (see labels). ***B***, ***C***, Number of HRP(+) vesicles (***B***) and the bulk endosome area (***C***) per square micrometer of synaptic cross-section are plotted versus the time before (Rest) and at 0 min (K+), 3 min, and 10 min after the end of KCl application in WT and $PKC_{\alpha}^{-/-}$ hippocampal cultures (mean + s.e.m., each group was from 100 –132 synaptic profiles from 4 –12 mice). The temperature before fixation was 22–24°C. ***D***, ***E***, Similar to ***B*** and ***C***, respectively, except that the temperature was 37°C before fixation. *, $p < 0.05$; **, $p < 0.01$; ***, $p < 0.001$ (t test).

While we examined bulk endocytosis with EM at a time scale of minutes, this does not mean that bulk endocytosis is completely independent of rapid and slow endocytosis measured at live synapses. Bulk endocytosis detected with capacitance measurements can be rapid or slow, within ~1–20 s after stimuli, and contributed to mediating rapid and slow endocytosis (Wu & Wu, 2007). Bulk endocytosis detected with EM after rapid freezing can be ultrafast, within hundreds of milliseconds after an action potential like stimulation in physiological temperature (Watanabe, Rost, et al., 2013). Thus, rapid and slow endocytosis may be due to formation of bulk endosome-like structures as well as regular-size vesicles.

2.3.4 CaM_2 Knockout mouse generation

Here we verified this suggestion by gene knockout, and more importantly, determined whether calcium binding with CaM is needed, the basic criteria for being a calcium sensor. Among 3 CaM genes (*CaM1*, *CaM2*, and *CaM3*) encoding the same CaM, we generated CaM_2^{loxP} mice by CRISPR technique as illustrated in Figure 2.3A. sgRNAs were designed by using CRISPR Design (https://zlab.bio/ guide-design-resources) to identify unique target sites through- out the mouse genome (Fig. 2.3A). sgRNAs were transcribed in vitro using the MEGAshortscript T7 Transcription Kit from synthetic double-strand DNAs and purified using MEGAclear kit (Fig. 2.3A). A mixture

of Cas9 mRNA, sgRNAs and ssDNA templates was injected into the cytoplasm of one cell-stage fertilized embryos harvested from C57BL/6J mice (Fig. 2.3A). Viable two- cell stage embryos were transferred into the oviducts of female surrogates to generate founder mice (Fig. 2.3A). Founders with loxP inserts were identified by PCR and sequencing, and were subsequently bred with C57BL/6J mice to generate heterozygous mice (Fig. 2.3A). CaM_2^{loxP} mouse was crossed with CMV-Cre mouse to generate $CaM_2^{-/-}$ mouse.

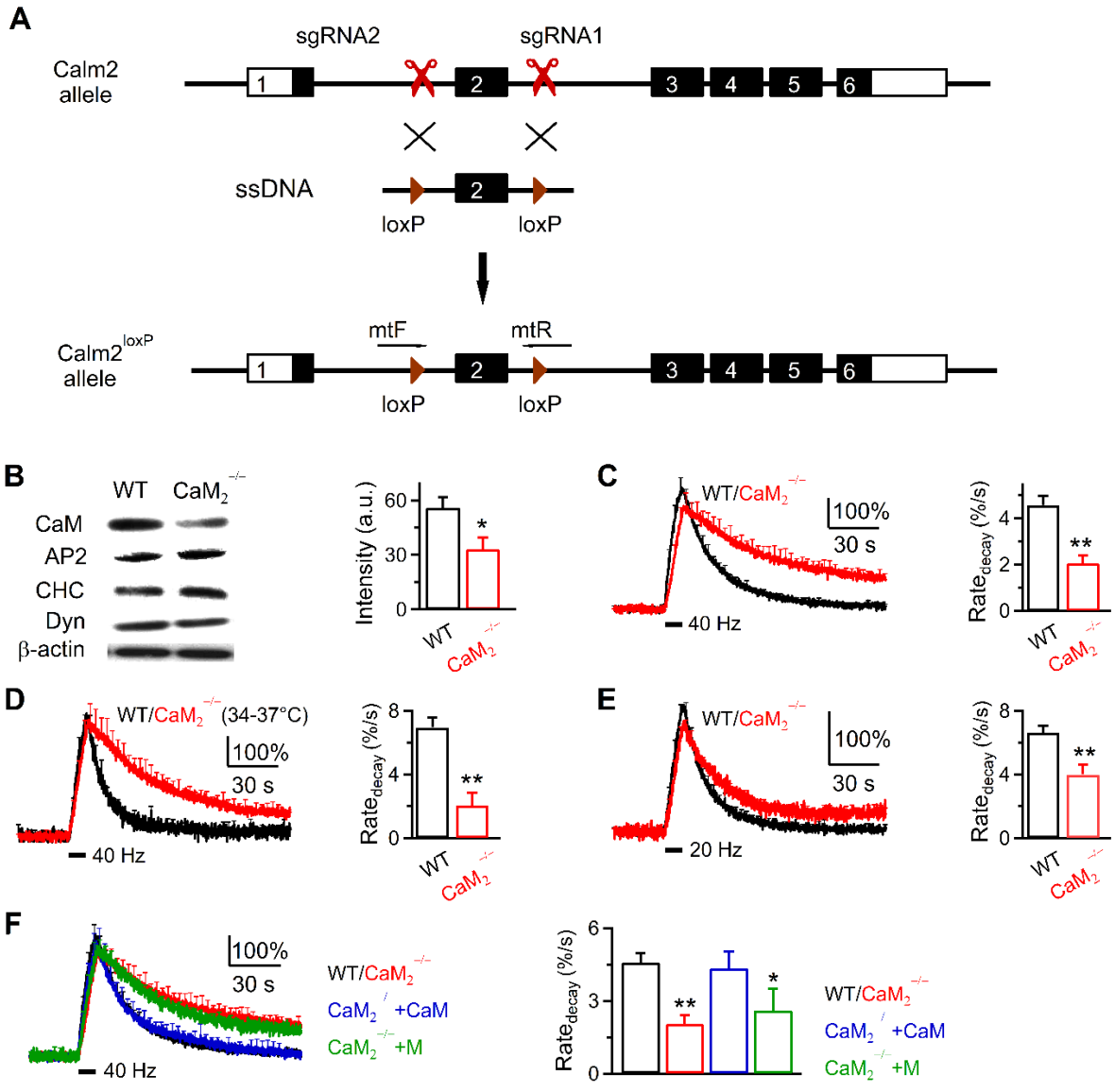

Figure 2.3. CaM and its calcium-binding domain are required for endocytosis at hippocampal synapses. ***A***, Generation of $Calm2^{loxP}$ mice (Calm2: Calmodulin 2 gene). sgRNAsweredesignedbyusing CRISPRDesign(https://zlab.bio/guide-design-resources) to identify uniquetarget sites throughoutthemousegenome. sgRNAsweretranscribed in vitro using the MEGAshortscript T7 Transcription Kit (Life Technologies) from synthetic double-strand DNAs purchased from IDT (Integrated DNA Technologies) and purified using MEGAclear kit (Life Technologies). A mixture of Cas9 mRNA (TriLink Biotechnologies, 100 ng/µl), sgRNAs (50 ng/µl), and ssDNA templates (100 ng/µl, synthesized by IDT) was injected into the cytoplasm of one cell-stage fertilized embryos harvested from C57BL/6J mice (The Jackson Laboratory, 000664). Viable two-cell stage embryos were transferred into the oviducts of female surrogates to generate founder mice. Founders with loxP inserts were identified by PCR and sequencing, and were subsequently bred with C57BL/6J mice to generate heterozygous mice. The primers used to identify the 5' and 3' loxP insertions were Calm2 mtF: 5'-CCATGAACCTTGAACCTGTAGGATCCA-3' and Calm2 mtR: 5'-ATGCTACATTCAACTTGTCACCATTCGAATTCA-3'. ***B***, Western blot of CaM, AP2, clathrin heavy chain (CHC), dynamin (Dyn), and β-actin in WT and $CaM_2^{-/-}$ brain. B, CaM Western blot intensity (CaM Int, a.u.) from WT or $CaM_2^{-/-}$ culture. ***C***, F_{SypH} traces (normalized to baseline) and $Rate_{decay}$ induced by $Train_{40Hz}$ (bar) in WT (n = 14 experiments) or $CaM_2^{-/-}$ (n = 8) hippocampal culture at 22–24°C (mean + s.e.m.). D, Similar to C, but at 34 –37°C (WT, n = 6; $CaM_2^{-/-}$, n = 4). ***E***, Similar to ***C***, but after a 10 s train at 20 Hz (WT, n = 16; $CaM_2^{-/-}$, n = 7). ***F***, F_{SypH} traces and $Rate_{decay}$ induced by $Train_{40Hz}$ in WT hippocampal boutons (n = 14 experiments, with SypH transfection), $CaM_2^{-/-}$ boutons (n = 8, with SypH transfection), $CaM_2^{-/-}$ boutons transfected with a plasmid containing CaM and mCherry (mCherry for recognition, SypH was cotransfected, n = 4, $CaM_2^{-/-}$+CaM), and $CaM_2^{-/-}$ boutons transfected with a plasmid containing CaM_{1234} and mCherry (n = 4, $CaM_2^{-/-}$+M). Temperature was 22–24°C. *, $p < 0.05$; **, $p < 0.01$ (t test). The transgenic mice were produced by Lin Gan. The data was produced by Yinghui Jin, Xinsheng Wu and me.

In $CaM_2^{-/-}$ hippocampal synapses, Western blot showed significant reduction of CaM, but not other major endocytic proteins (Fig. 2.3B).

2.3.5 Calmodulin calcium binding domain is needed for endocytosis at hippocampal synapses.

$Rate_{decay}$ was significantly reduced after a 40 or 20 Hz train, particularly the 40 Hz train at either 22–24°C or 34–37°C (Fig. 2.3C–E). Consistently, the time course of F_{SypH} decay at $CaM_2^{-/-}$ synapses was slower (Fig. 2.3C–E). The slower F_{SypH} decay was not due to slower reacidification, as revealed with acid-quenching of surface SypH (data not shown). Thus, CaM_2 knockout inhibits endocytosis, consistent with previous knockdown experiments (Sun et al., 2010). The $Rate_{decay}$ was rescued to the WT level by transfecting $CaM_2^{-/-}$ culture with SypH and WT CaM cDNA, but not with SypH and CaM_{1234} mutant

cDNA (Fig. 2.3F) where mutation in four calcium binding sites prevents calcium binding with CaM_{1234} (Xia et al., 1998). Thus, the calcium binding domain of CaM is needed to rescue endocytosis, suggesting that CaM serves as a calcium sensor.

2.3.6 EM suggests CaM involvement in endocytosis of regular vesicles and bulk endosome.

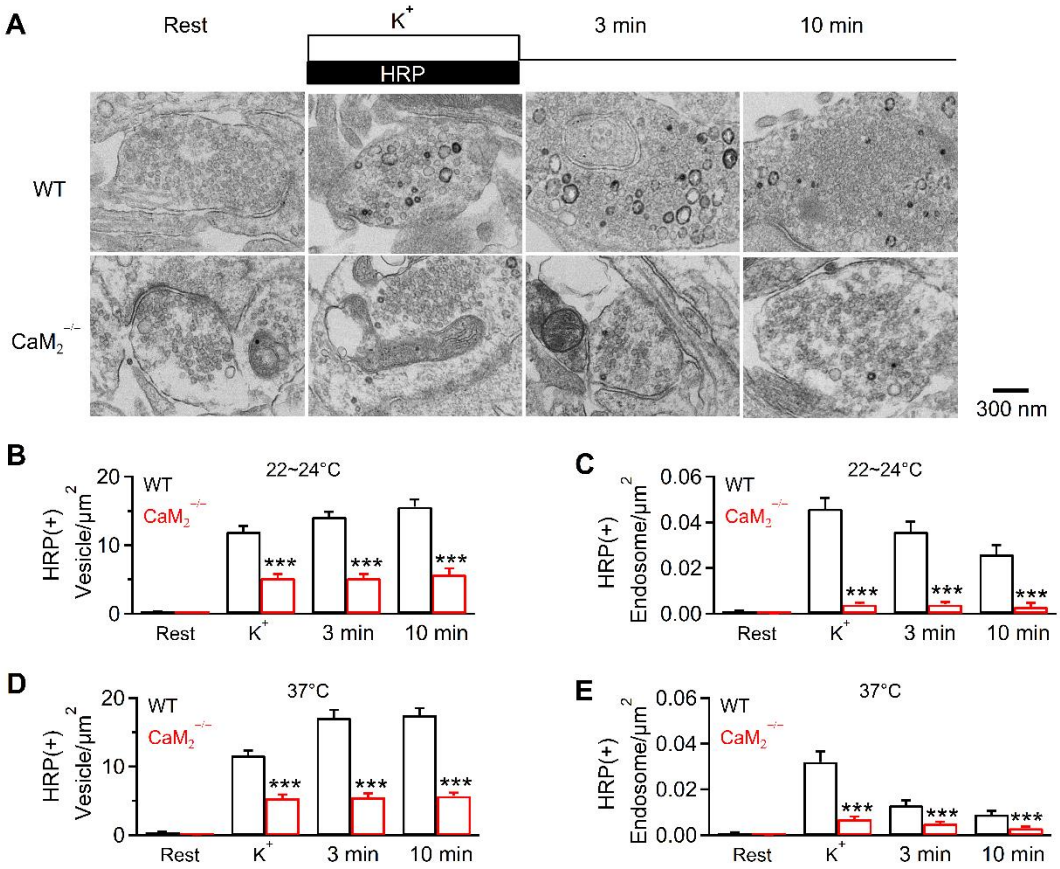

Figure 2.4. CaM_2 knockout affects endocytosis examined with EM at hippocampal synapses. ***A***, EM images of WT and $CaM_2^{-/-}$ hippocampal boutons at rest (Rest) and at 0 min (K^+), 3 min and 10 min after 1.5 min application of KCl and HRP (same arrangements as in Fig. 2.2A). ***B***, ***I***, The number of HRP(+) vesicles (***B***) and the bulk endosome area (***C***) per square micrometer of synaptic cross-section are plotted versus the time before (Rest) and at 0 min (K^+), 3 min, and 10 min after KCl/HRP application in WT and $CaM_2^{-/-}$ hippocampal cultures (22–24°C). Data are expressed as mean + s.e.m.; each group was from 100 – 132 synaptic profiles from 4 –12 mice. ***D***, ***E***, Similar to ***B*** and ***C***, respectively, except that the temperature was 37°C. ***, $p < 0.001$ (t test).

We examined $CaM_2^{-/-}$ hippocampal cultures with the same EM approach used for PKC knockout. HRP(+) vesicles were minimal at rest, but increased at 0–10 min after KCl application in WT, which reflected vesicle endocytosis (Fig. 2.4A, B). The in- crease of the HRP(+) vesicle number was substantially inhibited in $CaM_2^{-/-}$ boutons (Fig. 2.4A, B), confirming inhibition of endocytosis in $CaM_2^{-/-}$ boutons. HRP(+) bulk endosome was significantly reduced to near 0 at each time point (0 –10 min) after KCl application in $CaM_2^{-/-}$ boutons (Fig. 2.4C), suggesting involvement of CaM in bulk endocytosis. While results in Figure 7, G–I, were observed at room temperature, similar results were observed at physiological temperature (37°C; Fig. 2.4D, E), suggesting calmodulin involvement in endocytosis at both room and physiological temperature.

2.4 Discussion

We showed that PKC_α and PKC_β knockout (Fig. 2.1) inhibited slow endocytosis measured with SypH imaging after action potential trains at 20–40 Hz at cultured hippocampal synapses at 22–37°C. This inhibitory effect (by PKC_α knockout) was rescued by overexpressing WT PKC_α, but not $PKC_\alpha^{D/A}$ that could not bind calcium (Fig. 2.1). We generated $CaM_2^{-/-}$ mice and found that CaM_2 knockout inhibited slow and rapid endocytosis at calyces (Fig. 2.3), and inhibited slow endocytosis at hippocampal synapses, which could be rescued by overexpressing WT CaM, but not CaM_{1234} that could not bind calcium (Fig. 2.3). EM showed that PKC_α and CaM_2 knockout reduced HRP(+) vesicles and HRP(+) bulk endosomes generated via bulk endocytosis (Figs. 2.2, 2.4). Together, these results suggest that calcium binding with the calcium sensor PKC_α,

PKC_{β} and CaM mediate calcium- dependent trigger and speed up of slow, rapid and bulk endocytosis at synapses.

Early studies showed that PKC phosphorylates dynamin 1 and prevents dynamin 1 interaction with membrane phospholipids in vitro (Powell et al., 2000; Robinson et al., 1993). However, a subsequent study from the same lab shows that cyclin-dependent kinase 5, but not PKC phosphorylates dynamin 1 in vivo (Tan et al., 2003). The role of PKC in endocytosis has since not been considered. The present work suggests that calcium binding with PKC mediates calcium-stimulated slow and rapid endocytosis. PKC might stimulate endocytosis via phosphorylating serine/ threonine of its substrates (Cousin & Robinson, 2001).

Studies with pharmacology and knock-down suggest CaM involvement in endocytosis (Sun et al., 2010; Wu et al., 2009; Yamashita et al., 2010; Yao & Sakaba, 2012). By knocking out *Calm2* gene, we provided the first genetic evidence suggesting CaM involvement in bulk endocytosis (Figs. 2.4). Furthermore, by performing rescue experiments, we provided the missing evidence showing that CaM serves as a calcium sensor for endocytosis (Fig. 2.3). Potential downstream targets of CaM may include CaN and/or myosin light chain kinase (MLCK) for three reasons. First, both CaN and MLCK are activated by CaM; second, CaN dephosphorylates many endocytic proteins, and CaN knockout inhibits endocytosis at calyceal, hippocampal and cerebellar synapses; and third, MLCK, which is involved in controlling the readily releasable pool size (Srinivasan et al., 2008), facilitates endocytosis via actomyosin interaction, and actin is essential for synaptic vesicle endocytosis (Cousin & Robinson, 2001; Delvendahl et al., 2016; Li et

al., 2016; Soykan et al., 2017; Sun et al., 2010; X.-S. Wu et al., 2014; Wu et al., 2016; Yue & Xu, 2014).

We do not know why endocytosis involves two calcium sensors, PKC and CaM. Given that PKC mediates phosphorylation, and CaM may activate CaN or MLCK to mediate dephosphorylation or phosphorylation (Cousin & Robinson, 2001; Yue & Xu, 2014), we suggest that calcium triggers and facilitates endocytosis by phosphorylation and dephosphorylation of the endocytosis machinery. Since endocytosis may be composed of multiple steps, such as formation of a membrane pit, formation of a narrow pore, hemi-fission, and fission (Kononenko & Haucke, 2015; Mettlen et al., 2018; Shin et al., 2018; Zhao et al., 2016), it might be possible that PKC and CaM are involved in these different transitions.

Knockout or knock-down of synaptotagmin 1 led to slowdown of endocytosis, raising the possibility that synaptotagmin 1 may be another calcium sensor for endocytosis (Nicholson-Tomishima & Ryan, 2004; Poskanzer et al., 2006; J. Yao et al., 2012; L. H. Yao et al., 2012). However, a recent study shows that slower endocytosis in synaptotagmin 1 knockout synapses is due to asynchronous vesicle fusion caused by synaptotagmin 1 knockout (Li et al., 2017). Endocytosis after asynchronous fusion is slower than that after synchronous fusion, suggesting that synaptotagmin 1 is not an endocytosis calcium sensor (Li et al., 2017). While the evidence for transient calcium influx in stimulating endocytosis is overwhelming in a variety of stimulation conditions (see introduction), it has been suggested that prolonged calcium dialysis or calcium after a single action potential may not facilitate endocytosis, but inhibit endocytosis (Leitz & Kavalali, 2011; Li et al., 2017; Von Gersdorff & Matthews, 1994; Wu & Wu, 2014).

Caution is therefore needed when considering our findings in these conditions. It should be noted that a 1 ms APe induces rapid endocytosis with a τ of ~2 s, whereas $depol_{20ms}$ induces slow endocytosis with a τ of ~15–20 s at calyces (Wu et al., 2005). Similar results were observed at goldfish bipolar synapses and cerebellar mossy fiber boutons (Delvendahl et al., 2016; Von Gersdorff & Matthews, 1994). These observations may be explained by the prolonged global calcium increase caused by increased depolarization, which has been shown to inhibit endocytosis (Von Gersdorff & Matthews, 1994; Wu & Wu, 2014). Saturation of the endocytosis capacity, as previously proposed (Sankaranarayanan & Ryan, 2000; Sun et al., 2002; Wu et al., 2005) might also contribute to this observation.

Calcium triggers many forms of endocytosis, including rapid, slow, bulk, and overshoot endocytosis in nerve terminals (L.G. Wu et al., 2014), endocrine cells (Artalejo et al., 1995; Chiang et al., 2014; L.G. Wu et al., 2014) and dendrites (Kennedy & Ehlers, 2006). Our finding that calcium binding with the calcium sensors PKC and CaM mediates calcium-stimulated endocytosis may apply to these calcium-dependent forms of endocytosis in neurons and endocrine cells. It might also apply to the calcium-triggered fusion pore (Chiang et al., 2014; Shin et al., 2018) and fission pore closure (Wu et al., 2009) that control exo- and endocytosis efficiency, and to calcium- and endocytosis-dependent RRP replenishment that sustains synaptic transmission.

Chapter 3: Dynamin 1 controls vesicle size and endocytosis at hippocampal synapses

This chapter is derived from Shi, B., Jin, Y.H.*, Wu, L.G. (2022) Dynamin 1 controls vesicle size and endocytosis at hippocampal synapses. *Cell Calcium*, 103:102564. (*Shi, B. and Jin, Y.H. contributed equally to this work.)

*I am responsible for the project, and Yinghui Jin contributed some of the data.

3.1 Introduction

Calcium influx triggers vesicle fusion to release transmitters and hormones, which mediate synaptic transmission and control animal behaviors(L.-G. Wu et al., 2014). After vesicle fusion, exocytosed vesicles must be retrieved via endocytosis, which recycles exocytosed vesicles and thus maintains synaptic transmission (Gan & Watanabe, 2018; Kononenko & Haucke, 2015; Saheki & De Camilli, 2012; L.-G. Wu et al., 2014; Wu & Wu, 2014). Endocytosis must transform flat plasma membrane into oval/round vesicles (Heuser & Reese, 1973; Shin et al., 2021). Over the last several decades many proteins and lipids have been identified to be involved in this curvature transition processes. The most ubiquitous protein being identified in various forms of endocytosis is dynamin, a GTPase that catalyzes membrane fission, the last step of endocytosis that converts membrane pits into vesicles (Antonny et al., 2016). Despite these significant progresses, our understanding of the mechanisms that control the endocytic vesicle size remains poorly understood. For two reasons, vesicle size is important for nerve terminals to maintain calcium-triggered exocytosis that mediates synaptic transmission crucial for any neuronal circuits. First, if the vesicle is too big, a nerve terminal would contain much less vesicles that can be exhausted much more rapidly during high frequency firing, resulting in failure of synaptic transmission. Second, accumulated studies suggest that in addition

to vesicular transmitter concentration (Wu et al., 2007), vesicle size may determine the quantal size, a basic parameter that can determine and regulate synaptic strength (Zhang et al., 1998). More generally speaking, vesicle size is important in determining what endocytosis can take up, including large viruses or toxins, or small membrane-associated proteins and lipids, and in deciding the efficiency and strategy of endocytosis for a given cell – small but frequent versus large but infrequent vesicle making.

Deletion of AP180 increases the vesicle size by about ~20% and the quantal size by ~60%, suggesting that AP180 is involved in controlling vesicle size (Zhang et al., 1998). The involvement of AP180 in controlling vesicle seems to imply the involvement of clathrin in controlling vesicle size. However, perturbation of clathrin did not reach a consensus. For example, acute photoinactivation of clathrin light chain or clathrin heavy chain blocks vesicle generation, causes accumulation of large internal membrane compartments, and increases vesicle sizes at drosophila neuromuscular junctions (Heerssen et al., 2008; Kasprowicz et al., 2008). In contrast, mutation of clathrin heavy chain in *C. elegans*, which impairs receptor-mediated endocytosis, reduces synaptic vesicle size by ~14% (Sato et al., 2009). Knockdown of clathrin did not significantly affect ultrafast endocytosis or slow endocytosis at mouse hippocampal synapses (Kononenko, 2014; Watanabe et al., 2014) but see (Granseth et al., 2006), where electron microscopy was performed, but did not report vesicle size changes (Kononenko, 2014; Watanabe et al., 2014). In summary, our understanding of the endocytic molecules involved in controlling vesicle size is poor.

In the present work, we report that knockout of dynamin 1, the main dynamin isoform in the brain, increased the vesicle diameter by as much as ~40% at hippocampal

nerve terminals. This is a surprising finding, because dynamin has been well known for several decades as a GTPase responsible for the last step of endocytosis, fission, which forms a vesicle by cutting the neck of a membrane pit. Our finding suggests that dynamin 1 has an additional crucial function in endocytosis – controlling vesicle size at central synapses. Furthermore, we found that dynamin 1 plays a more critical role than previously recognized at central synapses, because dynamin 1 knockout at hippocampal synapses generated a much larger block of endocytosis measured after low and high frequency action potential trains than previously reported at cortical synapses (Ferguson et al., 2007; Raimondi et al., 2011).

3.2 Materials and Methods

3.2.1 Animals.

Animal care and use were carried out according to NIH guidelines and were approved by the NIH Animal Care and Use Committee. Dynamin $1^{+/-}$ ($Dnm1^{+/-}$) mice were purchased from the Jackson Laboratory. $Dnm1^{-/-}$ mice of either sex were obtained by heterozygous breeding using standard mouse husbandry procedures. Mouse genotypes were determined by PCR, and verified in some experiments with western blot. Wild-type littermates and wild-type non-littermates of either sex were used as control.

3.2.2 Hippocampal culture and imaging.

Mouse hippocampal culture was prepared as described previously (Sankaranarayanan and Ryan, 2000; Sun et al., 2010). Hippocampal CA1-CA3 regions from P0 mice were dissected, dissociated, and plated on Poly-D-lysine treated coverslips.

Cells were maintained at 37°C in a 5% CO_2 humidified incubator with a culture medium consisting of Neurobasal A (Invitrogen, Carlsbad, CA), 10% fetal bovine serum (Invitrogen, Carlsbad, CA), 2% B-27 (Invitrogen, Carlsbad, CA), 0.25% glutamax-1 (Invitrogen, Carlsbad, CA), and 0.25% insulin (Sigma, St. Louis, MO). On 5-7 days after plating, neurons were transfected with plasmids using Lipofectamine LTX (Invitrogen, Carlsbad, CA).

Hippocampal cultures were transfected with a plasmid containing SypH, provided by Dr. Yong-Ling Zhu (Zhu et al., 2009) for the imaging of endocytosis. cDNA encoding human Dnm1 wild-type was amplified from Dnm1-pmCherryN1 (Addgene #27697). Dnm1 plasmid was transfected along with SypH, and it contained mCherry, which was used for us to recognize the transfected cells. After transfection, neurons were maintained at 37°C in a 5% CO_2 humidified incubator for another 6-8 days before experiments.

Action potential was evoked by a 1 ms pulse (20 mA) through a platinum electrode. The bath solution contained (in mM): 119 NaCl, 2.5 KCl, 2 $CaCl_2$, 2 $MgCl_2$, 25 HEPES (buffered to pH 7.4), 30 glucose, 0.01 6-cyano-7-nitroquinoxaline-2, 3-dione (CNQX), and 0.05 D,L-2-amino-5-phosphonovaleric acid (AP-5). The culture chamber for imaging was heated using a temperature controller (TC344B, Warner Instruments, Hamden, CT), which set the temperature during imaging at 34-37ºC. Imaging was performed after the culture was at 34-37ºC for 15-30 min. The temperature was verified with another small thermometer (BAT-7001H, Physitemp Instruments, Clifton, NJ) in the chamber. SypH images were acquired at 10 Hz using Nikon A1 confocal microscope (60X, 1.4 NA), and analyzed with Nikon software.

3.2.3 Western blot.

For Western blot, neurons were washed three times with ice-cold PBS. Cell lysates were prepared in the modified RIPA buffer containing protease inhibitors (Thermo Scientific, Rockford, IL). Equal amounts of proteins, determined by BCA protein assay (Thermo Scientific, Rockford, IL), were loaded onto SDS-PAGE gel and immunoblotted using antibodies against clathrin heavy chain (1:1,000; BD Bioscience, San Jose, CA), dynamin (1:1,000; BD Bioscience, San Jose, CA, recognizing all dynamin isoforms, including 1, 2 and 3), dynamin 1 (1:1,000; Thermofisher, Waltham, MA) and β-actin (1:2,000; Abcam, Cambridge, United Kingdom).

3.2.4 Electron microscopy.

Hippocampal cultures were fixed with 4% glutaraldehyde (freshly prepared, Electron microscopy sciences, Hatfield, PA) in 0.1 N Na-cacodylate buffer solution containing for at least one hour at 22-24^{o}C, and stored in 4°C refrigerator overnight. The next day, cultures were washed with 0.1 N cacodylate buffer, and treated with 1% OsO_4 in cacodylate buffer for 1 hr on ice, and 0.25% uranyl acetate in acetate buffer at pH 5.0 overnight at 4°C, dehydrated with ethanol, and embedded in epoxy resin. Thin sections were counterstained with uranyl acetate and lead citrate then examined in a JEOL 200 CX TEM. Images were collected with a CCD digital camera system (XR-100 from AMT, Danvers, MA) at a primary magnification of 10,000-20,000X. Synapses were selected based on the structural specialization including synaptic vesicle clustering, synaptic cleft and the postsynaptic density.

3.2.5 Data collection and measurements of the decay time constant and $Rate_{decay}$.

The time constant (τ) of fluorescence decay was measured from exponential fit of the decay. For SypH signal in hippocampal cultures, the $Rate_{decay}$ was measured from boutons' SypH fluorescence trace in the first 4–10 s after stimulation.

3.2.6 Experimental Design and Statistical Analyses.

Means were presented as ± s.e.m. The statistical test was t-test. We used t test with equal variance, although t-test with unequal variance gave the same result. For pHluorin imaging, each experiment included 20-30 boutons showing fluorescence increase (region of interest: 2 μm X 2 μm). ~1-3 experiments were taken from 1 culture. Each culture was from 3-6 mice. Each group of data was obtained from at least four batches of cultures (4-7 cultures).

3.3 Results

3.3.1 Dynamin 1 knockout severely inhibits endocytosis after 5-40 Hz action potential trains.

Dynamin 1 knockout slows down endocytosis significantly only during high frequency firing, but not after high or low frequency firings at conventional small boutons of cortical synapses (Ferguson et al., 2007; Raimondi et al., 2011). To determine whether this observation applies beyond cortical synapses, we examined endocytosis at hippocampal synapses lacking dynamin 1. To detect endocytosis, we transfected the hippocampal cultures with pH sensitive synaptophysin-pHluorin2X (SypH). Application of a 10 s train of stimuli (1 ms/20 mA) at 20 Hz ($Train_{20Hz}$), which generated an action

potential train (Sankaranarayanan and Ryan, 2001; Sun et al., 2010), and it induced a F_{SypH} increase (ΔF) and then decline, which reflect exocytosis and sequent endocytosis (Fig. 3.1A, B) (Kavalali & Jorgensen, 2014).

In wild-type (WT) control culture at 22–24°C, the initial F_{SypH} decay rate ($Rate_{decay}$) was 5.5 ± 0.5%/s, which was calculated after normalizing the ΔF to 100%. ΔF/F was 316 ± 52% over the baseline fluorescence intensity F (n = 11 experiments, 1-3 experiments per culture, 6 cultures, each culture from 3–6 mice; Fig. 3.1C). In dynamin $1^{-/-}$ ($Dmn1^{-/-}$) cultures, dynamin 1 was knocked out, as verified with western blot (data not shown) (Ferguson et al., 2007); F_{SypH} decay was much slower as compared to control (Fig. 3.1A, B), the $Rate_{decay}$ was significantly reduced to ~41% of the WT level (Fig. 3.1C), and ΔF/F was also reduced substantially (Fig. 3.1A, C). While these results were obtained at room temperature, similar results were obtained at physiological temperature (34-37ºC) after action potential trains at 20 Hz (WT, 6 experiments; $Dmn1^{-/-}$, 4 experiments) or 40 Hz (WT, 5 experiments; $Dmn1^{-/-}$, 4 experiments; Fig. 3.2H-J). The slower F_{SypH} decay time course, smaller $Rate_{decay}$, and smaller ΔF were rescued to the control level by transfecting WT dynamin 1 (Dnm1) to $Dmn1^{-/-}$ cultures (Fig. 3.1A-C).

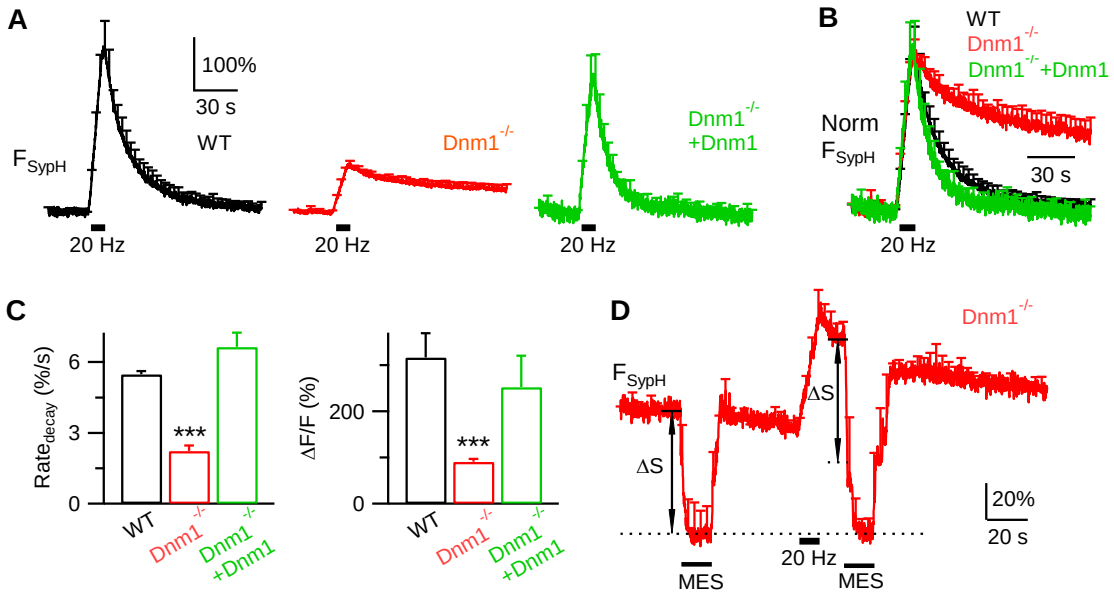

Figure 3.1. Dynamin 1 knockout severely inhibits endocytosis after repetitive firing at 20 Hz at hippocampal synapses. ***A-C***, F_{SypH} traces (A, B), $Rate_{decay}$ (C, left) and ΔF/F (C, right) induced by $Train_{20Hz}$ (10 s train of action potentials at 20 Hz) in wild-type (WT) cultures (n = 10 experiments), $Dnm1^{-/-}$ cultures (n = 6 experiments), or $Dnm1^{-/-}$ hippocampal cultures overexpressed with WT dynamin 1 ($Dnm1^{-/-}$ + Dnm1; containing mCherry for recognition, n = 5). F_{SypH} traces in panel B are the same as those in panel A, but with the peak F_{SypH} rescaled (Norm F_{SypH}) to the same amplitude for better comparison of time courses. Temperature and data analysis (applies to Figs. 1-4, if not specifically mentioned): 22–24°C; data expressed as mean+s.e.m. ***, $p < 0.001$ (t test, compared to WT). ***D***, Applying MES solution (pH: 5.5) quenched F_{SypH} (mean + s.e.m.) to a similar level (lowest dash line) before and after a 10 s train of stimuli in $Dnm1^{-/-}$ cultures (n = 5 experiments, 22–24°C). *ΔS*: SypH at resting plasma membrane quenched by MES (see main text for more description).

To exclude the possibility that the slower F_{SypH} decay in $Dnm1^{-/-}$ culture is not due to slower reacidification, we applied the MES solution with a pH of 5.5 before and after the $Train_{20Hz}$. Before $Train_{20Hz}$, the MES solution quenched F_{SypH} to the background level, resulting in a decrease of F_{SypH} by ΔS (Fig. 3.1D), which reflected the preexisting SypH molecules at the plasma membrane surface. Washing out MES solution led to recovery of F_{SypH} to baseline (Fig. 3.1D). We then applied $Train_{20Hz}$ to induce exo-endocytosis (Fig. 3.1D). At 10 s after $Train_{20Hz}$, at which F_{SypH} remained well above the baseline, we applied the MES solution again, which quenched F_{SypH} to a level similar to that during

MES application before $Train_{20Hz}$ (lower dotted line; Fig. 3.1D), but much lower than that predicted (F_{SypH} decrease by ΔS) if F_{SypH} decay is due to reacidification (upper dotted line; Fig. 3.1D, n = 5). F_{SypH} recovered above baseline after MES washout, confirming the prolonged presence of SypH at the plasma membrane (Fig. 3.1D). Thus, slower F_{SypH} decay in $Dmn1^{-/-}$ cultures primarily reflected slower endocytosis.

The slower F_{SypH} decay was accompanied by a reduction of ΔF, suggesting that exocytosis is reduced. Reduction of ΔF is not the reason for the slower F_{SypH} decay, because smaller ΔF induced by a 2 s train of stimulation at 20 Hz or by a lower frequency stimulation train does not prolong F_{SypH} decay (Sun et al., 2010; Wu et al., 2016) (see also Fig. 3.2, 5-Hz train). Inhibition of endocytosis may account for the reduction of ΔF, because endocytosis may facilitate vesicle replenishment to the readily releasable pool during repetitive stimulation by facilitation of the active zone clearance after exocytosis (Hosoi et al., 2009; L.-G. Wu et al., 2014; Wu et al., 2009). Consistent with this explanation, inhibition of proteins involved in endocytosis, such as dynamin, CaN, CaM, actin and potassium channel Kv3.3, has all been shown to slow down endocytosis and reduce exocytosis during repetitive stimulation (Jin et al., 2019; Sun et al., 2010; Wu et al., 2009; Wu et al., 2021; Wu et al., 2016).

Next, we determined whether the slower F_{SypH} decay in $Dmn1^{-/-}$ cultures depended on the frequency of stimulation. We found that F_{SypH} decay was slower with a smaller $Rate_{decay}$ after a 10 s action potential train at 40 Hz (Fig. 3.2A-C) or at 5 Hz (Fig. 3.2D-F) in $Dmn1^{-/-}$ cultures. $Rate_{decay}$ was 65 ± 12% (n = 8) of WT control after the 5-Hz train, but 41 ± 2% (n = 6) and 33 ± 8% (n = 6) of WT control after the 20-Hz and 40-Hz train, respectively (Fig. 3.2G). The $Rate_{decay}$ reduction after the 5-Hz train was not as

significant as those after 20-Hz or 40-Hz train (Fig. 3.2G). Thus, dynamin 1 is important in mediating endocytosis after both low and high frequency firing, but more crucial after higher frequency firing.

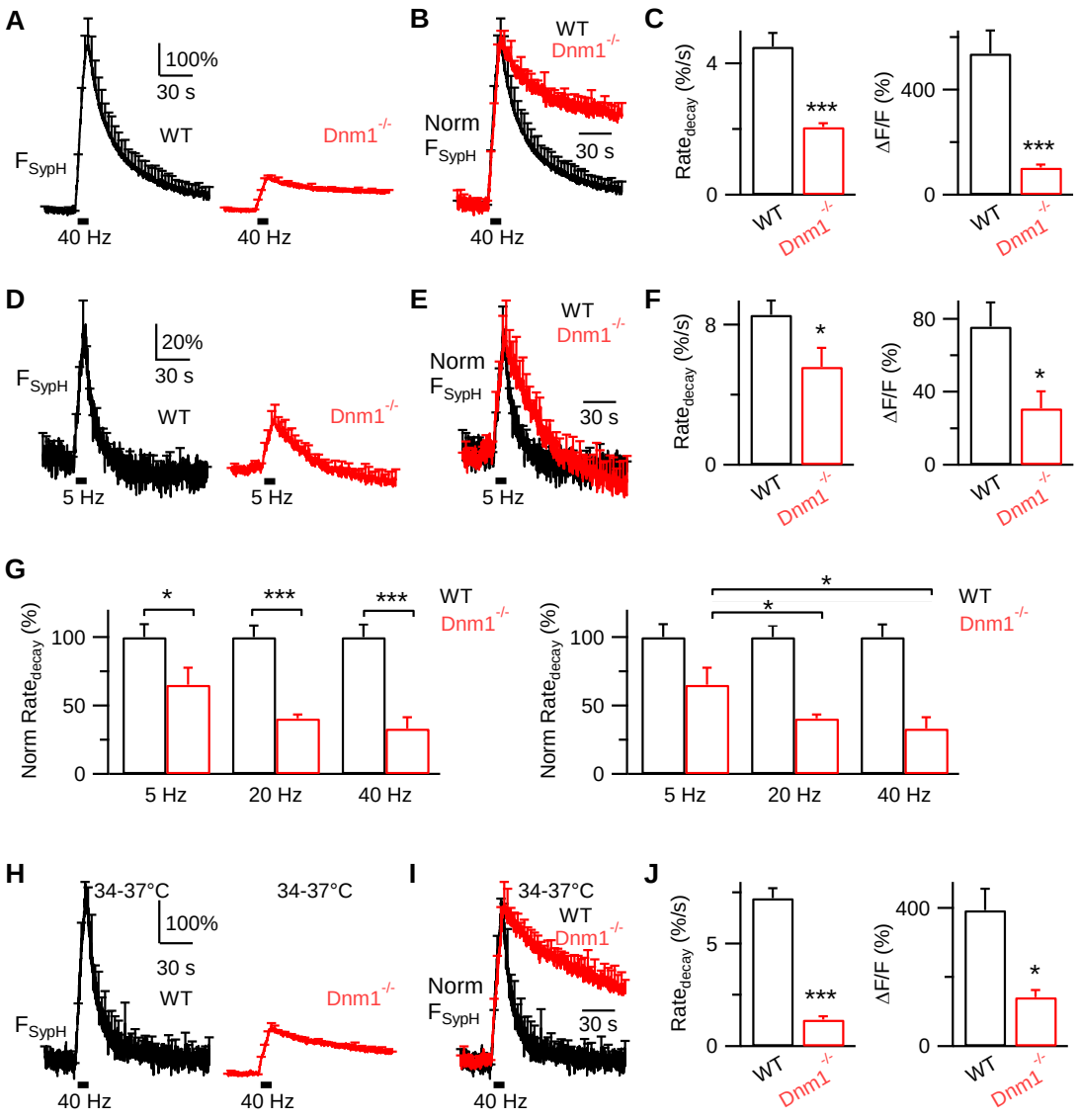

Figure 3.2. Dynamin 1 knockout inhibits endocytosis after repetitive firing at 5 or 40 Hz at hippocampal synapses. ***A-C***, F_{SypH} traces (A, B), $Rate_{decay}$ (C, left) and ΔF/F (C, right) induced by a 10-s train of action potentials at 40 Hz) in wild-type (WT) cultures (n = 14 experiments) or $Dnm1^{-/-}$ cultures (n = 6 experiments). F_{SypH} traces in panel B are the same as those in panel A, but with the peak F_{SypH} rescaled to the same amplitude for better comparison of time courses. ***D-F***, Similar arrangement as ***A-C*** respectively, except that the stimulation was a 10-s train of action potentials at 5 Hz (WT, 9 experiments; $Dnm1^{-/-}$, 8

experiments). ***G***, $Rate_{decay}$ after 5, 20, and 40 Hz action potential train in the WT and $Dnm1^{-/-}$ culture. For each frequency of stimulation, $Rate_{decay}$ was normalized to the mean of the corresponding WT $Rate_{decay}$. This plot aims for comparing the degree of reduction of $Rate_{decay}$ at different frequencies. 5 Hz: WT, n = 9; $Dnm1^{-/-}$, n = 8 (original data from Fig. ***3.2D-F***). 20 Hz: WT, n = 10, $Dnm1^{-/-}$, n = 6 (original data from Fig. ***3.1A-C***). 40 Hz: WT, n = 14, $Dnm1^{-/-}$, n = 5 (original data from Fig. ***3.2A-C***). ***H-J***, Similar arrangement as ***A-C*** respectively, except that the experiments at physiological temperature (WT, 5 experiments; $Dnm1^{-/-}$, 4 experiments), ***, $p < 0.001$; *, $p < 0.05$ (t test, compared to WT).

3.3.2 Dynamin 1 knockout enlarges the size of synaptic vesicles.

In WT hippocampal cultures, the vesicle diameter, examined with electron microscopy (EM), ranged from 17 to 249 nm with a mean of 38.6 ± 0.2 nm (n = 2170 vesicles, 22 boutons, 4 cultures, Fig. 3A-C). Among these vesicles, 98.9% (2146 out of 2170 vesicles) had a diameter < 80 nm; their mean diameter was 37.6 ± 0.1 nm (n = 2146 vesicles, Fig. 3.3D), which reflects the mean diameter of synaptic vesicles. The remaining 1.1% had a diameter > 80 nm, which is previously defined as endosome-like structures (Wu et al., 2016; Y. Wu et al., 2014). These WT control results were similar to previous reports (Wu et al., 2016; Y. Wu et al., 2014).

In $Dnm1^{-/-}$ culture, the vesicle diameter ranged from 22 to 315 nm with a mean of 63.2 ± 0.5 nm (n = 2628 vesicles, 49 boutons, 5 cultures), which was on average ~64% larger than that (38.6 ± 0.2 nm) in WT control (Fig. 3.3A-C). 80% of vesicles (2101 out of 2628) in $Dnm1^{-/-}$ culture had a diameter < 80 nm; their mean diameter was 52.5 ± 0.3 nm (n = 2101 vesicles), which was on average ~40% larger than the corresponding control (37.6 ± 0.1 nm, n = 2146 vesicles, Fig. 3.3D). The percentage of vesicles with a diameter > 80 nm was 20%, which was much larger than the corresponding WT control (1.1%). In summary, the mean diameter of all vesicles and synaptic vesicles (diameter < 80 nm) in $Dnm1^{-/-}$ culture were on average ~40-64% larger than the

corresponding WT control, suggesting that dynamin 1 is crucial in controlling synaptic vesicle size.

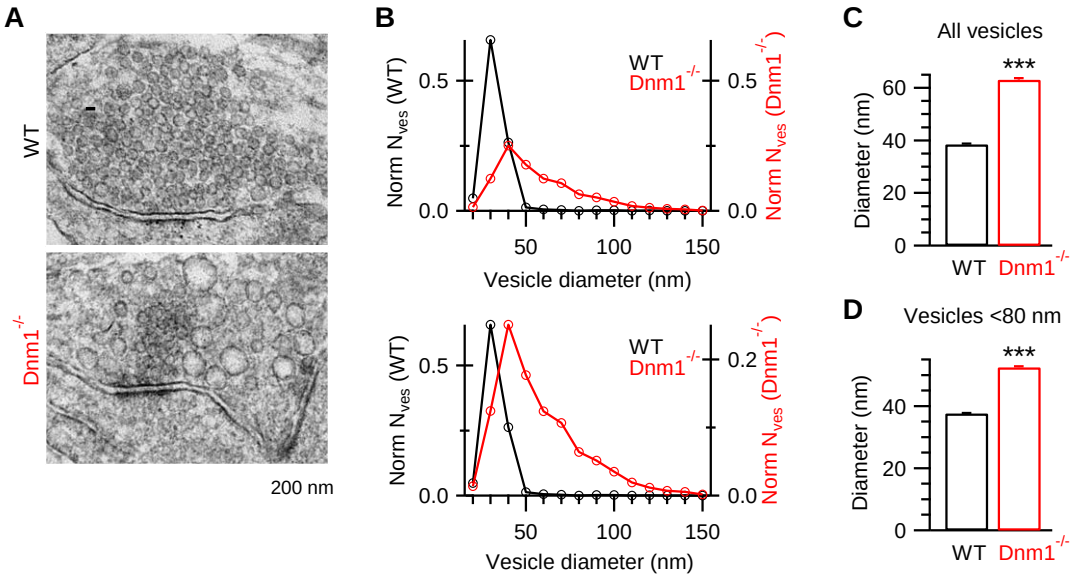

Figure 3.3. Dynamin 1 knockout significantly increases the vesicle size at hippocampal synapses. ***A***, Electron microscopic image of synaptic boutons from wild-type (WT) or Dnm1$^{-/-}$ hippocampal culture. ***B, Upper:*** Vesicle diameter distribution: The normalized number of vesicles (Norm N_{ves}) plotted versus the vesicle diameter in WT (left axis) or Dnm1$^{-/-}$ (right axis) hippocampal cultures. Vesicles with a diameter difference within 10 nm is binned together. The total vesicle number is normalized as 1 for each group of data. WT: 2170 vesicles, 22 boutons, 4 cultures, each culture from 6 mice; Dnm1$^{-/-}$: 2628 vesicles, 49 boutons, 5 cultures, each culture from 3-5 mice. ***Lower:*** Same as in left panel, but with the WT and Dnm1$^{-/-}$ data plotted at different scales such that the peak N_{ves} (norm) for WT and Dnm1$^{-/-}$ cultures is at the same vertical level, which shows a clear right shift of the distribution for Dnm1$^{-/-}$ cultures. ***C***, Mean (± s.e.m.) vesicle diameter from WT (2170 vesicles) and Dnm1$^{-/-}$ (2628 vesicles) culture. Vesicles with a diameter between 17-315 nm are all included. ***D***, Mean (± s.e.m.) vesicle diameter for vesicles with a diameter less than 80 nm from WT (2101 vesicles) and Dnm1$^{-/-}$ (2146 vesicles) culture. ***, $p < 0.001$ (t test, compared to WT).

To determine whether the increase in vesicle size in Dnm1$^{-/-}$ nerve terminals is due to formation of large pits, we examined membrane pits in boutons before, and 0, 3, and 10 min after 90 mM KCl application for 1.5 min. Membrane pits, which may appear as Λ-shape (or dome shape), inverse U-shape or Ω-shape (Fig. 3.4A); they were defined as having a height >15 nm, a base of 20-120 nm, and a height/base ratio >0.15

(Fig. 3.4A). The pit number per bouton (cross section) reached the peak at 3-10 min after KCl application (Fig. 3.4B), likely because endocytosis continued for > 10 min after KCl (Y. Wu et al., 2014). In Dnm1$^{-/-}$ boutons, the pit number after KCl was significantly higher than control boutons at every time point measured (Fig. 3.4B), likely because the block of fission dynamin 1 knockout caused pit accumulation. The pit height (from base membrane) was also significantly higher in Dnm1$^{-/-}$ boutons than in control boutons at any time point before or after KCl application (Fig. 3.4C). These results suggest that that in Dnm1$^{-/-}$ boutons larger pits are generated after depolarization-induced exocytosis (Fig. 3.4), which eventually form larger vesicles observed in resting conditions (Fig. 3.3). Dynamin 1 is thus a crucial molecule controlling the vesicle size at hippocampal synapses.

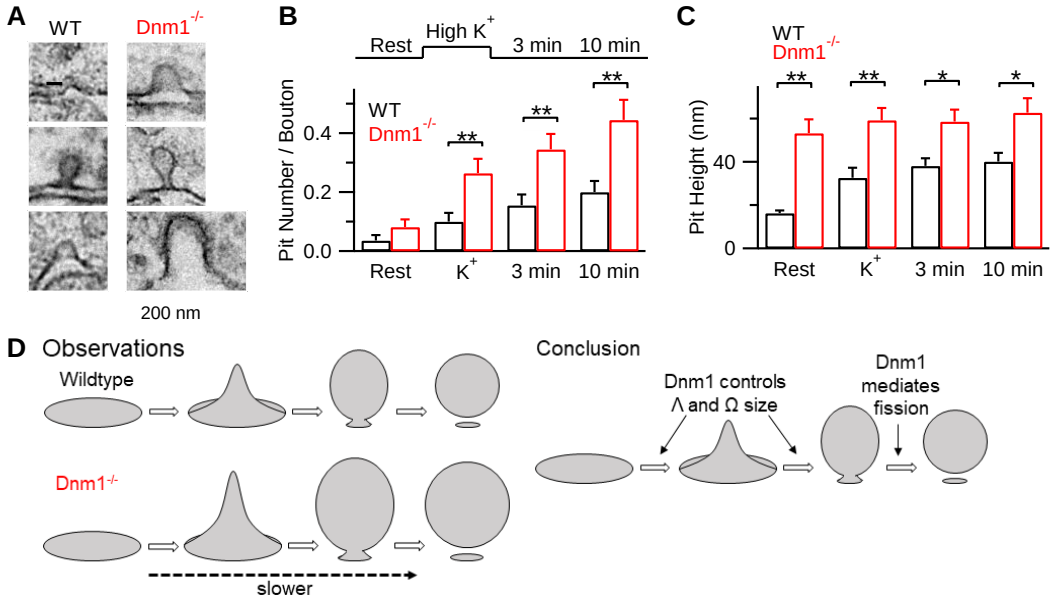

Figure 3.4. Dynamin 1 knockout significantly increases the membrane pit size at hippocampal synapses. ***A***, Sampled EM images of membrane pits from WT (upper) and Dnm1$^{-/-}$ (lower) boutons. ***B***, The number of pits per bouton cross section before (R) and at 0, 3, and 10 min after KCl application (90 mM, 1.5 min) in WT boutons (110 boutons, 3 cultures) and in Dnm1$^{-/-}$ boutons (110 boutons, 3 cultures) boutons. Each

culture was from 3-5 mice. ***C***, The pit height before (R) and at 0, 3, and 10 min after KCl application (90 mM, 1.5 min) in WT boutons (110 boutons, 3 cultures) and in Dnm1$^{-/-}$ boutons (110 boutons, 3 cultures) boutons, *, $p < 0.05$; **, $p < 0.01$ (t test, compared to WT). ***D***, A model for the Dnm1 function during endocytosis based on the results.

3.4 Discussion

We found that dynamin 1 knockout significantly slowed down endocytosis after action potential trains at 5-40 Hz with more slowdown observed at higher frequency at cultured hippocampal synapses (Figs. 3.1, 3.2). More importantly, dynamin 1 knockout increased the diameter of synaptic vesicles (less than 80 nm vesicles) by as much as ~40% (Fig. 3.3). Such an increase was accompanied by an increase of the size of membrane pits, the precursor for forming larger vesicles (Fig. 3.4). These results suggest that dynamin 1 is crucial for not only membrane fission as generally thought, but also controlling synaptic vesicle sizes at hippocampal synapses. Furthermore, we found that dynamin 1 plays a more crucial role than being recognized previously at small conventional boutons.

Our observation that synaptic vesicle diameter was enlarged by as large as ~40% in Dnm1$^{-/-}$ hippocampal synapses is a surprising finding. Previous studies reported only ~8-10% increase in vesicle diameter in Dnm1$^{-/-}$ cortical synapses and calyx-type synapses (Ferguson et al., 2007; Lou et al., 2008). Even with dynamin 1 and 3 knockout, the vesicle diameter was increased by only ~14% (Raimondi et al., 2011). While these results may suggest that dynamin regulates vesicle size, the small degrees of increase have led to a general neglection of this potentially important function of dynamin over the years. The large degree of increase (~40%) at Dnm1$^{-/-}$ hippocampal synapses reported here re-established dynamin as an important regulator of vesicle size. This function must take

place before fission, because we found that membrane pits generated after depolarization were much larger in Dnm1$^{-/-}$ synapses than in WT (Fig. 3.4). Our finding is consistent with studies suggesting that dynamin facilitates clathrin-coated pit maturation before fission (for review, see (Mettlen et al., 2018)). We thus suggest modifying dynamin models by including a new function beyond fission – control of the endocytic membrane pit size and thus the resulting endocytic vesicle size.

One may ask why dynamin 1 knockout did not increase the vesicle size at cortical synapses and calyx-type synapses as large as at hippocampal synapses reported here. Although we do not know the answer, one possibility could be dynamin 1 does not play at these synapses as important endocytic roles as at hippocampal synapses. Consistent with this possibility, dynamin 1 knockout at conventional small-boutons cortical synapses inhibited endocytosis severely only during, but not after high frequency firing (Ferguson et al., 2007; Raimondi et al., 2011). These studies had led to a view that dynamin 1 is essential only when exocytosis is intense during high frequency firing that requires a large endocytic capacity to retrieve intensely exocytosed vesicles. Otherwise, other dynamin isoforms may have overlapped roles with dynamin 1 and may exert their roles in the absence of dynamin 1. The present work showed that knockout of dynamin 1 alone is sufficient to inhibit endocytosis after low and high frequency firing (Figs. 3.1, 3.2), suggesting that dynamin 1's role in endocytosis after repetitive firings at low and high frequency at hippocampal synapses is much larger than that at cortical synapses. Consistent with this suggestion, dynamin 1 knockout at the large calyx-type synapse also inhibits endocytosis after prolonged depolarizing pulses (Lou et al., 2008). In summary, the present work reveals a much more important role than previously recognized for

dynamin 1 in mediating endocytosis and especially in controlling vesicle size at a step before fission at hippocampal small-bouton synapses.

Chapter 4: Clathrin is essential for endocytosis of synaptic vesicle proteins at mammalian central synapses

*The transgenic mice were produced by Lin Gan. The pHluorin imaging data was produced by Zhen Zhang, Sunghoon Lee, Xinsheng Wu and me. I am responsible for EM data.

4.1 Introduction

Synaptic vesicle endocytosis retrieves fused vesicles from the plasma membrane to sustain synaptic transmission, the fundamental building block for the function of the neural circuits (Saheki & De Camilli, 2012). The discovery of Synaptic vesicle endocytosis in 1970s began an intensedebate on whether Synaptic vesicle endocytosis is mediated by a classical clathrin-dependent mechanism, involving membrane invagination, coated pit formation, and fission, or by kiss-and-run, involving only fusion pore opening and closure (Alabi & Tsien, 2013; Aravanis et al., 2003; Ceccarelli et al., 1973; Fernández-Alfonso & Ryan, 2004; Gandhi & Stevens, 2003; Granseth et al., 2009; He & Wu, 2007; He et al., 2006; Heuser & Reese, 1973; Zhang et al., 2009). Clathrin-dependent endocytosis has been supported by many sets of circumstantial evidence, such as the observation of the clathrin-coated pits after exocytosis and accumulation of clathrin-coated pits after block ofvesicle recycling (Ferguson et al., 2007; Kononenko & Haucke, 2015; Saheki & De Camilli, 2012; Shupliakov, 1997). Accordingly, clathrin-dependent endocytosis has often been considered a major form of Synaptic vesicle endocytosis for several decades (Saheki & De Camilli, 2012). However, crucial testing of the clathrin hypothesis by perturbing clathrin or AP2 led to controversial results. At hippocampal synapses at room temperature, an early study reported that knockdown of clathrin nearly entirely blocks synaptic vesicle protein endocytosis (Granseth et al.,

2006), suggesting an indispensable role of clathrin in synaptic vesicle endocytosis. In contrast, recent studies at hippocampal synapses at room temperature reported that clathrin knockdown, conditional knockout of AP2 (Kononenko, 2014), or ~96% knockdown of AP2 (Kim & Ryan, 2009) only inhibits vesicle protein endocytosis to a rather minor extent, suggesting that clathrin is dispensable for vesicular protein endocytosis (Kononenko, 2014). Ultrastructural examination suggests that clathrin is required in vesicle budding from endosome (Kononenko, 2014). Using 'flash-and-freeze' electron microscopy (EM), where high-pressure freezing is timed after action potentials evoked by light-induced channelrhodopsin activation, recent studies suggest that an ultrafast (~50-100 ms) clathrin-independent mechanism, which forms large endosomes from the plasma membrane, mediates Synaptic vesicle endocytosis at physiological temperature, whereas clathrin mediates vesicle budding from endosomes (Watanabe, Liu, et al., 2013; Watanabe, Rost, et al., 2013; Watanabe et al., 2014). Only at room temperature, clathrin mediates Synaptic vesicle endocytosis (Watanabe et al., 2014). Consistent with these EM results, acute photo-inactivation of clathrin light chain or clathrin heavy chain does not inhibit membrane internalization, but blocks vesicle budding from endosome in drosophila neuromuscular junction (Heerssen et al., 2008; Kasprowicz et al., 2008); reducing clathrin in *Caenorhabditis elegans* does not affect vesicle number in nerve terminals and spontaneous release (Sato et al., 2009). Taken together, except an early study (Granseth et al., 2006), most recent studies seem to agree that endocytosis is mediated by a clathrin-independent mechanism. However, even for these apparently agreeable studies, the detail does not agree with each other. For example, the flash-and-freeze EM suggests a clathrin-independent synaptic vesicle

endocytosis only in physiological temperature, but a clathrin-dependent synaptic vesicle endocytosis at room temperature inhippocampal synapses (Watanabe et al., 2014), which is in conflict with a study suggesting that clathrin is dispensable at room temperature in hippocampal synapses (Kononenko, 2014).

In the present work, my lab examined whether Synaptic vesicle endocytosis depends on clathrin at hippocampal synapses by performing conditional clathrin knockout for the first time in mammalian synapses and by recording Synaptic vesicle endocytosis with imaging of synaptic vesicular membrane proteins. We found that endocytosis of vesicular proteins in hippocampal synapses was slow and clathrin-dependent after a wide range of stimulation conditions, at physiological temperature, suggesting an essential role of clathrin in vesicular protein endocytosis. We found that the clathrin-dependency was not evident until clathrin was reduced by ~80% or more, which may help to reconcile the conflict regarding whether clathrin is essential for vesicular protein endocytosis at hippocampal synapses (Granseth et al., 2006; Kononenko, 2014).

4.2 Methods and Materials

4.2.1 Animals.

Animal care and use were performed according to National Institutes of Health (NIH) guidelines and were approved by the NIH Animal Care and Use Committee. $CHC^{Loxp/Loxp}$ mouse generation is described in Fig. 4.1A and legends. Conditional knockout mice of either sex were obtained by heterozygous and homozygous breeding using standard mouse husbandry procedures. Mouse genotypes were determined by PCR.

4.2.2 Hippocampal culture and imaging.

Mouse hippocampal culture was prepared as described previously (Sankaranarayanan & Ryan, 2000; Sun et al., 2010). Hippocampal CA1-CA3 regions from P0 mice were dissected, dissociated, and plated on Poly-D-lysine-treated coverslips. Cells were maintained at 37°C in a 5% CO_2 humidified incubator with a culture medium consisting of Neurobasal A (Invitrogen), 10% fetal bovine serum (Invitrogen), 2% B-27 (Invitrogen), 1% Glutamax-1 (Invitrogen). On 5–7 d after plating, neurons were transfected with plasmids using Lipofectamine LTX (Invitrogen).

Hippocampal cultures were transfected with a plasmid containing synaptophysin tagged with the SypH, provided by Dr. Yong-Ling Zhu (Zhu et al., 2009) alone (control) or with L309 plasmid containing Cre/mCherry. A nuclear localization sequence was tagged at the N-terminal of Cre, and cloned into L309 vector via BamHI and EcoRI sites. Accordingly, mCherry was expressed in the nucleus.

Action potential was evoked by a 1 ms pulse (20 mA) through a platinum electrode. The bath solution contained the following (in mM): 119 NaCl, 2.5 KCl, 2 $CaCl_2$, 2 $MgCl_2$, 25 HEPES, 30 glucose, 0.01 6-cyano-7- nitroquinoxaline-2, 3-dione (CNQX), and 0.05 D,L-2-amino-5- phosphonovaleric acid (AP-5), pH 7.4 , adjusted with NaOH. In temperature experiments, we heated the culture chamber using a temperature controller (TC344B; Warner Instruments, Hamden, CT). Imaging was performed after the culture was at 34 –37°C for 15–30 min. The temperature was verified with another small thermometer (BAT-7001H; Physitemp Instruments) in the chamber. SypH images

were acquired at 1 Hz using Nikon A1 confocal microscope (60X, 1.4 numerical aperture [NA]), and analyzed with Nikon software.

4.2.3 Immunohistochemistry.

Neurons were fixed with 4% paraformaldehyde, permeabilized with 0.3% Triton X-100, and subsequently incubated with primary and secondary antibodies. Primary antibodies were diluted in PBS containing 10% donkey serum and incubated with cells for 1 h at room temperature. After several rinses in PBS, cells were incubated with fluorescence-conjugated donkey anti- mouse, anti-sheep, or anti-rabbit IgG (1:1000, Invitrogen) for 2 h at room temperature. Primary antibodies included mouse anti-CHC (1:500, Abcam). mCherry fluorescence imaging was performed simultaneously to identify cells transfected with Cre/mCherry.

4.2.4 Data collection and measurements of T and $Rate_{decay}$.

For SypH signal in hippocampal cultures, the $Rate_{decay}$ was measured from boutons' SypH fluorescence trace in the first 4 –10 s after stimulation.

4.2.5 AAV-Cre-mCherry plasmid construction and virus packaging.

Cre-mCherry was amplified from the plasmid L309-Cre-mCherry, and replaced the Cre-GFP fragment from AAV-Cre/GFP plasmid (from Dr. Huaibin Cai Lab, or Addgene #49056, Watertown, MA, USA) via EcoRI and XhoI sites. The plasmid was packaged into serotype AAV-DJ by Vigene Biosciences (Rockville, MD).

4.2.6 Western blot.

Neurons were washed three times with ice-cold PBS. Cell lysates were prepared in the modified RIPA buffer containing protease inhibitors (Thermo Scientific). Equal amounts of proteins, determined by BCA protein assay (Thermo Scientific), were loaded onto SDS-PAGE gel and immunoblotted using antibodies against clathrin heavy chain (1:1000; BD Bioscience) and β-actin (1:2000; Abcam).

4.2.7 Electron microscopy.

Hippocampal cultures were fixed with 4% glutaraldehyde (freshly prepared, Electron microscopy sciences, Hatfield, PA) in 0.1 M Na-cacodylate buffer solution containing for at least 1 h at 22–24°C and stored in 4°C refrigerator overnight. The next day, cultures were washed with 0.1 M cacodylate buffer, and treated with 1% OsO_4 in cacodylate buffer for1h on ice, and 0.25% uranyl acetate in acetate buffer at pH 5.0 overnight at 4°C, dehydrated with ethanol, and embedded in epoxy resin. Thin sections were counterstained with uranyl acetate and lead citrate then examined in a JEOL200CX TEM. Images were collected with a CCD digital camera system (XR-100; AMT) at a primary magnification of 10,000–20,000X. Synapses were selected based on the structural specialization including synaptic vesicle clustering, synaptic cleft and the postsynaptic density.

4.2.8 Experimental design and statistical analyses.

Data are presented as means ± s.e.m. The statistical test used was t test with equal variance, although t test with unequal variance gave the same result.

For pHluorin imaging, each experiment included 20–30 boutons showing fluorescence increase (region of interest: 2 μm X 2 μm). Approximately one to three experiments were taken from each culture. Each culture was from 3–5 mice. Each group of data was obtained from at least four batches of cultures (4–12 cultures).

For electron microscopy, synapses were selected based on the structural specialization, including synaptic vesicle clustering, synaptic cleft, and the postsynaptic density. Each group of data was taken from 100–101 synaptic profiles from 4 –12 mice.

4.3 Results

4.3.1 Clathrin conditional knockout.

We generated clathrin heavy chain (CHC) conditional knockout ($CHC^{LoxP/LoxP}$) mice by floxing CHC Exon 2 (Fig. 4.1A). Breeding $CHC^{LoxP/LoxP}$ mice with actin β-Cre or synapsin-Cre mice that express Cre broadly produced no *CHC* knockout mice (> 30 pups from > 5 litters), likely due to embryonic death. We thus induced *CHC* gene deletion by transfecting a plasmid containing Cre and mCherry to hippocampal neurons cultured from $CHC^{LoxP/LoxP}$ mice (Fig. 4.1B). At 6 days after Cre transfection ($Day6_{Cre}$), CHC antibody staining in neuronal somata expressing mCherry was reduced to 12% of control, the neighboring un-transfected neurons (Fig. 4.1B).

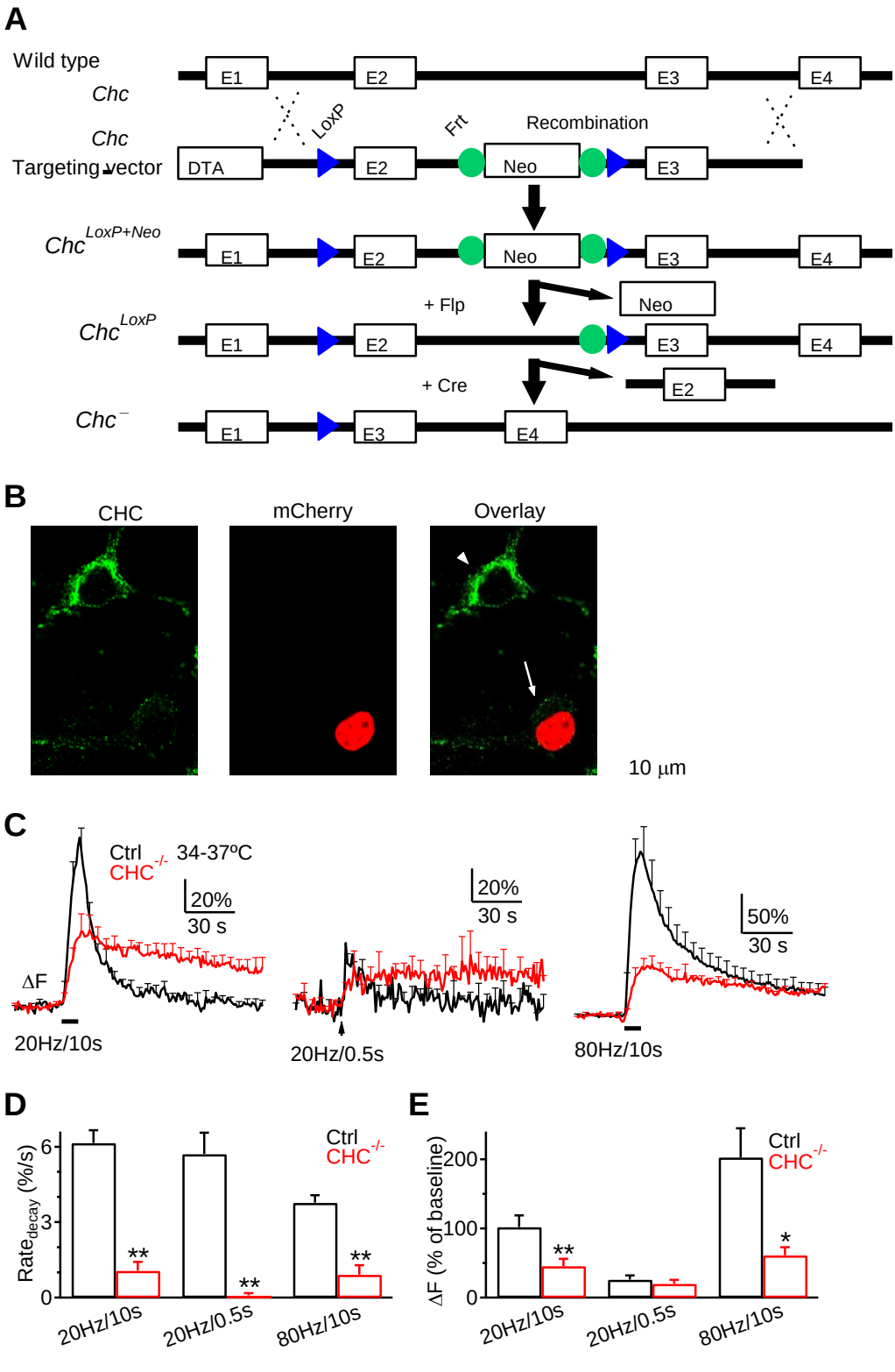
A
Wild type
Chc
E1
E2
E3
E4
Chc
Targeting vector
LoxP
Frt
Recombination
DTA
Neo
Chc LoxP+Neo
+ Flp
Chc LoxP
+ Cre
Chc⁻
B
CHC
mCherry
Overlay
10 μm
C
Ctrl
CHC -/-
34-37ºC
20%
30 s
ΔF
20Hz/10s
20Hz/0.5s
80Hz/10s
50%
D
Rate decay (%/s)
E
ΔF (% of baseline)
**
*

Figure 4.1. Inhibition of F_{SypH} decay after AP trains at $Day6_{Cre}$ hippocampal synapses by Lipofectamine transfection at 34-37 ºC. ***A***, Procedure for generating CHC conditional knockout mouse. Wild-type *CHC*: endogenous CHC contains E1, E2, E3, and E4 exons. *CHC* targeting construct: A 7.7 kb *CHC* genomic DNA fragment containing E2 and E3 was used as the homologous arm, and was subcloned at the *SacII* and *NotI* sites of the cloning vector containing a negative selection marker, diphtheria toxin A gene (DTA). A loxP site was inserted at 538 bp upstream of E2 and a Frt-loxP-flanked Neomycin (Neo) cassette was inserted at 640 bp downstream of E2 for positive selection. $CHC^{LoxP+Neo}$: The *CHC* targeting construct was linearized and electroporated into G4 embryonic stem (ES) cells as described previously[4]. Targeted ES cells were selected by Neo selectant, G418, and identified by Southern blot. Targeted ES cells were injected into C57BL/6J blastocysts implanted in ICR females, giving rise to mouse chimeras. Chimeric mice were bred with C57BL/6J mice to generate *CHC* targeted germline mice ($CHC^{Neo+LoxP}$). CHC^{LoxP}: Crossing $CHC^{Neo+LoxP}$ mice with ROSA26-FLPe mice (Jackson Laboratory) removed the FRT-flanked Neo gene in off springs, leading to generation of *CHC* conditional knockout (CHC^{Loxp}) mice. CHC^{-}: introducing the Cre recombinase deletes E2 and creates a premature termination codon in E3, giving rise to the *CHC* null (CHC^{-}) allele. ***B***, Sampled CHC antibody staining at 6 days after Cre/mCherry transfection to $CHC^{Loxp/Loxp}$ hippocampal culture. Arrow: Cre/mCherry-transfected neuron (lower CHC staining); triangle: un-transfected neuron (higher CHC staining). ***C-E***, F_{SypH} traces (d), $Rate_{decay}$ (e) and ΔF (e) induced by $AP_{20H/10s}$, $AP_{20H/0.5s}$ and $AP_{80H/10s}$ in Ctrl (black) and $Day6_{Cre}$ (red) culture at 34-37ºC. $Rate_{decay}$ (%/s, mean + s.e.m) was measured from normalized F_{SypH} traces with ΔF = 100%, ΔF refers to the percent increase of F_{SypH} over baseline. Ctrl: $CHC^{Loxp/Loxp}$ synapses transfected with SypH alone for 6 days. *, $p < 0.05$; **, $p < 0.01$ (t test). The transgenic mice were produced by Lin Gan. The F_{SypH} traces was produced by Zhen Zhang, Sunghoon Lee, Xinsheng Wu and me.

4.3.2 F_{SpH} decay is clathrin-dependent at 34-37ºC.

We transfected $CHC^{LoxP/LoxP}$ hippocampal neurons with pH-sensitive synaptophysin-pHluorin 2x (SypH) alone (control) or plus Cre/mCherry to delete *CHC*. 6 days later, we performed SypH imaging of endocytosis induced by 3 action potential (AP) trains, 20 Hz for 10 s ($AP_{20Hz/10s}$) or 0.5 s ($AP_{20Hz/0.5s}$) and 80 Hz for 10 s ($AP_{80Hz/10s}$). In control at 34-37ºC, ΔF after $AP_{20Hz/10s}$ decayed bi-exponentially with τ of 7.4 ± 0.5 s (weight: 0.8) and 46.0 ± 7.1 s, respectively (n = 9); ΔF after $AP_{20Hz/0.5s}$ decayed mono-exponentially with a τ of 12.2 ± 2.1 s (n = 5); ΔF after $AP_{80Hz/10s}$ decayed bi-exponential with τ of 13.1 ± 1.3 s (weight: 0.5) and 56.0 ± 0.5 s, respectively (n = 7, Fig. 4.1C). At 34-37ºC at $Day6_{Cre}$ synapses, both fast and slow components were abolished, suggesting that clathrin is involved in these different speeds of endocytosis; $Rate_{decay}$ was reduced to 2-24% of control (Fig. 4.1C, D, n = 4-11); ΔF after $AP_{20Hz/10s}$ and $AP_{80Hz/10s}$, but not after $AP_{20Hz/0.5s}$, was reduced that depleted the

readily releasable pool (Fig. 4.1E). Thus, $Rate_{decay}$ was substantially reduced at $Day6_{Cre}$ synapses at both room (data not shown) and physiological (Fig. 4.1C-E) temperature.

Co-transfection of wild-type CHC with SpH/Cre/mCherry to $CHC^{Loxp/Loxp}$ cultures for 6 days rescued CHC expression to a level similar to or higher than control, and rescued $Rate_{decay}$ to the control level (data not shown).

4.3.3 EM suggests clathrin involvement in endocytosis of regular vesicles and bulk endosomes.

To examine ultrastructural changes, we transduced AAV-Cre into hippocampal cultures for 48 hours, remove AAV by change media, and then culture for another 6 days ($Day8_{AAV\text{-}Cre}$), which reduced CHC detected with Western blotting to 21.6 ± 2.4% of control (Fig. 4.2A, B), suggesting that most neurons were transfected with Cre. Similar to $Day6_{Cre}$ cultures, ΔF_{SypH} decay after $Train_{20Hz/10s}$ was blocked in $Day8_{AAV\text{-}Cre}$ cultures. Electron microscopic examination in $Day8_{AAV\text{-}Cre}$ cultures showed that synapses appeared normal for bouton areas. Vesicle numbers (79.22±4.80 per μm^2, n=100) was significantly less than in control (101.21±9.03 per μm^2, n=100, Fig. 4.2C). Moreover, vesicle diameter (41.96 ± 0.26 nm, n = 983) was slightly but significantly larger than in control (37.94 ± 0.16 nm, n = 1088, Fig. 4.2D).

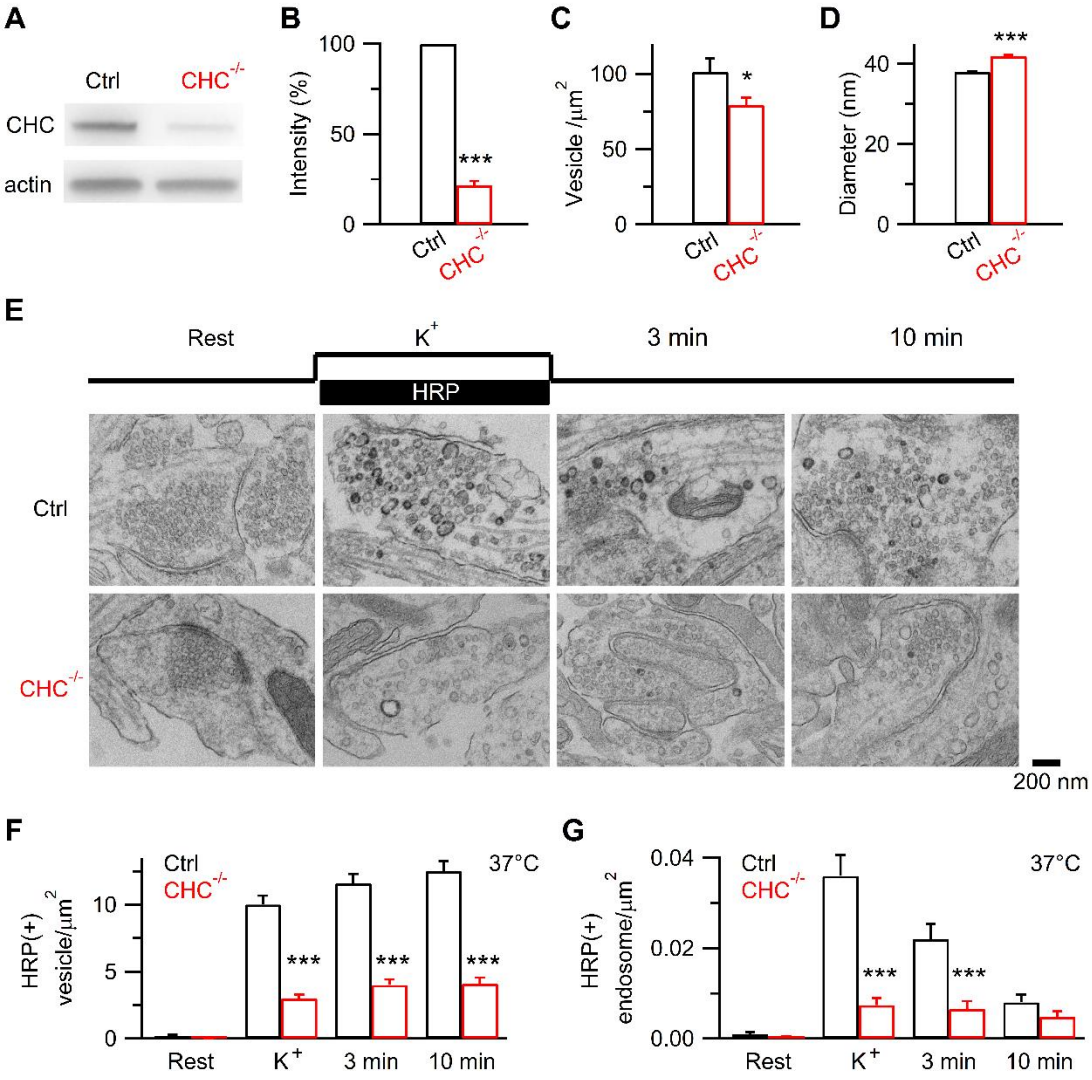

Figure 4.2. AAV-Cre induction into $CHC^{LoxP/LoxP}$ cultures reduces clathrin expression and block endocytosis examined with EM at hippocampal synapses at 37 ºC. ***A***, Western blot of CHC and actin in Ctrl and $Day12_{AAV\text{-}Cre}$ hippocampal cultures. Control cultures were taken from $CHC^{LoxP/LoxP}$ cultures. ***B***, Normalized Western blot intensity from Ctrl (3 cultures) or $Day12_{AAV\text{-}Cre}$ hippocampal cultures (AAV-Cre, 3 experiments). The Ctrl culture include wild-type and $CHC^{LoxP/LoxP}$ culture without Cre transduction. ***C***, Vesicle number per μm^2 in Ctrl and $Day8_{AAV\text{-}Cre}$ hippocampal boutons at rest. ***D***, Vesicle diameter in Ctrl and $Day8_{AAV\text{-}Cre}$ hippocampal boutons at rest. ***E***, EM images of Ctrl and $Day8_{AAV\text{-}Cre}$ hippocampal boutons at rest (Rest) and at 0 min (KCl), 3 min and 10 min after 1.5 min application of 90 mM KCl. Rest: HRP included for 1.5 min; Other groups: HRP included only during 1.5 min KCl application. ***F***, ***G***, The number of HRP(+) vesicles (left) and bulk endosome area (right, per μm^2 synaptic cross section) plotted versus the time before (Rest) and at 0 min (KCl), 3 min and 10 min after KCl/HRP application in Ctrl (black) and $Day8_{AAV\text{-}Cre}$ (red) cultures (mean + s.e.m.). Each group: 100-101 synaptic profiles, 3 cultures. *, $p < 0.05$; ***, $p < 0.001$ (t test).

Horseradish peroxidase (HRP, 5 mg/ml, bath) was added for assay of vesicular uptake at physiological temperature. At rest, HRP-positive [HRP(+)] vesicles were minimal; most vesicles were HRP-negative [HRP(-)] (Fig. 4.2E, F); the number of HRP(+) and HRP(-) vesicles and their sum in boutons were similar in control and $CHC^{-/-}$ cultures (data not shown). To examine endocytosis, we applied 90 mM KCl with HRP for 1.5 min, and fixed samples at 0, 3 and 10 min after KCl/HRP application. In control boutons, compared with the resting condition, HRP(+) vesicles increased from time 0 to 10 min after KCl, reflecting vesicle endocytosis (Fig. 4.2E, F) as previously shown (Wu et al., 2016; Y. Wu et al., 2014). Compared with control boutons, HRP(+) vesicles were significantly reduced at each time point after KCl in $CHC^{-/-}$ boutons (Fig. 4.2E, F), suggesting inhibition of endocytosis.

In the control group, HRP(+) bulk endosomes were observed in the boutons (Fig. 4.2E), defined as vesicles with a diameter 80 nm or with a cross section area more than that of a 80 nm vesicle (~0.005 μm^2). The area of HRP(+) bulk endosomes raised after high potassium application (time 0 min), then decreased during the two following time points (3 and 10 min) (Fig. 4.2E, G), suggesting generation of bulk endosomes and subsequent conversion to vesicles as previously shown (Wu et al., 2016; Y. Wu et al., 2014). Compared with control boutons, HRP(+) vesicles were significantly reduced at 0 and 3 min time point after KCl in $CHC^{-/-}$ boutons (Fig. 4.2E, G). The bulk endosome in knockout broke down very slow and there was no significant difference with control (Fig. 4.2G), suggesting inhibition of bulk endocytosis. These EM data confirmed the involvement of CHC in endocytosis at physiological temperature (37°C).

4.4 Discussion

In the results shown so far, my lab used a wide range of AP trains, but not a single AP yet, one of the main stimulus used in the flash-and-freeze EM studies (Watanabe, Rost, et al., 2013; Watanabe et al., 2014). One may wonder whether ultrafast clathrin-independent endocytosis dominates after a single AP. To address this question, my colleague quantified endocytosis after single AP. 18.5 ± 1.6% was ultrafast endocytosis (< 1 s), 39.0 ± 3.7% was fast (1-10 s), 22.0 ± 2.4% was slow (10-70 s), and 20.5 ± 2.6% was ultra-slow.

Consequently, we found that clathrin is essential for endocytosis at live hippocampal synapses after a wide range of stimuli, including 1- 800 APs by performing conditional CHC knockout in mice.

My lab also tested whether the $Rate_{decay}$ reduction depended on the extent of CHC reduction, another colleague performed SypH imaging at 2, 4, 5 and 6 days after Cre transfection, at which CHC was reduced to a value ranging from ~86% to 12% of control. We found that from day 2 to 6 at 22- 24^{o}C, $Rate_{decay}$ after $AP_{20Hz/10s}$ decreased. The decrease was minor at day 2 and 4, at which CHC was ~86% and 26% of control, respectively; the decrease was dramatic at day 5 and6, at which CHC was ~22% and 12% of control, respectively. These results showed a dose-dependent relation between $Rate_{decay}$ and CHC level. These results provide crucial evidence establishing clathrin as an indispensable molecule for synaptic vesicle protein endocytosis in a variety of physiological stimulation conditions at hippocampal synapses and help to explain the often-negative effects of clathrin inhibition on Synaptic vesicle endocytosis. Given the involvement of clathrin, synaptic vesicle protein endocytosis must be analogous to

classical clathrin-dependent endocytosis, involving membrane invagination, coated pit formation and fission (Saheki & De Camilli, 2012).

Whether Synaptic vesicle endocytosis is mediated in a similar manner as the classical receptor-mediated endocytosis, in which clathrin plays an essential role, has been intensely debated for many years (see Introduction). Crucial test of this idea relies on knocking down or photo-inactivating clathrin. With few exception (Granseth et al., 2006), most studies (Heerssen et al., 2008; Kasprowicz et al., 2008; Kononenko, 2014; Sato et al., 2009; Watanabe et al., 2014) did not reveal a significant block of Synaptic vesicle endocytosis, but endosomal vesicle budding, leading to a current view that clathrin is dispensable for Synaptic vesicle endocytosis (Kononenko & Haucke, 2015; Kononenko, 2014; Watanabe et al., 2014). Flash-and-freeze EM works in hippocampal synapses suggest that the clathrin-independent mechanism is ultrafast at physiological temperature but is replaced with slow clathrin-dependent endocytosis at room temperature (Watanabe, Rost, et al., 2013; Watanabe et al., 2014). Our finding that reducing CHC by ~74% and ~88% caused negligible and substantial inhibition of SypH endocytosis, respectively. Our results may account for the minor or lack of effects in most manipulations of clathrin and thus may help to reconcile the controversy regarding the role of clathrin in Synaptic vesicle endocytosis. For example, at the same hippocampal synapse, a study reported that reducing clathrin by ~70-75% did not substantially block vesicular protein endocytosis, suggesting that clathrin is dispensable for Synaptic vesicle endocytosis (Kononenko, 2014). In contrast, another study found that reducing clathrin by ~88% substantially blocked of vesicular protein endocytosis, suggesting that clathrin is indispensable for Synaptic vesicle endocytosis (Granseth et al.,

2006). This sharp conflict could be due to the seemingly subtle differences in the clathrin knockdown by ~70-75% and by ~88%.

Knockdown or knockout of clathrin adaptor AP2 affects synaptic vesicular protein endocytosis or membrane endocytosis to a minor or negligible extent (Gu et al., 2008; Kim & Ryan, 2009; Kononenko, 2014). This observation may not necessarily contradict our finding, because other adaptor proteins, such as AP1, AP3, stonin, and AP180, might compensate for AP2 loss. Our results do not exclude the presence of clathrin-independent endocytosis at other cells. For example, with pharmacological tools to perturb clathrin function, rapid endocytosis with a time constant of ~1 s or less has been suggested to be mediated by a clathrin-independent mechanism in chromaffin cells, goldfish retinal bipolar nerve terminals, and mossy fiber boutons (Artalejo et al., 1995; Delvendahl et al., 2016; Jockusch et al., 2005).

Our results are in apparent conflict with recent flash-and-freeze EM works suggesting that Synaptic vesicle endocytosis is slow and clathrin-dependent at room temperature, but ultrafast and clathrin- independent at physiological temperature at hippocampal synapses (Watanabe et al., 2014). The stimulation used in flash-and-freeze EM work was 1-100 AP induced optogenetically at 20 Hz with 4 mM extracellular calcium at room temperature and physiological temperature, whereas we used 1-800 AP at 0.03-80 Hz with 2-4 mM extracellular calcium in both temperatures. Thus, the discrepancy is unlikely to be due to different stimulation conditions.

The possibility that might account for the apparent difference in our results and the flash-and-freeze EM works is the differences in the methods used to measure and interpret ultrafast endocytosis. SypH endocytosis were measured in live synapses in the

present work, whereas ultrafast endocytosis was interpreted largely based on the ultra-transient appearance of putative endocytic intermediates observed under the EM from different boutons frozen at various times after light-induced channelrhodopsin activation (Watanabe, Rost, et al., 2013; Watanabe et al., 2014). While the interpretation of ultrafast endocytosis seems reasonable, it is unclear whether every putative endocytic intermediate observed is due to endocytosis. For example, the ultra-transient appearance of membrane invagination is interpreted as the intermediate of bulk endocytosis but could be membrane folding due to addition of exocytosed vesicle membrane that increases the plasma membrane area. While large Ω-shaped membrane profile is interpreted as a result of membrane invagination followed by formation of the Ω- profile, the possibility that it is due to fusion that generates an Ω-profile could not be completely excluded. The fusion-generated Ω-profile (without collapse) might move from the release site to the peri-active zone and enlarge to some extent as recently observed in chromaffin cells (Chiang et al., 2014), which might account for the reported transient appearance of large Ω-profiles at the peri-active zone (Watanabe, Rost, et al., 2013; Watanabe et al., 2014). The possibility that delayed exocytosis, including compound exocytosis of large vesicles (due to vesicle-vesicle fusion) (He et al., 2009; Matthews & Sterling, 2008) at the peri-active zone, contributes to the reported ultra-transient appearance of Ω-profiles at the peri-active zone (Watanabe, Rost, et al., 2013; Watanabe et al., 2014) could not be fully excluded either.

In addition to revealing clathrin as the essential molecule for synaptic vesicular protein endocytosis, the present work generated $CHC^{Loxp/Loxp}$ mice for the first time, which makes it possible to reduce clathrin to a greater extent than the knockdown technique. This provides a powerful tool to study the role of clathrin in endocytosis,

intracellular trafficking, and many other biological processes where clathrin may be crucial, yet relatively insensitive to traditional clathrin knockdown.

Chapter 5: NSF is involved in mediating endocytosis at synapses

*The transgenic mice were produced by Lin Gan. I am responsible for the data.

5.1 Introduction

Exocytosis releases transmitters to mediate synaptic transmission. It is well established that exocytosis is catalyzed by the SNARE complex, composed of synaptobrevin at the vesicle membrane and SNAP-25 and syntaxin at the plasma membrane (Jackson & Chapman, 2008; Südhof, 2004). After exocytosis, the SNARE complex is disassembled by the ATPase NSF for the next round of exocytosis (Südhof, 2004), and endocytosis takes place to retrieve the fused vesicle membrane and proteins within a few seconds to tens of seconds (Wu et al., 2007). Endocytosis may involve membrane invagination and fission, which are mediated by an array of endocytic proteins, such as dynamin, clathrin, AP2, AP180, endophilin, synaptojanin, intersectin, and auxilin, which are different from core exocytosis proteins mentioned above (Dittman & Ryan, 2009). Moreover, all three SNARE proteins play roles in endocytosis in calyx and hippocampal synapses (Xu et al., 2013; Zhang et al., 2013). Here I tested whether NSF is also involved in mediating synaptic vesicle endocytosis. I found that indeed NSF is involved in mediating endocytosis. My results suggest new endocytosis model in which newly disassembled SNARE proteins by NSF are involved in endocytosis by binding and recruiting endocytosis proteins to mediate endocytosis.

5.2 Methods and Materials

5.2.1 Animals.

Animal care and use were performed according to National Institutes of Health (NIH) guidelines and were approved by the NIH Animal Care and Use Committee. *NSF*$^{Loxp/Loxp}$ mouse generation is produced by our previous lab member Lin Gan. Conditional knockout mice of either sex were obtained by heterozygous and homozygous breeding using standard mouse husbandry procedures. Mouse genotypes were determined by PCR.

5.2.2 Hippocampal culture and imaging.

Mouse hippocampal culture was prepared as described previously (Sankaranarayanan & Ryan, 2000; Sun et al., 2010). Hippocampal CA1-CA3 regions from P0 mice were dissected, dissociated, and plated on Poly-D-lysine-treated coverslips. Cells were maintained at 37°C in a 5% CO_2 humidified incubator with a culture medium consisting of Neurobasal A (Invitrogen), 10% fetal bovine serum (Invitrogen), 2% B-27 (Invitrogen), 1% Glutamax-1 (Invitrogen). On 7–10 days after plating, neurons were transfected with plasmids using Lipofectamine LTX (Invitrogen).

Hippocampal cultures were transfected with a plasmid containing SypH, provided by Dr. Yong-Ling Zhu (Zhu et al., 2009) alone (control) or with L309 plasmid containing Cre/mCherry. A nuclear localization sequence was tagged at the N-terminal of Cre, and cloned into L309 vector via BamHI and EcoRI sites. Accordingly, mCherry was expressed in the nucleus.

The cDNA encoding NSF (Novopro) or NSF_{E329Q} (Genecopoeia), was subcloned into EBFP2-C1 (Addgene #54665), and EBFP2 was used for us to recognize transfected cells. For the rescue experiments (see Fig. 5), we transfected NSF or NSF_{E329Q} plasmid

along with SypH and Cre/mCherry. After transfection, neurons were maintained at 37°C in a 5% CO_2-humidified incubator for another 2 day before experiments.

Action potential was evoked by a 1 ms pulse (20 mA) through a platinum electrode. The bath solution contained the following (in mM): 119 NaCl, 2.5 KCl, 2 $CaCl_2$, 2 $MgCl_2$, 25 HEPES, 30 glucose, 0.01 6-cyano-7- nitroquinoxaline-2, 3-dione (CNQX), and 0.05 D,L-2-amino-5- phosphonovaleric acid (AP-5), pH 7.4 , adjusted with NaOH. In temperature experiments, we heated the culture chamber using a temperature controller (TC344B; Warner Instruments, Hamden, CT). Imaging was performed after the culture was at 34 –37°C for 15–30 min. The temperature was verified with another small thermometer (BAT-7001H; Physitemp Instruments) in the chamber. SypH images were acquired at 1 Hz using Nikon A1 confocal microscope (60X, 1.4 numerical aperture [NA]), and analyzed with Nikon software.

5.2.3 Data collection and measurements of T and $Rate_{decay}$.

For SypH signal in hippocampal cultures, the $Rate_{decay}$ was measured from boutons' SypH fluorescence trace in the first 4 –10 s after stimulation.

5.2.4 Experimental design and statistical analyses.

Data are presented as means ± s.e.m. The statistical test used was t test with equal variance, although t test with unequal variance gave the same result.

For pHluorin imaging, each experiment included 20–30 boutons showing fluorescence increase (region of interest: 2 μm X 2 μm). Approximately one to three

experiments were taken from each culture. Each culture was from 3–5 mice. Each group of data was obtained from at least four batches of cultures (4–12 cultures).

5.3 Results

5.3.1 NSF involvement in slow endocytosis at room temperature.

We transfected *NSF*$^{LoxP/LoxP}$ hippocampal neurons with pH-sensitive synaptophysin-pHluorin 2x (SypH) alone (control) or plus Cre/mCherry to delete *NSF* 5-6 days later, we performed SypH imaging of endocytosis at room temperature (the same for below, if not mentioned). An action potential train of 10 s at 20 Hz ($AP_{20Hz/10s}$) induced a fluorescence increase then decrease, reflecting exocytosis and endocytosis. In control, the initial decay rate was 3.9%/s, and the peak of the ΔF over the baseline (ΔF/F) is 161.0%. In NSF KO cultures, decay rate was ~74.6% slower than control (Fig. 5A-C). Decay rate in NSF KO culture was rescued to the control level by transfection of WT NSF. After an action potential train for 10 s at 40 Hz ($AP_{40Hz/10s}$) in WT cultures, the initial decay rate was 3.5%/s in control, and the peak of the ΔF is 223.9%. In NSF KO cultures, the decay rate was ~75.7% slower than control (Fig. 5D-F). Following a 10 s action potential train at 5 Hz ($AP_{5Hz/10s}$), the initial decay rate was 5.4%/s in control, and the peak of the ΔF is 36.7%. In NSF KO cultures, decay rate was ~60.3% slower than control (Fig. 5G-I). These results suggest that NSF is crucial in mediating endocytosis at 5-40 Hz of stimulation.

5.3.2 NSF involvement in slow endocytosis at physiological temperature.

Ultrafast endocytosis has been shown to occur only in physiological temperature (add citation). To determine whether NSF involvement in endocytosis observed at room temperature (Fig. 5) is applicable to physiological temperature we repeated experiments at physiological temperature. $AP_{20Hz/10s}$ induced an initial decay rate of 5.2%/s in control, and ΔF amplitude of 192.3%. In NSF KO cultures, the decay rate was ~74.9% slower than control (Fig. 5J-L). The decay rate was ~74.6% slower at room temperature, suggesting the NSF involvement in endocytosis at both room temperature and physiological temperature.

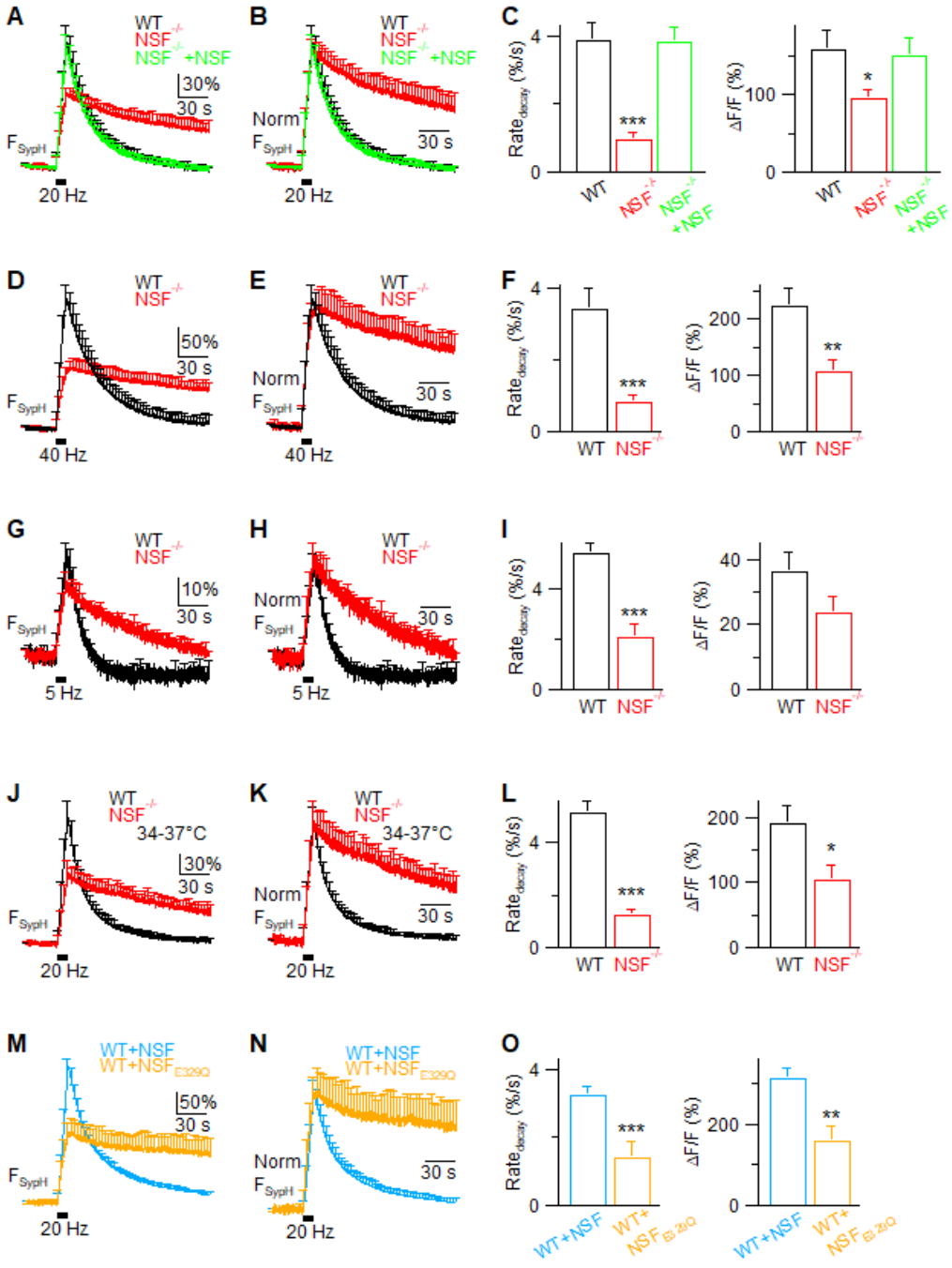

Figure 5. NSF and its ATP hydrolyzing function are required for endocytosis at hippocampal synapses. ***A-C***, F_{SypH} traces (***A***, ***B***), $Rate_{decay}$ (C, left) and ΔF/F (C, right) induced by $Train_{20Hz}$ (10 s train of action potentials at 20 Hz) in wild-type (WT) cultures (n = 20 experiments), $NSF^{-/-}$ cultures (n = 19 experiments), or $NSF^{-/-}$ hippocampal cultures overexpressed with WT NSF ($NSF^{-/-}$ + NSF; containing EBFP2 for recognition, n = 23). F_{SypH} traces in panel B are the same as those in panel A, but with the peak F_{SypH} rescaled (Norm F_{SypH}) to the same amplitude for better comparison of time courses. ***D-F***, Similar arrangement as ***A-C*** respectively, except that the stimulation was a 10-s train of action potentials at 40 Hz (WT, 11 experiments; $NSF^{-/-}$, 10 experiments). ***G-I***, Similar arrangement as ***A-C*** respectively, except that the stimulation was a 10-s train of action potentials at 5 Hz (WT, 11 experiments; $NSF^{-/-}$, 10 experiments).

Temperature (applies to Figs. ***A-I***, ***M-O***): 22–24°C. ***J-L***, Similar arrangement as ***A-C*** respectively, except that the temperature is 34-37°C (WT, 19 experiments; $NSF^{-/-}$, 9 experiments). ***M-O***, Similar arrangement as ***A-C*** respectively, except that the temperature is in wild-type (WT) cultures with overexpressed WT NSF (n = 34 experiments), or mutant NSF (n = 8 experiments); data expressed as mean+s.e.m.; *, $p < 0.05$; **, $p < 0.01$; ***, $p < 0.001$ (t test).

5.3.3 ATP hydrolyzing is required for endocytosis at hippocampal synapses.

The mutant, NSF_{E329Q}, loses the function to hydrolyze ATP and thus to disassemble SNARE proteins (Whiteheart et al., 1994). We found that $AP_{20Hz/10s}$ induced the initial decay rate of 3.3%/s in control with transfection of WT NSF, but a decay rate ~55.9% slower than the control with transfection of NSF_{E329Q} (Fig. 5M-O). These results suggest that NSF-mediated ATP hydrolysis and SNARE disassembly are required for endocytosis. NSF may thus contribute to coupling between exocytosis and endocytosis.

5.4 Discussion

5.4.1 Comparison and reconciliation with previous studies.

While it seems rather surprising that NSF is involved in endocytosis at hippocampal synapses with NSF knockout, its endocytic role is consistent with studies in systems other than vesicular exo-endocytosis. For example, NSF is involved in AMPA receptor endocytosis at dendrites (Lee et al., 2002).

Moreover, our lab previously found that three SNARE proteins play roles in endocytosis in calyx and hippocampal synapses (Xu et al., 2013; Zhang et al., 2013). Assigning four core exocytosis proteins (three SNAREs plus NSF) into the endocytosis model is likely to have a wide application, considering that NSF and SNARE proteins mediate vesicle fusion at synapses, non-neuronal secretory cells, and many intracellular fusion events (Südhof, 2004).

The involvement of exocytosis proteins in endocytosis may not be limited to NSF and SNARE complex. Synaptotagmin is involved in endocytosis after action potential trains at drosophila synapses and hippocampal synapses (Nicholson-Tomishima & Ryan, 2004; Poskanzer et al., 2006; J. Yao et al., 2012). However, a recent study did not find such a role during a $depol_{20ms}$ or $depol_{20msX10}$ at calyces (Wu et al., 2009). The discrepancy might be due to different stimuli. It remains possible that with prolonged 20 ms depolarization, the calcium sensor for mediating endocytosis might shift (Yao & Sakaba, 2012).

The dual role of core exocytosis proteins suggests that exo- and endocytosis may take place at the same location or nearby. Consistent with this possibility, NSF, SNARE proteins, and classical endocytosis proteins are physically connected to calcium channels (Khanna, Li, Bewersdorf, et al., 2007; Khanna, Li, Schlichter, et al., 2007), and clathrin-mediated endocytosis occurs near active zones at snake neuromuscular junctions (Teng & Wilkinson, 2000).

Although ATP hydrolysis is required for endocytosis (Heidelberger, 2001), its underlying mechanism was unclear. The present work suggests that it is largely due to the ATPase NSF. Photolysis of a caged NSF peptide after ~10 s stimulation did not block a form of endocytosis that lasts for ~5 min at squid synapses, leading to the conclusion that NSF is not involved in endocytosis (Kuner et al., 2008). However, the discrepancy can be reconciled by the possibility that NSF may have disassembled the SNARE complex after exocytosis that takes place during the 10 s stimulation period, making it too late for the NSF peptide uncaged after the 10 s stimulation to inhibit SNARE disassembly.

5.4.2 A model to account for the coupling between exo- and endocytosis.

We found that NSF, which disassembles the SNARE complex after exocytosis, and three SNARE proteins are involved in endocytosis. Since clostridial toxins cleave SNARE proteins only when SNARE proteins are disassembled (Niemann et al., 1994) and could inhibit endocytosis without affecting exocytosis (Xu et al., 2013), they must inhibit endocytosis by cleaving the newly disassembled SNARE proteins after exocytosis. These results led to a model in which three SNARE proteins disassembled by NSF after exocytosis are required to mediate endocytosis.

Our model may account for the exo-endocytosis coupling with respect to the time and the amount. The SNARE complex disassembly may signal the endocytosis starting time and thus explain why endocytosis follows exocytosis, because the endocytic machinery may need and thus wait for newly disassembled SNARE proteins to participate in endocytosis. The amount of newly disassembled SNARE proteins, which is proportional to the amount of recently exocytosed vesicles, may signal the amount of endocytosis to match the exocytosis amount, likely because more vesicle retrieval may require participation of more disassembled SNARE proteins. This model may also explain why no endocytosis occurs when calcium influx, which can trigger endocytosis (Clayton & Cousin, 2009; Hosoi et al., 2009; Wu et al., 2009; Yao et al., 2009), does not induce exocytosis (Wu et al., 2005; Yamashita et al., 2005). At single boutons, the release probability during an action potential is often low (Zucker & Regehr, 2002). The requirement of newly disassembled SNARE proteins to initiate or mediate endocytosis may thus prevent futile endocytosis in the absence of exocytosis during an action potential. We therefore suggest that both calcium influx and the SNARE complex

disassembly are required to initiate or mediate compensatory endocytosis, which follows and matches the amount of exocytosis.

Although we suggested that newly disassembled SNARE proteins by NSF are involved in endocytosis, we could not rule out the possibility that pre-existing free SNARE proteins are involved in endocytosis. However, pre-existing SNARE proteins may not necessarily conflict with newly disassembled one, because they might exist at a concentration too low to mediate endocytosis, or might be bound with other proteins (e.g., calcium channels or other SNAREs). Newly disassembled SANREs may provide a locally high concentration of free SNAREs soon after exocytosis to mediate endocytosis.

We found that endocytosis was not entirely abolished by NSF knockout. Whether the remaining endocytosis is due to the remaining NSF/SNAREs or independent of NSF/SNAREs is unclear. Addressing this question in the future would allow us to determine whether NSF and SNARE proteins play a regulatory or essential role in endocytosis.

Bibliography

Alabi, A. A., & Tsien, R. W. (2013). Perspectives on Kiss-and-Run: Role in Exocytosis, Endocytosis, and Neurotransmission. *Annual Review of Physiology*, *75*(1), 393-422. https://doi.org/10.1146/annurev-physiol-020911-153305

Albillos, A., Dernick, G., Horstmann, H., Almers, W., De Toledo, G. A., & Lindau, M. (1997). The exocytotic event in chromaffin cells revealed by patch amperometry. *Nature*, *389*(6650), 509-512. https://doi.org/10.1038/39081

Antonny, B. (2011). Mechanisms of Membrane Curvature Sensing. *Annual Review of Biochemistry*, *80*(1), 101-123. https://doi.org/10.1146/annurev-biochem-052809-155121

Antonny, B., Burd, C., De Camilli, P., Chen, E., Daumke, O., Faelber, K., Ford, M., Frolov, V. A., Frost, A., Hinshaw, J. E., Kirchhausen, T., Kozlov, M. M., Lenz, M., Low, H. H., McMahon, H., Merrifield, C., Pollard, T. D., Robinson, P. J., Roux, A., & Schmid, S. (2016). Membrane fission by dynamin: what we know and what we need to know. *The EMBO Journal*, *35*(21), 2270-2284. https://doi.org/10.15252/embj.201694613

Aravanis, A. M., Pyle, J. L., & Tsien, R. W. (2003). Single synaptic vesicles fusing transiently and successively without loss of identity. *Nature*, *423*(6940), 643-647. https://doi.org/10.1038/nature01686

Artalejo, C. R., Henley, J. R., McNiven, M. A., & Palfrey, H. C. (1995). Rapid endocytosis coupled to exocytosis in adrenal chromaffin cells involves Ca2+, GTP, and dynamin but not clathrin. *Proceedings of the National Academy of Sciences*, *92*(18), 8328-8332. https://doi.org/10.1073/pnas.92.18.8328

Avinoam, O., Schorb, M., Beese, C. J., Briggs, J. A. G., & Kaksonen, M. (2015). Endocytic sites mature by continuous bending and remodeling of the clathrin coat. *Science*, *348*(6241), 1369-1372. https://doi.org/10.1126/science.aaa9555

Balaji, J., Armbruster, M., & Ryan, T. A. (2008). Calcium Control of Endocytic Capacity at a CNS Synapse. *Journal of Neuroscience*, *28*(26), 6742-6749. https://doi.org/10.1523/jneurosci.1082-08.2008

Beck, K. A., & Keen, J. H. (1991). Interaction of phosphoinositide cycle intermediates with the plasma membrane-associated clathrin assembly protein AP-2. *Journal of Biological Chemistry*, *266*(7), 4442-4447. https://doi.org/10.1016/s0021-9258(20)64342-3

Behnia, R., & Munro, S. (2005). Organelle identity and the signposts for membrane traffic. *Nature*, *438*(7068), 597-604. https://doi.org/10.1038/nature04397

Bittner, G. D., & Kennedy, D. (1970). QUANTITATIVE ASPECTS OF TRANSMITTER RELEASE. *Journal of Cell Biology*, *47*(3), 585-592. https://doi.org/10.1083/jcb.47.3.585

Braell, W. A., Schlossman, D. M., Schmid, S. L., & Rothman, J. E. (1984). Dissociation of clathrin coats coupled to the hydrolysis of ATP: role of an uncoating ATPase. *Journal of Cell Biology*, *99*(2), 734-741. https://doi.org/10.1083/jcb.99.2.734

Burston, H. E., Maldonado-Báez, L., Davey, M., Montpetit, B., Schluter, C., Wendland, B., & Conibear, E. (2009). Regulators of yeast endocytosis identified by systematic quantitative analysis. *Journal of Cell Biology*, *185*(6), 1097-1110. https://doi.org/10.1083/jcb.200811116

Ceccarelli, B., Hurlbut, W. P., & Mauro, A. (1973). TURNOVER OF TRANSMITTER AND SYNAPTIC VESICLES AT THE FROG NEUROMUSCULAR JUNCTION. *Journal of Cell Biology*, *57*(2), 499-524. https://doi.org/10.1083/jcb.57.2.499

Chanaday, N. L., Cousin, M. A., Milosevic, I., Watanabe, S., & Morgan, J. R. (2019). The Synaptic Vesicle Cycle Revisited: New Insights into the Modes and Mechanisms. *The Journal of Neuroscience*, *39*(42), 8209-8216. https://doi.org/10.1523/jneurosci.1158-19.2019

Chanaday, N. L., & Kavalali, E. T. (2018). Time course and temperature dependence of synaptic vesicle endocytosis. *FEBS Letters*, *592*(21), 3606-3614. https://doi.org/10.1002/1873-3468.13268

Chiang, H.-C., Shin, W., Zhao, W.-D., Hamid, E., Sheng, J., Baydyuk, M., Wen, P. J., Jin, A., Momboisse, F., & Wu, L.-G. (2014). Post-fusion structural changes and their roles in exocytosis and endocytosis of dense-core vesicles. *Nature Communications*, *5*(1). https://doi.org/10.1038/ncomms4356

Clayton, E. L., Anggono, V., Smillie, K. J., Chau, N., Robinson, P. J., & Cousin, M. A. (2009). The Phospho-Dependent Dynamin-Syndapin Interaction Triggers Activity-Dependent Bulk Endocytosis of Synaptic Vesicles. *Journal of Neuroscience*, *29*(24), 7706-7717. https://doi.org/10.1523/jneurosci.1976-09.2009

Clayton, E. L., & Cousin, M. A. (2009). The molecular physiology of activity-dependent bulk endocytosis of synaptic vesicles. *Journal of Neurochemistry*, *111*(4), 901-914. https://doi.org/10.1111/j.1471-4159.2009.06384.x

Clayton, E. L., Evans, G. J. O., & Cousin, M. A. (2008). Bulk Synaptic Vesicle Endocytosis Is Rapidly Triggered during Strong Stimulation. *Journal of Neuroscience*, *28*(26), 6627-6632. https://doi.org/10.1523/jneurosci.1445-08.2008

Cocucci, E., Aguet, F., Boulant, S., & Kirchhausen, T. (2012). The First Five Seconds in the Life of a Clathrin-Coated Pit. *Cell*, *150*(3), 495-507. https://doi.org/10.1016/j.cell.2012.05.047

Cottrell, J. R., Li, B., Kyung, J. W., Ashford, C. J., Mann, J. J., Horvath, T. L., Ryan, T. A., Kim, S. H., & Gerber, D. J. (2016). Calcineurin Aγ is a Functional Phosphatase That Modulates Synaptic Vesicle Endocytosis. *Journal of Biological Chemistry*, *291*(4), 1948-1956. https://doi.org/10.1074/jbc.m115.705319

Cousin, M. A., & Robinson, P. J. (2001). The dephosphins: dephosphorylation by calcineurin triggers synaptic vesicle endocytosis. *Trends in Neurosciences*, *24*(11), 659-665. https://doi.org/10.1016/s0166-2236(00)01930-5

De Toledo, G. A., Fernández-Chacón, R., & Fernández, J. M. (1993). Release of secretory products during transient vesicle fusion. *Nature*, *363*(6429), 554-558. https://doi.org/10.1038/363554a0

Delgado, R., Maureira, C., Oliva, C., Kidokoro, Y., & Labarca, P. (2000). Size of Vesicle Pools, Rates of Mobilization, and Recycling at Neuromuscular Synapses of a Drosophila mutant, shibire. *Neuron*, *28*(3), 941-953. https://doi.org/10.1016/s0896-6273(00)00165-3

Delvendahl, I., Nicholas, Henrique, & Hallermann, S. (2016). Fast, Temperature-Sensitive and Clathrin-Independent Endocytosis at Central Synapses. *Neuron*, *90*(3), 492-498. https://doi.org/10.1016/j.neuron.2016.03.013

Den Otter, W. K., & Briels, W. J. (2011). The Generation of Curved Clathrin Coats from Flat Plaques. *Traffic*, *12*(10), 1407-1416. https://doi.org/10.1111/j.1600-0854.2011.01241.x

Diril, M. K., Wienisch, M., Jung, N., Klingauf, J., & Haucke, V. (2006). Stonin 2 Is an AP-2-Dependent Endocytic Sorting Adaptor for Synaptotagmin Internalization and Recycling. *Developmental Cell*, *10*(2), 233-244. https://doi.org/10.1016/j.devcel.2005.12.011

Dittman, J., & Ryan, T. A. (2009). Molecular Circuitry of Endocytosis at Nerve Terminals. *Annual Review of Cell and Developmental Biology*, *25*(1), 133-160. https://doi.org/10.1146/annurev.cellbio.042308.113302

Dittman, J. S., & Kaplan, J. M. (2006). Factors regulating the abundance and localization of synaptobrevin in the plasma membrane. *Proceedings of the National Academy of Sciences*, *103*(30), 11399-11404. https://doi.org/10.1073/pnas.0600784103

Edeling, M. A., Smith, C., & Owen, D. (2006). Life of a clathrin coat: insights from clathrin and AP structures. *Nature Reviews Molecular Cell Biology*, *7*(1), 32-44. https://doi.org/10.1038/nrm1786

Edvardson, S., Cinnamon, Y., Ta-Shma, A., Shaag, A., Yim, Y.-I., Zenvirt, S., Jalas, C., Lesage, S., Brice, A., Taraboulos, A., Kaestner, K. H., Greene, L. E., & Elpeleg, O. (2012). A Deleterious Mutation in DNAJC6 Encoding the Neuronal-Specific Clathrin-Uncoating Co-Chaperone Auxilin, Is Associated with Juvenile Parkinsonism. *PLoS ONE*, *7*(5), e36458. https://doi.org/10.1371/journal.pone.0036458

Elhamdani, A. (2006). Double Patch Clamp Reveals That Transient Fusion (Kiss-and-Run) Is a Major Mechanism of Secretion in Calf Adrenal Chromaffin Cells: High Calcium Shifts the Mechanism from Kiss-and-Run to Complete Fusion. *Journal of Neuroscience*, *26*(11), 3030-3036. https://doi.org/10.1523/jneurosci.5275-05.2006

Evans, G. J. O., & Cousin, M. A. (2007). Activity-Dependent Control of Slow Synaptic Vesicle Endocytosis by Cyclin-Dependent Kinase 5. *Journal of Neuroscience*, *27*(2), 401-411. https://doi.org/10.1523/jneurosci.3809-06.2007

Farsad, K., Ringstad, N., Takei, K., Floyd, S. R., Rose, K., & De Camilli, P. (2001). Generation of high curvature membranes mediated by direct endophilin bilayer interactions. *Journal of Cell Biology*, *155*(2), 193-200. https://doi.org/10.1083/jcb.200107075

Fergestad, T., & Broadie, K. (2001). Interaction of Stoned and Synaptotagmin in Synaptic Vesicle Endocytosis. *The Journal of Neuroscience*, *21*(4), 1218-1227. https://doi.org/10.1523/jneurosci.21-04-01218.2001

Ferguson, S. M., Brasnjo, G., Hayashi, M., Wolfel, M., Collesi, C., Giovedi, S., Raimondi, A., Gong, L. W., Ariel, P., Paradise, S., O'Toole, E., Flavell, R., Cremona, O., Miesenbock, G., Ryan, T. A., & De Camilli, P. (2007). A Selective Activity-Dependent Requirement for Dynamin 1 in Synaptic Vesicle Endocytosis. *Science*, *316*(5824), 570-574. https://doi.org/10.1126/science.1140621

Ferguson, S. M., & De Camilli, P. (2012). Dynamin, a membrane-remodelling GTPase. *Nature Reviews Molecular Cell Biology*, *13*(2), 75-88. https://doi.org/10.1038/nrm3266

Fernández-Alfonso, T., & Ryan, T. A. (2004). The Kinetics of Synaptic Vesicle Pool Depletion at CNS Synaptic Terminals. *Neuron*, *41*(6), 943-953. https://doi.org/10.1016/s0896-6273(04)00113-8

Fioravante, D., Chu, Y., Michael, Leitges, M., & Wade. (2011). Calcium-Dependent Isoforms of Protein Kinase C Mediate Posttetanic Potentiation at the Calyx of Held. *Neuron*, *70*(5), 1005-1019. https://doi.org/10.1016/j.neuron.2011.04.019

Ford, M. G. J., Mills, I. G., Peter, B. J., Vallis, Y., Praefcke, G. J. K., Evans, P. R., & McMahon, H. T. (2002). Curvature of clathrin-coated pits driven by epsin. *Nature*, *419*(6905), 361-366. https://doi.org/10.1038/nature01020

Frost, A., Perera, R., Roux, A., Spasov, K., Destaing, O., Egelman, E. H., De Camilli, P., & Unger, V. M. (2008). Structural Basis of Membrane Invagination by F-BAR Domains. *Cell*, *132*(5), 807-817. https://doi.org/10.1016/j.cell.2007.12.041

Frost, A., Unger, V. M., & De Camilli, P. (2009). The BAR Domain Superfamily: Membrane-Molding Macromolecules. *Cell*, *137*(2), 191-196. https://doi.org/10.1016/j.cell.2009.04.010

Gallop, J. L., Jao, C. C., Kent, H. M., Butler, P. J. G., Evans, P. R., Langen, R., & McMahon, H. T. (2006). Mechanism of endophilin N-BAR domain-mediated membrane curvature. *The EMBO Journal*, *25*(12), 2898-2910. https://doi.org/10.1038/sj.emboj.7601174

Gan, Q., & Watanabe, S. (2018). Synaptic Vesicle Endocytosis in Different Model Systems. *Front Cell Neurosci*, *12*, 171. https://doi.org/10.3389/fncel.2018.00171

Gandhi, S. P., & Stevens, C. F. (2003). Three modes of synaptic vesicular recycling revealed by single-vesicle imaging. *Nature*, *423*(6940), 607-613. https://doi.org/10.1038/nature01677

Granseth, B., Odermatt, B., Royle, S. J., & Lagnado, L. (2009). Comment on "The dynamic control of kiss-and-run and vesicular reuse probed with single nanoparticles". *Science*, *325*(5947), 1499; author reply 1499. https://doi.org/10.1126/science.1175790

Granseth, B., Odermatt, B., Stephen, & Lagnado, L. (2006). Clathrin-Mediated Endocytosis Is the Dominant Mechanism of Vesicle Retrieval at Hippocampal Synapses. *Neuron*, *51*(6), 773-786. https://doi.org/10.1016/j.neuron.2006.08.029

Gu, M., Schuske, K., Watanabe, S., Liu, Q., Baum, P., Garriga, G., & Jorgensen, E. M. (2008). μ2 adaptin facilitates but is not essential for synaptic vesicle recycling in Caenorhabditis elegans. *Journal of Cell Biology*, *183*(5), 881-892. https://doi.org/10.1083/jcb.200806088

Haucke, V. (1999). AP-2 Recruitment to Synaptotagmin Stimulated by Tyrosine-Based Endocytic Motifs. *Science*, *285*(5431), 1268-1271. https://doi.org/10.1126/science.285.5431.1268

Haucke, V., Neher, E., & Sigrist, S. J. (2011). Protein scaffolds in the coupling of synaptic exocytosis and endocytosis. *Nature Reviews Neuroscience*, *12*(3), 127-138. https://doi.org/10.1038/nrn2948

Hayashi, M., Raimondi, A., O'Toole, E., Paradise, S., Collesi, C., Cremona, O., Ferguson, S. M., & De Camilli, P. (2008). Cell- and stimulus-dependent heterogeneity of synaptic vesicle endocytic recycling mechanisms revealed by studies of dynamin 1-null neurons. *Proceedings of the National Academy of Sciences*, *105*(6), 2175-2180. https://doi.org/10.1073/pnas.0712171105

He, L., & Wu, L.-G. (2007). The debate on the kiss-and-run fusion at synapses. *Trends in Neurosciences*, *30*(9), 447-455. https://doi.org/10.1016/j.tins.2007.06.012

He, L., Wu, X.-S., Mohan, R., & Wu, L.-G. (2006). Two modes of fusion pore opening revealed by cell-attached recordings at a synapse. *Nature*, *444*(7115), 102-105. https://doi.org/10.1038/nature05250

He, L., Xue, L., Xu, J., McNeil, B. D., Bai, L., Melicoff, E., Adachi, R., & Wu, L.-G. (2009). Compound vesicle fusion increases quantal size and potentiates synaptic transmission. *Nature*, *459*(7243), 93-97. https://doi.org/10.1038/nature07860

Heerssen, H., Fetter, R. D., & Davis, G. W. (2008). Clathrin Dependence of Synaptic-Vesicle Formation at the Drosophila Neuromuscular Junction. *Current Biology*, *18*(6), 401-409. https://doi.org/10.1016/j.cub.2008.02.055

Heidelberger, R. (2001). ATP Is Required at an Early Step in Compensatory Endocytosis in Synaptic Terminals. *The Journal of Neuroscience*, *21*(17), 6467-6474. https://doi.org/10.1523/jneurosci.21-17-06467.2001

Heuser, J. (1980). Three-dimensional visualization of coated vesicle formation in fibroblasts. *Journal of Cell Biology*, *84*(3), 560-583. https://doi.org/10.1083/jcb.84.3.560

Heuser, J. (1989). The role of coated vesicles in recycling of synaptic vesicle membrane. *Cell Biol Int Rep*, *13*(12), 1063-1076. https://doi.org/10.1016/0309-1651(89)90020-9

Heuser, J. E., & Reese, T. S. (1973). EVIDENCE FOR RECYCLING OF SYNAPTIC VESICLE MEMBRANE DURING TRANSMITTER RELEASE AT THE FROG NEUROMUSCULAR JUNCTION. *Journal of Cell Biology*, *57*(2), 315-344. https://doi.org/10.1083/jcb.57.2.315

Heuser, J. E., & Reese, T. S. (1981). Structural changes after transmitter release at the frog neuromuscular junction. *Journal of Cell Biology*, *88*(3), 564-580. https://doi.org/10.1083/jcb.88.3.564

Holt, M., Cooke, A., Wu, M. M., & Lagnado, L. (2003). Bulk Membrane Retrieval in the Synaptic Terminal of Retinal Bipolar Cells. *The Journal of Neuroscience*, *23*(4), 1329-1339. https://doi.org/10.1523/jneurosci.23-04-01329.2003

Hosoi, N., Holt, M., & Sakaba, T. (2009). Calcium Dependence of Exo- and Endocytotic Coupling at a Glutamatergic Synapse. *Neuron*, *63*(2), 216-229. https://doi.org/10.1016/j.neuron.2009.06.010

Jackson, L. P., Kelly, B. T., McCoy, A. J., Gaffry, T., James, L. C., Collins, B. M., Höning, S., Evans, P. R., & Owen, D. J. (2010). A Large-Scale Conformational Change Couples Membrane Recruitment to Cargo Binding in the AP2 Clathrin Adaptor Complex. *Cell*, *141*(7), 1220-1229. https://doi.org/10.1016/j.cell.2010.05.006

Jackson, M. B., & Chapman, E. R. (2008). The fusion pores of Ca2+-triggered exocytosis. *Nature Structural & Molecular Biology*, *15*(7), 684-689. https://doi.org/10.1038/nsmb.1449

Jin, Y.-H., Wu, X.-S., Shi, B., Zhang, Z., Guo, X., Gan, L., Chen, Z., & Wu, L.-G. (2019). Protein Kinase C and Calmodulin Serve As Calcium Sensors for Calcium-Stimulated Endocytosis at Synapses. *The Journal of Neuroscience*, *39*(48), 9478-9490. https://doi.org/10.1523/jneurosci.0182-19.2019

Jockusch, W. J., Praefcke, G. J. K., McMahon, H. T., & Lagnado, L. (2005). Clathrin-Dependent and Clathrin-Independent Retrieval of Synaptic Vesicles in Retinal Bipolar Cells. *Neuron*, *46*(6), 869-878. https://doi.org/10.1016/j.neuron.2005.05.004

John, Christine, Gowrisankaran, S., Amandeep, Soukup, S.-F., Vidal, R., Capece, V., Freytag, S., Fischer, A., Verstreken, P., Bonn, S., Raimundo, N., & Milosevic, I. (2016). Endophilin-A Deficiency Induces the Foxo3a-Fbxo32 Network in the Brain and Causes Dysregulation of Autophagy and the Ubiquitin-Proteasome System. *Cell Reports*, *17*(4), 1071-1086. https://doi.org/10.1016/j.celrep.2016.09.058

Jorgensen, E. M., Hartwieg, E., Schuske, K., Nonet, M. L., Jin, Y., & Horvitz, H. R. (1995). Defective recycling of synaptic vesicles in synaptotagmin mutants of Caenorhabditis elegans. *Nature*, *378*(6553), 196-199. https://doi.org/10.1038/378196a0

Kaksonen, M., & Roux, A. (2018). Mechanisms of clathrin-mediated endocytosis. *Nature Reviews Molecular Cell Biology*, *19*(5), 313-326. https://doi.org/10.1038/nrm.2017.132

Kasprowicz, J., Kuenen, S., Miskiewicz, K., Habets, R. L. P., Smitz, L., & Verstreken, P. (2008). Inactivation of clathrin heavy chain inhibits synaptic recycling but allows bulk membrane uptake. *Journal of Cell Biology*, *182*(5), 1007-1016. https://doi.org/10.1083/jcb.200804162

Kasprowicz, J., Kuenen, S., Swerts, J., Miskiewicz, K., & Verstreken, P. (2014). Dynamin photoinactivation blocks Clathrin and α-adaptin recruitment and induces bulk membrane retrieval. *Journal of Cell Biology*, *204*(7), 1141-1156. https://doi.org/10.1083/jcb.201310090

Kavalali, E. T., & Jorgensen, E. M. (2014). Visualizing presynaptic function. *Nature Neuroscience*, *17*(1), 10-16. https://doi.org/10.1038/nn.3578

Kawasaki, F., Hazen, M., & Ordway, R. W. (2000). Fast synaptic fatigue in shibire mutants reveals a rapid requirement for dynamin in synaptic vesicle membrane trafficking. *Nature Neuroscience*, *3*(9), 859-860. https://doi.org/10.1038/78753

Kelly, B. T., Graham, S. C., Liska, N., Dannhauser, P. N., Honing, S., Ungewickell, E. J., & Owen, D. J. (2014). AP2 controls clathrin polymerization with a membrane-activated switch. *Science*, *345*(6195), 459-463. https://doi.org/10.1126/science.1254836

Kennedy, M. J., & Ehlers, M. D. (2006). ORGANELLES AND TRAFFICKING MACHINERY FOR POSTSYNAPTIC PLASTICITY. *Annual Review of Neuroscience*, *29*(1), 325-362. https://doi.org/10.1146/annurev.neuro.29.051605.112808

Kessels, M. M., & Qualmann, B. (2021). Interplay between membrane curvature and the actin cytoskeleton. *Current Opinion in Cell Biology*, *68*, 10-19. https://doi.org/10.1016/j.ceb.2020.08.008

Khanna, R., Li, Q., Bewersdorf, J., & Stanley, E. F. (2007). The presynaptic CaV2.2 channel-transmitter release site core complex. *European Journal of Neuroscience*, *26*(3), 547-559. https://doi.org/10.1111/j.1460-9568.2007.05680.x

Khanna, R., Li, Q., Schlichter, L. C., & Stanley, E. F. (2007). The transmitter release-site CaV2.2 channel cluster is linked to an endocytosis coat protein complex.

European Journal of Neuroscience, *26*(3), 560-574. https://doi.org/10.1111/j.1460-9568.2007.05681.x

Kim, S. H., & Ryan, T. A. (2009). Synaptic Vesicle Recycling at CNS Synapses without AP-2. *Journal of Neuroscience*, *29*(12), 3865-3874. https://doi.org/10.1523/jneurosci.5639-08.2009

Kirchhausen, T. (2009). Imaging endocytic clathrin structures in living cells. *Trends in Cell Biology*, *19*(11), 596-605. https://doi.org/10.1016/j.tcb.2009.09.002

Klyachko, V. A., & Jackson, M. B. (2002). Capacitance steps and fusion pores of small and large-dense-core vesicles in nerve terminals. *Nature*, *418*(6893), 89-92. https://doi.org/10.1038/nature00852

Koch, M., & Holt, M. (2012). Coupling exo- and endocytosis: An essential role for PIP2 at the synapse. *Biochimica et Biophysica Acta (BBA) - Molecular and Cell Biology of Lipids*, *1821*(8), 1114-1132. https://doi.org/10.1016/j.bbalip.2012.02.008

Koenig, J., & Ikeda, K. (1989). Disappearance and reformation of synaptic vesicle membrane upon transmitter release observed under reversible blockage of membrane retrieval. *The Journal of Neuroscience*, *9*(11), 3844-3860. https://doi.org/10.1523/jneurosci.09-11-03844.1989

Koenig, J. H., & Ikeda, K. (1996). Synaptic vesicles have two distinct recycling pathways. *Journal of Cell Biology*, *135*(3), 797-808. https://doi.org/10.1083/jcb.135.3.797

Kononenko, N. L., Diril, M. K., Puchkov, D., Kintscher, M., Koo, S. J., Pfuhl, G., Winter, Y., Wienisch, M., Klingauf, J., Breustedt, J., Schmitz, D., Maritzen, T., & Haucke, V. (2013). Compromised fidelity of endocytic synaptic vesicle protein sorting in the absence of stonin 2. *Proceedings of the National Academy of Sciences*, *110*(6), E526-E535. https://doi.org/10.1073/pnas.1218432110

Kononenko, N. L., & Haucke, V. (2015). Molecular Mechanisms of Presynaptic Membrane Retrieval and Synaptic Vesicle Reformation. *Neuron*, *85*(3), 484-496. https://doi.org/10.1016/j.neuron.2014.12.016

Kononenko, N. L., Puchkov,D., Classen,G.A., Walter,A.M., Pechstein,A., Sawade,L., Kaempf,N., Trimbuch,T., Lorenz,D., Rosenmund,C., Maritzen,T., and Haucke,V. (2014). Clathrin/AP-2 Mediate Synaptic Vesicle Reformation from Endosome-like Vacuoles but Are Not Essential for Membrane Retrieval at Central Synapses. *Neuron*, *82*(5), 981-988. https://doi.org/10.1016/j.neuron.2014.05.007

Koo, S. J., Markovic, S., Puchkov, D., Mahrenholz, C. C., Beceren-Braun, F., Maritzen, T., Dernedde, J., Volkmer, R., Oschkinat, H., & Haucke, V. (2011). SNARE motif-mediated sorting of synaptobrevin by the endocytic adaptors clathrin assembly lymphoid myeloid leukemia (CALM) and AP180 at synapses. *Proceedings of the National Academy of Sciences*, *108*(33), 13540-13545. https://doi.org/10.1073/pnas.1107067108

Krauß, M., & Haucke, V. (2007). Phosphoinositide-metabolizing enzymes at the interface between membrane traffic and cell signalling. *EMBO reports*, *8*(3), 241-246. https://doi.org/10.1038/sj.embor.7400919

Krauss, M., Kukhtina, V., Pechstein, A., & Haucke, V. (2006). Stimulation of phosphatidylinositol kinase type I-mediated phosphatidylinositol (4,5)-bisphosphate synthesis by AP-2 -cargo complexes. *Proceedings of the National*

Academy of Sciences, *103*(32), 11934-11939. https://doi.org/10.1073/pnas.0510306103

Krebs, C. E., Karkheiran, S., Powell, J. C., Cao, M., Makarov, V., Darvish, H., Di Paolo, G., Walker, R. H., Shahidi, G. A., Buxbaum, J. D., De Camilli, P., Yue, Z., & Paisán-Ruiz, C. (2013). The Sac1 Domain of SYNJ 1 Identified Mutated in a Family with Early-Onset Progressive P arkinsonism with Generalized Seizures. *Human Mutation*, *34*(9), 1200-1207. https://doi.org/10.1002/humu.22372

Kuner, T., Li, Y., Gee, K. R., Bonewald, L. F., & Augustine, G. J. (2008). Photolysis of a caged peptide reveals rapid action of N-ethylmaleimide sensitive factor before neurotransmitter release. *Proceedings of the National Academy of Sciences*, *105*(1), 347-352. https://doi.org/10.1073/pnas.0707197105

Lampe, M., Vassilopoulos, S., & Merrifield, C. (2016). Clathrin coated pits, plaques and adhesion. *Journal of Structural Biology*, *196*(1), 48-56. https://doi.org/10.1016/j.jsb.2016.07.009

Larkin, J. M., Donzell, W. C., & Anderson, R. G. (1986). Potassium-dependent assembly of coated pits: new coated pits form as planar clathrin lattices. *The Journal of Cell Biology*, *103*(6), 2619-2627. https://doi.org/10.1083/jcb.103.6.2619

Lauwers, E., Goodchild, R., & Verstreken, P. (2016). Membrane Lipids in Presynaptic Function and Disease. *Neuron*, *90*(1), 11-25. https://doi.org/10.1016/j.neuron.2016.02.033

Le Clainche, C., Pauly, B. S., Zhang, C. X., Engqvist-Goldstein, Å. E. Y., Cunningham, K., & Drubin, D. G. (2007). A Hip1R–cortactin complex negatively regulates actin assembly associated with endocytosis. *The EMBO Journal*, *26*(5), 1199-1210. https://doi.org/10.1038/sj.emboj.7601576

Lee, A., Frank, D. W., Marks, M. S., & Lemmon, M. A. (1999). Dominant-negative inhibition of receptor-mediated endocytosis by a dynamin-1 mutant with a defective pleckstrin homology domain. *Current Biology*, *9*(5), 261-265. https://doi.org/10.1016/s0960-9822(99)80115-8

Lee, S. H., Liu, L., Wang, Y. T., & Sheng, M. (2002). Clathrin Adaptor AP2 and NSF Interact with Overlapping Sites of GluR2 and Play Distinct Roles in AMPA Receptor Trafficking and Hippocampal LTD. *Neuron*, *36*(4), 661-674. https://doi.org/10.1016/s0896-6273(02)01024-3

Leitz, J., & Kavalali, E. T. (2011). Ca2+ Influx Slows Single Synaptic Vesicle Endocytosis. *Journal of Neuroscience*, *31*(45), 16318-16326. https://doi.org/10.1523/jneurosci.3358-11.2011

Lemmon, M. A. (2008). Membrane recognition by phospholipid-binding domains. *Nature Reviews Molecular Cell Biology*, *9*(2), 99-111. https://doi.org/10.1038/nrm2328

Li, L., Wu, X., Yue, H.-Y., Zhu, Y.-C., & Xu, J. (2016). Myosin light chain kinase facilitates endocytosis of synaptic vesicles at hippocampal boutons. *Journal of Neurochemistry*, *138*(1), 60-73. https://doi.org/10.1111/jnc.13635

Li, Y. C., Chanaday, N. L., Xu, W., & Kavalali, E. T. (2017). Synaptotagmin-1- and Synaptotagmin-7-Dependent Fusion Mechanisms Target Synaptic Vesicles to Kinetically Distinct Endocytic Pathways. *Neuron*, *93*(3), 616-631.e613. https://doi.org/10.1016/j.neuron.2016.12.010

Littleton, J. T., Bai, J., Vyas, B., Desai, R., Baltus, A. E., Garment, M. B., Carlson, S. D., Ganetzky, B., & Chapman, E. R. (2001). synaptotagmin Mutants Reveal Essential

Functions for the C2B Domain in Ca2+-Triggered Fusion and Recycling of Synaptic VesiclesIn Vivo. *The Journal of Neuroscience*, *21*(5), 1421-1433. https://doi.org/10.1523/jneurosci.21-05-01421.2001

Lou, X., Paradise, S., Ferguson, S. M., & De Camilli, P. (2008). Selective saturation of slow endocytosis at a giant glutamatergic central synapse lacking dynamin 1. *Proceedings of the National Academy of Sciences*, *105*(45), 17555-17560. https://doi.org/10.1073/pnas.0809621105

Maritzen, T., Podufall, J., & Haucke, V. (2010). Stonins-Specialized Adaptors for Synaptic Vesicle Recycling and Beyond? *Traffic*, *11*(1), 8-15. https://doi.org/10.1111/j.1600-0854.2009.00971.x

Martin, T. F. J. (2015). PI(4,5)P2-binding effector proteins for vesicle exocytosis. *Biochimica et Biophysica Acta (BBA) - Molecular and Cell Biology of Lipids*, *1851*(6), 785-793. https://doi.org/10.1016/j.bbalip.2014.09.017

Masuda, M., Takeda, S., Sone, M., Ohki, T., Mori, H., Kamioka, Y., & Mochizuki, N. (2006). Endophilin BAR domain drives membrane curvature by two newly identified structure-based mechanisms. *The EMBO Journal*, *25*(12), 2889-2897. https://doi.org/10.1038/sj.emboj.7601176

Matteis, M. A. D., & Godi, A. (2004). PI-loting membrane traffic. *Nature Cell Biology*, *6*(6), 487-492. https://doi.org/10.1038/ncb0604-487

Matthews, G., & Sterling, P. (2008). Evidence That Vesicles Undergo Compound Fusion on the Synaptic Ribbon. *Journal of Neuroscience*, *28*(21), 5403-5411. https://doi.org/10.1523/jneurosci.0935-08.2008

Mettlen, M., Chen, P.-H., Srinivasan, S., Danuser, G., & Schmid, S. L. (2018). Regulation of Clathrin-Mediated Endocytosis. *Annual Review of Biochemistry*, *87*(1), 871-896. https://doi.org/10.1146/annurev-biochem-062917-012644

Miller, T. M., & Heuser, J. E. (1984). Endocytosis of synaptic vesicle membrane at the frog neuromuscular junction. *Journal of Cell Biology*, *98*(2), 685-698. https://doi.org/10.1083/jcb.98.2.685

Milosevic, I., Giovedi, S., Lou, X., Raimondi, A., Collesi, C., Shen, H., Paradise, S., O'Toole, E., Ferguson, S., Cremona, O., & Pietro. (2011). Recruitment of Endophilin to Clathrin-Coated Pit Necks Is Required for Efficient Vesicle Uncoating after Fission. *Neuron*, *72*(4), 587-601. https://doi.org/10.1016/j.neuron.2011.08.029

Morgan, J. R., Zhao, X., Womack, M., Prasad, K., Augustine, G. J., & Lafer, E. M. (1999). A Role for the Clathrin Assembly Domain of AP180 in Synaptic Vesicle Endocytosis. *The Journal of Neuroscience*, *19*(23), 10201-10212. https://doi.org/10.1523/jneurosci.19-23-10201.1999

Moser, T., & Beutner, D. (2000). Kinetics of exocytosis and endocytosis at the cochlear inner hair cell afferent synapse of the mouse. *Proceedings of the National Academy of Sciences*, *97*(2), 883-888. https://doi.org/10.1073/pnas.97.2.883

Mullen, G. P., Grundahl, K. M., Gu, M., Watanabe, S., Hobson, R. J., Crowell, J. A., McManus, J. R., Mathews, E. A., Jorgensen, E. M., & Rand, J. B. (2012). UNC-41/Stonin Functions with AP2 to Recycle Synaptic Vesicles in Caenorhabditis elegans. *PLoS ONE*, *7*(7), e40095. https://doi.org/10.1371/journal.pone.0040095

Nalefski, E. A., & Falke, J. J. (1996). The C2 domain calcium-binding motif: Structural and functional diversity. *Protein Science*, *5*(12), 2375-2390. https://doi.org/10.1002/pro.5560051201

Neher, E. (2010). What is Rate-Limiting during Sustained Synaptic Activity: Vesicle Supply or the Availability of Release Sites. *Front Synaptic Neurosci*, *2*, 144. https://doi.org/10.3389/fnsyn.2010.00144

Neves, G., Gomis, A., & Lagnado, L. (2001). Calcium influx selects the fast mode of endocytosis in the synaptic terminal of retinal bipolar cells. *Proceedings of the National Academy of Sciences*, *98*(26), 15282-15287. https://doi.org/10.1073/pnas.261311698

Newton, A. C. (2010). Protein kinase C: poised to signal. *Am J Physiol Endocrinol Metab*, *298*(3), E395-402. https://doi.org/10.1152/ajpendo.00477.2009

Nguyen, T. H., Qiu, X., Sun, J., & Meunier, F. A. (2014). Bulk endocytosis at neuronal synapses. *Science China Life Sciences*, *57*(4), 378-383. https://doi.org/10.1007/s11427-014-4636-z

Nicholson-Fish, J. C., Kokotos, A. C., Gillingwater, T. H., Smillie, K. J., & Cousin, M. A. (2015). VAMP4 Is an Essential Cargo Molecule for Activity-Dependent Bulk Endocytosis. *Neuron*, *88*(5), 973-984. https://doi.org/10.1016/j.neuron.2015.10.043

Nicholson-Tomishima, K., & Ryan, T. A. (2004). Kinetic efficiency of endocytosis at mammalian CNS synapses requires synaptotagmin I. *Proceedings of the National Academy of Sciences*, *101*(47), 16648-16652. https://doi.org/10.1073/pnas.0406968101

Niemann, H., Blasi, J., & Jahn, R. (1994). Clostridial neurotoxins: new tools for dissecting exocytosis. *Trends in Cell Biology*, *4*(5), 179-185. https://doi.org/10.1016/0962-8924(94)90203-8

Nonet, M. L., Holgado, A. M., Brewer, F., Serpe, C. J., Norbeck, B. A., Holleran, J., Wei, L., Hartwieg, E., Jorgensen, E. M., & Alfonso, A. (1999). UNC-11, a Caenorhabditis elegans AP180 Homologue, Regulates the Size and Protein Composition of Synaptic Vesicles. *Molecular Biology of the Cell*, *10*(7), 2343-2360. https://doi.org/10.1091/mbc.10.7.2343

Paillart, C., Li, J., Matthews, G., & Sterling, P. (2003). Endocytosis and Vesicle Recycling at a Ribbon Synapse. *The Journal of Neuroscience*, *23*(10), 4092-4099. https://doi.org/10.1523/jneurosci.23-10-04092.2003

Perrais, D., Kleppe, I. C., Taraska, J. W., & Almers, W. (2004). Recapture after exocytosis causes differential retention of protein in granules of bovine chromaffin cells. *The Journal of Physiology*, *560*(2), 413-428. https://doi.org/10.1113/jphysiol.2004.064410

Peter, B. J. (2004). BAR Domains as Sensors of Membrane Curvature: The Amphiphysin BAR Structure. *Science*, *303*(5657), 495-499. https://doi.org/10.1126/science.1092586

Poskanzer, K. E., Fetter, R. D., & Davis, G. W. (2006). Discrete Residues in the C2B Domain of Synaptotagmin I Independently Specify Endocytic Rate and Synaptic Vesicle Size. *Neuron*, *50*(1), 49-62. https://doi.org/10.1016/j.neuron.2006.02.021

Poskanzer, K. E., Marek, K. W., Sweeney, S. T., & Davis, G. W. (2003). Synaptotagmin I is necessary for compensatory synaptic vesicle endocytosis in vivo. *Nature*, *426*(6966), 559-563. https://doi.org/10.1038/nature02184

Posor, Y., Eichhorn-Grünig, M., & Haucke, V. (2015). Phosphoinositides in endocytosis. *Biochimica et Biophysica Acta (BBA) - Molecular and Cell Biology of Lipids*, *1851*(6), 794-804. https://doi.org/10.1016/j.bbalip.2014.09.014

Powell, K. A., Valova, V. A., Malladi, C. S., Jensen, O. N., Larsen, M. R., & Robinson, P. J. (2000). Phosphorylation of Dynamin I on Ser-795 by Protein Kinase C Blocks Its Association with Phospholipids. *Journal of Biological Chemistry*, *275*(16), 11610-11617. https://doi.org/10.1074/jbc.275.16.11610

Preta, G., Cronin, J. G., & Sheldon, I. M. (2015). Dynasore - not just a dynamin inhibitor. *Cell Communication and Signaling*, *13*(1). https://doi.org/10.1186/s12964-015-0102-1

Raimondi, A., Ferguson, S. M., Lou, X., Armbruster, M., Paradise, S., Giovedi, S., Messa, M., Kono, N., Takasaki, J., Cappello, V., O'Toole, E., Ryan, T. A., & De Camilli, P. (2011). Overlapping role of dynamin isoforms in synaptic vesicle endocytosis. *Neuron*, *70*(6), 1100-1114. https://doi.org/10.1016/j.neuron.2011.04.031

Renard, H. F., & Boucrot, E. (2021). Unconventional endocytic mechanisms. *Curr Opin Cell Biol*, *71*, 120-129. https://doi.org/10.1016/j.ceb.2021.03.001

Renden, R., & von Gersdorff, H. (2007). Synaptic vesicle endocytosis at a CNS nerve terminal: faster kinetics at physiological temperatures and increased endocytotic capacity during maturation. *J Neurophysiol*, *98*(6), 3349-3359. https://doi.org/10.1152/jn.00898.2007

Ringstad, N., Nemoto, Y., & De Camilli, P. (2001). Differential Expression of Endophilin 1 and 2 Dimers at Central Nervous System Synapses. *Journal of Biological Chemistry*, *276*(44), 40424-40430. https://doi.org/10.1074/jbc.m106338200

Robinson, P. J., Sontag, J.-M., Liu, J.-P., Fykse, E. M., Slaughter, C., McMahontt, H., & Südhof, T. C. (1993). Dynamin GTPase regulated by protein kinase C phosphorylation in nerve terminals. *Nature*, *365*(6442), 163-166. https://doi.org/10.1038/365163a0

Saffarian, S., Cocucci, E., & Kirchhausen, T. (2009). Distinct Dynamics of Endocytic Clathrin-Coated Pits and Coated Plaques. *PLoS Biology*, *7*(9), e1000191. https://doi.org/10.1371/journal.pbio.1000191

Saheki, Y., & De Camilli, P. (2012). Synaptic Vesicle Endocytosis. *Cold Spring Harbor Perspectives in Biology*, *4*(9), a005645-a005645. https://doi.org/10.1101/cshperspect.a005645

Sakaba, T., Kononenko, N. L., Bacetic, J., Pechstein, A., Schmoranzer, J., Yao, L., Barth, H., Shupliakov, O., Kobler, O., Aktories, K., & Haucke, V. (2013). Fast neurotransmitter release regulated by the endocytic scaffold intersectin. *Proceedings of the National Academy of Sciences*, *110*(20), 8266-8271. https://doi.org/10.1073/pnas.1219234110

Sankaranarayanan, S., & Ryan, T. A. (2000). Real-time measurements of vesicle-SNARE recycling in synapses of the central nervous system. *Nature Cell Biology*, *2*(4), 197-204. https://doi.org/10.1038/35008615

Sankaranarayanan, S., & Ryan, T. A. (2001). Calcium accelerates endocytosis of vSNAREs at hippocampal synapses. *Nature Neuroscience*, *4*(2), 129-136. https://doi.org/10.1038/83949

Sato, K., Ernstrom, G. G., Watanabe, S., Weimer, R. M., Chen, C. H., Sato, M., Siddiqui, A., Jorgensen, E. M., & Grant, B. D. (2009). Differential requirements for clathrin in receptor-mediated endocytosis and maintenance of synaptic vesicle pools. *Proceedings of the National Academy of Sciences*, *106*(4), 1139-1144. https://doi.org/10.1073/pnas.0809541106

Schlossman, D. M., Schmid, S. L., Braell, W. A., & Rothman, J. E. (1984). An enzyme that removes clathrin coats: purification of an uncoating ATPase. *Journal of Cell Biology*, *99*(2), 723-733. https://doi.org/10.1083/jcb.99.2.723

Schmid, E. M., & McMahon, H. T. (2007). Integrating molecular and network biology to decode endocytosis. *Nature*, *448*(7156), 883-888. https://doi.org/10.1038/nature06031

Schuske, K. R., Richmond, J. E., Matthies, D. S., Davis, W. S., Runz, S., Rube, D. A., Van Der Bliek, A. M., & Jorgensen, E. M. (2003). Endophilin Is Required for Synaptic Vesicle Endocytosis by Localizing Synaptojanin. *Neuron*, *40*(4), 749-762. https://doi.org/10.1016/s0896-6273(03)00667-6

Sharon, Daniela, Stephen, Höning, S., Margaret, Andrew, & David. (2011). The Molecular Basis for the Endocytosis of Small R-SNAREs by the Clathrin Adaptor CALM. *Cell*, *147*(5), 1118-1131. https://doi.org/10.1016/j.cell.2011.10.038

Shi, B., Jin, Y.H., Wu, L.G. (2022) Dynamin 1 controls vesicle size and endocytosis at hippocampal synapses. *Cell Calcium,* 103:102564. https://doi.org/10.1016/j.ceca.2022.102564

Shimada, A., Niwa, H., Tsujita, K., Suetsugu, S., Nitta, K., Hanawa-Suetsugu, K., Akasaka, R., Nishino, Y., Toyama, M., Chen, L., Liu, Z.-J., Wang, B.-C., Yamamoto, M., Terada, T., Miyazawa, A., Tanaka, A., Sugano, S., Shirouzu, M., Nagayama, K., . . . Yokoyama, S. (2007). Curved EFC/F-BAR-Domain Dimers Are Joined End to End into a Filament for Membrane Invagination in Endocytosis. *Cell*, *129*(4), 761-772. https://doi.org/10.1016/j.cell.2007.03.040

Shin, W., Ge, L., Arpino, G., Villarreal, S. A., Hamid, E., Liu, H., Zhao, W.-D., Wen, P. J., Chiang, H.-C., & Wu, L.-G. (2018). Visualization of Membrane Pore in Live Cells Reveals a Dynamic-Pore Theory Governing Fusion and Endocytosis. *Cell*, *173*(4), 934-945.e912. https://doi.org/10.1016/j.cell.2018.02.062

Shin, W., Wei, L., Arpino, G., Ge, L., Guo, X., Chan, C. Y., Hamid, E., Shupliakov, O., Bleck, C. K. E., & Wu, L. G. (2021). Preformed Ω-profile closure and kiss-and-run mediate endocytosis and diverse endocytic modes in neuroendocrine chromaffin cells. *Neuron*. https://doi.org/10.1016/j.neuron.2021.07.019

Shupliakov, O. (1997). Synaptic Vesicle Endocytosis Impaired by Disruption of Dynamin-SH3 Domain Interactions. *Science*, *276*(5310), 259-263. https://doi.org/10.1126/science.276.5310.259

Simonsen, A., Wurmser, A. E., Emr, S. D., & Stenmark, H. (2001). The role of phosphoinositides in membrane transport. *Current Opinion in Cell Biology*, *13*(4), 485-492. https://doi.org/10.1016/s0955-0674(00)00240-4

Slepnev, V. I., & De Camilli, P. (2000). Accessory factors in clathrin-dependent synaptic vesicle endocytosis. *Nature Reviews Neuroscience*, *1*(3), 161-172. https://doi.org/10.1038/35044540

Smillie, K. J., Pawson, J., Perkins, E. M., Jackson, M., & Cousin, M. A. (2013). Control of synaptic vesicle endocytosis by an extracellular signalling molecule. *Nat Commun*, *4*, 2394. https://doi.org/10.1038/ncomms3394

Smith, C., & Neher, E. (1997). Multiple Forms of Endocytosis In Bovine Adrenal Chromaffin Cells. *Journal of Cell Biology*, *139*(4), 885-894. https://doi.org/10.1083/jcb.139.4.885

Soykan, T., Kaempf, N., Sakaba, T., Vollweiter, D., Goerdeler, F., Puchkov, D., Kononenko, N. L., & Haucke, V. (2017). Synaptic Vesicle Endocytosis Occurs on Multiple Timescales and Is Mediated by Formin-Dependent Actin Assembly. *Neuron*, *93*(4), 854-866.e854. https://doi.org/10.1016/j.neuron.2017.02.011

Srinivasan, G., Kim, J. H., & von Gersdorff, H. (2008). The pool of fast releasing vesicles is augmented by myosin light chain kinase inhibition at the calyx of Held synapse. *J Neurophysiol*, *99*(4), 1810-1824. https://doi.org/10.1152/jn.00949.2007

Südhof, T. C. (2004). THE SYNAPTIC VESICLE CYCLE. *Annual Review of Neuroscience*, *27*(1), 509-547. https://doi.org/10.1146/annurev.neuro.26.041002.131412

Sun, J.-Y., & Wu, L.-G. (2001). Fast Kinetics of Exocytosis Revealed by Simultaneous Measurements of Presynaptic Capacitance and Postsynaptic Currents at a Central Synapse. *Neuron*, *30*(1), 171-182. https://doi.org/10.1016/s0896-6273(01)00271-9

Sun, J.-Y., Wu, X.-S., & Wu, L.-G. (2002). Single and multiple vesicle fusion induce different rates of endocytosis at a central synapse. *Nature*, *417*(6888), 555-559. https://doi.org/10.1038/417555a

Sun, T., Wu, X. S., Xu, J., McNeil, B. D., Pang, Z. P., Yang, W., Bai, L., Qadri, S., Molkentin, J. D., Yue, D. T., & Wu, L. G. (2010). The Role of Calcium/Calmodulin-Activated Calcineurin in Rapid and Slow Endocytosis at Central Synapses. *Journal of Neuroscience*, *30*(35), 11838-11847. https://doi.org/10.1523/jneurosci.1481-10.2010

Tan, T. C., Valova, V. A., Malladi, C. S., Graham, M. E., Berven, L. A., Jupp, O. J., Hansra, G., McClure, S. J., Sarcevic, B., Boadle, R. A., Larsen, M. R., Cousin, M. A., & Robinson, P. J. (2003). Cdk5 is essential for synaptic vesicle endocytosis. *Nature Cell Biology*, *5*(8), 701-710. https://doi.org/10.1038/ncb1020

Teng, H., & Wilkinson, R. S. (2000). Clathrin-Mediated Endocytosis near Active Zones in Snake Motor Boutons. *The Journal of Neuroscience*, *20*(21), 7986-7993. https://doi.org/10.1523/jneurosci.20-21-07986.2000

Thomas, P., Lee, A., Wong, J., & Almers, W. (1994). A triggered mechanism retrieves membrane in seconds after Ca(2+)-stimulated exocytosis in single pituitary cells. *Journal of Cell Biology*, *124*(5), 667-675. https://doi.org/10.1083/jcb.124.5.667

Ullrich, B., Li, C., Zhang, J. Z., McMahon, H., Anderson, R. G. W., Geppert, M., & Südhof, T. C. (1994). Functional properties of multiple synaptotagmins in brain. *Neuron*, *13*(6), 1281-1291. https://doi.org/10.1016/0896-6273(94)90415-4

Ungewickell, E. (1985). The 70-kd mammalian heat shock proteins are structurally and functionally related to the uncoating protein that releases clathrin triskelia from

coated vesicles. *The EMBO Journal*, *4*(13A), 3385-3391. https://doi.org/10.1002/j.1460-2075.1985.tb04094.x

Ungewickell, E., Ungewickell, H., Holstein, S. E. H., Lindner, R., Prasad, K., Barouch, W., Martini, B., Greene, L. E., & Eisenberg, E. (1995). Role of auxilin in uncoating clathrin-coated vesicles. *Nature*, *378*(6557), 632-635. https://doi.org/10.1038/378632a0

Vallis, Y., Wigge, P., Marks, B., Evans, P. R., & McMahon, H. T. (1999). Importance of the pleckstrin homology domain of dynamin in clathrin-mediated endocytosis. *Current Biology*, *9*(5), 257-263. https://doi.org/10.1016/s0960-9822(99)80114-6

Von Gersdorff, H., & Matthews, G. (1994). Inhibition of endocytosis by elevated internal calcium in a synaptic terminal. *Nature*, *370*(6491), 652-655. https://doi.org/10.1038/370652a0

von Kleist, L., Stahlschmidt, W., Bulut, H., Gromova, K., Puchkov, D., Mark, Kylie, Tomilin, N., Pechstein, A., Chau, N., Chircop, M., Sakoff, J., Jens, Saenger, W., Kräusslich, H.-G., Shupliakov, O., Phillip, McCluskey, A., & Haucke, V. (2011). Role of the Clathrin Terminal Domain in Regulating Coated Pit Dynamics Revealed by Small Molecule Inhibition. *Cell*, *146*(3), 471-484. https://doi.org/10.1016/j.cell.2011.06.025

Walter, A. M., Müller, R., Tawfik, B., Wierda, K. D., Pinheiro, P. S., Nadler, A., McCarthy, A. W., Ziomkiewicz, I., Kruse, M., Reither, G., Rettig, J., Lehmann, M., Haucke, V., Hille, B., Schultz, C., & Sørensen, J. B. (2017). Phosphatidylinositol 4,5-bisphosphate optical uncaging potentiates exocytosis. *eLife*, *6*. https://doi.org/10.7554/elife.30203

Watanabe, S., Liu, Q., Davis, M. W., Hollopeter, G., Thomas, N., Jorgensen, N. B., & Jorgensen, E. M. (2013). Ultrafast endocytosis at Caenorhabditis elegans neuromuscular junctions. *eLife*, *2*. https://doi.org/10.7554/elife.00723

Watanabe, S., Mamer, L. E., Raychaudhuri, S., Luvsanjav, D., Eisen, J., Trimbuch, T., Söhl-Kielczynski, B., Fenske, P., Milosevic, I., Rosenmund, C., & Jorgensen, E. M. (2018). Synaptojanin and Endophilin Mediate Neck Formation during Ultrafast Endocytosis. *Neuron*, *98*(6), 1184-1197.e1186. https://doi.org/10.1016/j.neuron.2018.06.005

Watanabe, S., Rost, B. R., Camacho-Pérez, M., Davis, M. W., Söhl-Kielczynski, B., Rosenmund, C., & Jorgensen, E. M. (2013). Ultrafast endocytosis at mouse hippocampal synapses. *Nature*, *504*(7479), 242-247. https://doi.org/10.1038/nature12809

Watanabe, S., Trimbuch, T., Camacho-Pérez, M., Rost, B. R., Brokowski, B., Söhl-Kielczynski, B., Felies, A., Davis, M. W., Rosenmund, C., & Jorgensen, E. M. (2014). Clathrin regenerates synaptic vesicles from endosomes. *Nature*, *515*(7526), 228-233. https://doi.org/10.1038/nature13846

Weissenhorn, W. (2005). Crystal Structure of the Endophilin-A1 BAR Domain. *Journal of Molecular Biology*, *351*(3), 653-661. https://doi.org/10.1016/j.jmb.2005.06.013

Whiteheart, S. W., Rossnagel, K., Buhrow, S. A., Brunner, M., Jaenicke, R., & Rothman, J. E. (1994). N-ethylmaleimide-sensitive fusion protein: a trimeric ATPase whose hydrolysis of ATP is required for membrane fusion. *Journal of Cell Biology*, *126*(4), 945-954. https://doi.org/10.1083/jcb.126.4.945

Willox, A. K., & Royle, S. J. (2012). Stonin 2 Is a Major Adaptor Protein for Clathrin-Mediated Synaptic Vesicle Retrieval. *Current Biology*, *22*(15), 1435-1439. https://doi.org/10.1016/j.cub.2012.05.048

Wu, L.-G., & Borst, J. G. G. (1999). The Reduced Release Probability of Releasable Vesicles during Recovery from Short-Term Synaptic Depression. *Neuron*, *23*(4), 821-832. https://doi.org/10.1016/s0896-6273(01)80039-8

Wu, L.-G., Hamid, E., Shin, W., & Chiang, H.-C. (2014). Exocytosis and Endocytosis: Modes, Functions, and Coupling Mechanisms. *Annual Review of Physiology*, *76*(1), 301-331. https://doi.org/10.1146/annurev-physiol-021113-170305

Wu, L. G., Ryan, T. A., & Lagnado, L. (2007). Modes of Vesicle Retrieval at Ribbon Synapses, Calyx-Type Synapses, and Small Central Synapses. *Journal of Neuroscience*, *27*(44), 11793-11802. https://doi.org/10.1523/jneurosci.3471-07.2007

Wu, W., & Wu, L. G. (2007). Rapid bulk endocytosis and its kinetics of fission pore closure at a central synapse. *Proceedings of the National Academy of Sciences*, *104*(24), 10234-10239. https://doi.org/10.1073/pnas.0611512104

Wu, W., Xu, J., Wu, X. S., & Wu, L. G. (2005). Activity-Dependent Acceleration of Endocytosis at a Central Synapse. *Journal of Neuroscience*, *25*(50), 11676-11683. https://doi.org/10.1523/jneurosci.2972-05.2005

Wu, X.-S., McNeil, B. D., Xu, J., Fan, J., Xue, L., Melicoff, E., Adachi, R., Bai, L., & Wu, L.-G. (2009). Ca2+ and calmodulin initiate all forms of endocytosis during depolarization at a nerve terminal. *Nature Neuroscience*, *12*(8), 1003-1010. https://doi.org/10.1038/nn.2355

Wu, X.-S., Subramanian, S., Zhang, Y., Shi, B., Xia, J., Li, T., Guo, X., El-Hassar, L., Szigeti-Buck, K., Henao-Mejia, J., Flavell, R. A., Horvath, T. L., Jonas, E. A., Kaczmarek, L. K., & Wu, L.-G. (2021). Presynaptic Kv3 channels are required for fast and slow endocytosis of synaptic vesicles. *Neuron*, *109*(6), 938-946.e935. https://doi.org/10.1016/j.neuron.2021.01.006

Wu, X.-S., Zhang, Z., Zhao, W.-D., Wang, D., Luo, F., & Wu, L.-G. (2014). Calcineurin Is Universally Involved in Vesicle Endocytosis at Neuronal and Nonneuronal Secretory Cells. *Cell Reports*, *7*(4), 982-988. https://doi.org/10.1016/j.celrep.2014.04.020

Wu, X. S., Lee, S. H., Sheng, J., Zhang, Z., Zhao, W. D., Wang, D., Jin, Y., Charnay, P., Ervasti, J. M., & Wu, L. G. (2016). Actin Is Crucial for All Kinetically Distinguishable Forms of Endocytosis at Synapses. *Neuron*, *92*(5), 1020-1035. https://doi.org/10.1016/j.neuron.2016.10.014

Wu, X. S., & Wu, L. G. (2009). Rapid Endocytosis Does Not Recycle Vesicles within the Readily Releasable Pool. *Journal of Neuroscience*, *29*(35), 11038-11042. https://doi.org/10.1523/jneurosci.2367-09.2009

Wu, X. S., & Wu, L. G. (2014). The Yin and Yang of Calcium Effects on Synaptic Vesicle Endocytosis. *Journal of Neuroscience*, *34*(7), 2652-2659. https://doi.org/10.1523/jneurosci.3582-13.2014

Wu, Y., O'Toole, E. T., Girard, M., Ritter, B., Messa, M., Liu, X., McPherson, P. S., Ferguson, S. M., & De Camilli, P. (2014). A dynamin 1-, dynamin 3- and clathrin-independent pathway of synaptic vesicle recycling mediated by bulk endocytosis. *eLife*, *3*. https://doi.org/10.7554/elife.01621

Xia, X. M., Fakler, B., Rivard, A., Wayman, G., Johnson-Pais, T., Keen, J. E., Ishii, T., Hirschberg, B., Bond, C. T., Lutsenko, S., Maylie, J., & Adelman, J. P. (1998). Mechanism of calcium gating in small-conductance calcium-activated potassium channels. *Nature*, *395*(6701), 503-507. https://doi.org/10.1038/26758

Xing, Y., Böcking, T., Wolf, M., Grigorieff, N., Kirchhausen, T., & Harrison, S. C. (2010). Structure of clathrin coat with bound Hsc70 and auxilin: mechanism of Hsc70-facilitated disassembly. *The EMBO Journal*, *29*(3), 655-665. https://doi.org/10.1038/emboj.2009.383

Xu, J., Luo, F., Zhang, Z., Xue, L., Wu, X.-S., Chiang, H.-C., Shin, W., & Wu, L.-G. (2013). SNARE Proteins Synaptobrevin, SNAP-25, and Syntaxin Are Involved in Rapid and Slow Endocytosis at Synapses. *Cell Reports*, *3*(5), 1414-1421. https://doi.org/10.1016/j.celrep.2013.03.010

Xu, J., Wu, X. S., Sheng, J., Zhang, Z., Yue, H. Y., Sun, L., Sgobio, C., Lin, X., Peng, S., Jin, Y., Gan, L., Cai, H., & Wu, L. G. (2016). -Synuclein Mutation Inhibits Endocytosis at Mammalian Central Nerve Terminals. *Journal of Neuroscience*, *36*(16), 4408-4414. https://doi.org/10.1523/jneurosci.3627-15.2016

Xue, L., McNeil, B. D., Wu, X. S., Luo, F., He, L., & Wu, L. G. (2012). A Membrane Pool Retrieved via Endocytosis Overshoot at Nerve Terminals: A Study of Its Retrieval Mechanism and Role. *Journal of Neuroscience*, *32*(10), 3398-3404. https://doi.org/10.1523/jneurosci.5943-11.2012

Xue, L., & Wu, L.-G. (2010). Post-tetanic potentiation is caused by two signalling mechanisms affecting quantal size and quantal content. *The Journal of Physiology*, *588*(24), 4987-4994. https://doi.org/10.1113/jphysiol.2010.196964

Yamashita, T., Eguchi, K., Saitoh, N., Von Gersdorff, H., & Takahashi, T. (2010). Developmental shift to a mechanism of synaptic vesicle endocytosis requiring nanodomain Ca2+. *Nature Neuroscience*, *13*(7), 838-844. https://doi.org/10.1038/nn.2576

Yamashita, T., Hige, T., & Takahashi, T. (2005). Vesicle endocytosis requires dynamin-dependent GTP hydrolysis at a fast CNS synapse. *Science*, *307*(5706), 124-127. https://doi.org/10.1126/science.1103631

Yao, C.-K., Liu, Y.-T., Lee, I. C., Wang, Y.-T., & Wu, P.-Y. (2017). A Ca2+ channel differentially regulates Clathrin-mediated and activity-dependent bulk endocytosis. *PLoS Biology*, *15*(4), e2000931. https://doi.org/10.1371/journal.pbio.2000931

Yao, C. K., Lin, Y. Q., Ly, C. V., Ohyama, T., Haueter, C. M., Moiseenkova-Bell, V. Y., Wensel, T. G., & Bellen, H. J. (2009). A synaptic vesicle-associated Ca2+ channel promotes endocytosis and couples exocytosis to endocytosis. *Cell*, *138*(5), 947-960. https://doi.org/10.1016/j.cell.2009.06.033

Yao, J., Kwon, S. E., Gaffaney, J. D., Dunning, F. M., & Chapman, E. R. (2012). Uncoupling the roles of synaptotagmin I during endo- and exocytosis of synaptic vesicles. *Nature Neuroscience*, *15*(2), 243-249. https://doi.org/10.1038/nn.3013

Yao, L., & Sakaba, T. (2012). Activity-dependent modulation of endocytosis by calmodulin at a large central synapse. *Proceedings of the National Academy of Sciences*, *109*(1), 291-296. https://doi.org/10.1073/pnas.1100608109

Yao, L. H., Rao, Y., Varga, K., Wang, C. Y., Xiao, P., Lindau, M., & Gong, L. W. (2012). Synaptotagmin 1 Is Necessary for the Ca2+ Dependence of Clathrin-Mediated

Endocytosis. *Journal of Neuroscience*, *32*(11), 3778-3785. https://doi.org/10.1523/jneurosci.3540-11.2012

Yao, P. J., & Coleman, P. D. (1998). Reduced O-glycosylated clathrin assembly protein AP180: implication for synaptic vesicle recycling dysfunction in Alzheimer's disease. *Neuroscience Letters*, *252*(1), 33-36. https://doi.org/10.1016/s0304-3940(98)00547-3

Yao, P. J., Zhang, P., Mattson, M. P., & Furukawa, K. (2003). Heterogeneity of endocytic proteins: distribution of clathrin adaptor proteins in neurons and glia. *Neuroscience*, *121*(1), 25-37. https://doi.org/10.1016/s0306-4522(03)00431-7

Yim, Y. I., Sun, T., Wu, L. G., Raimondi, A., De Camilli, P., Eisenberg, E., & Greene, L. E. (2010). Endocytosis and clathrin-uncoating defects at synapses of auxilin knockout mice. *Proceedings of the National Academy of Sciences*, *107*(9), 4412-4417. https://doi.org/10.1073/pnas.1000738107

Yue, H. Y., & Xu, J. (2014). Myosin Light Chain Kinase Accelerates Vesicle Endocytosis at the Calyx of Held Synapse. *Journal of Neuroscience*, *34*(1), 295-304. https://doi.org/10.1523/jneurosci.3744-13.2014

Zhang, B., Koh, Y. H., Beckstead, R. B., Budnik, V., Ganetzky, B., & Bellen, H. J. (1998). Synaptic Vesicle Size and Number Are Regulated by a Clathrin Adaptor Protein Required for Endocytosis. *Neuron*, *21*(6), 1465-1475. https://doi.org/10.1016/s0896-6273(00)80664-9

Zhang, J. Z., Davletov, B. A., Südhof, T. C., & Anderson, R. G. W. (1994). Synaptotagmin I is a high affinity receptor for clathrin AP-2: Implications for membrane recycling. *Cell*, *78*(5), 751-760. https://doi.org/10.1016/s0092-8674(94)90442-1

Zhang, Q., Li, Y., & Tsien, R. W. (2009). The Dynamic Control of Kiss-And-Run and Vesicular Reuse Probed with Single Nanoparticles. *Science*, *323*(5920), 1448-1453. https://doi.org/10.1126/science.1167373

Zhang, Z., Wang, D., Sun, T., Xu, J., Chiang, H. C., Shin, W., & Wu, L. G. (2013). The SNARE Proteins SNAP25 and Synaptobrevin Are Involved in Endocytosis at Hippocampal Synapses. *Journal of Neuroscience*, *33*(21), 9169-9175. https://doi.org/10.1523/jneurosci.0301-13.2013

Zhao, W.-D., Hamid, E., Shin, W., Wen, P. J., Krystofiak, E. S., Villarreal, S. A., Chiang, H.-C., Kachar, B., & Wu, L.-G. (2016). Hemi-fused structure mediates and controls fusion and fission in live cells. *Nature*, *534*(7608), 548-552. https://doi.org/10.1038/nature18598

Zhu, Y., Xu, J., & Heinemann, S. F. (2009). Two pathways of synaptic vesicle retrieval revealed by single-vesicle imaging. *Neuron*, *61*(3), 397-411. https://doi.org/10.1016/j.neuron.2008.12.024

Zucker, R. S., & Regehr, W. G. (2002). Short-Term Synaptic Plasticity. *Annual Review of Physiology*, *64*(1), 355-405. https://doi.org/10.1146/annurev.physiol.64.092501.114547